

©Copyright 2012
Erin E. Mulkearns-Hubert

The “intelligent adaptor” Dab2 regulates clathrin-mediated endocytosis

Erin E. Mulkearns-Hubert

A dissertation

submitted in partial fulfillment of the

requirements for the degree of

Doctor of Philosophy

University of Washington

2012

Reading Committee:

Jonathan Cooper, Chair

Robert Eisenman

Paul Lampe

Program Authorized to Offer Degree:

Molecular and Cellular Biology

Abstract

Clathrin-mediated endocytosis (CME) is an essential process by which cells internalize plasma membrane proteins. The master regulator of the process is thought to be the adaptor protein AP2, which organizes receptors, clathrin, and other necessary factors at the plasma membrane. Disabled-2 (Dab2) is an adaptor protein that allows AP2 to internalize receptors to which it cannot directly bind, such as the low-density lipoprotein receptor (LDLR) and integrin $\beta 1$. Dab2 has been shown to function independently of AP2 under some conditions. I hypothesized that this AP2-independent function of Dab2 might require Dab2 to interact directly with various endocytic accessory proteins normally recruited by AP2. Here I report the direct interaction of Dab2 with three endocytic accessory proteins, the F-BAR protein FCHO2 and the EH domain proteins Eps15 and Intersectin (ITSN). Interestingly, FCHO2 and the EH domain proteins are both important for the organization and structure of clathrin-coated pits (CCPs). FCHO2 and EH domain proteins are required for CME and their interaction with Dab2 is required for Dab2-mediated endocytosis. The mere presence of EH domain proteins in CCPs is not sufficient for internalization of Dab2 cargoes; Eps15 and ITSN must directly bind to Dab2 to permit receptor endocytosis. This suggests that a cargo-adaptor-EH domain protein complex is required for CME. I also give evidence that Dab2 exists in both “open” and “closed” states and that the change between the two may be regulated by cargo binding. While common perception holds that adaptor proteins simply link two incompatible proteins together, I propose that Dab2 is an “intelligent adaptor” which senses the presence of one molecule and undergoes a conformational change to permit the binding of others.

Table of Contents

List of Figures	iii
List of Tables	iv
Chapter 1 – Introduction	1
I. Clathrin-mediated endocytosis: mechanism and hub proteins	1
II. Accessory proteins in CME.....	5
III. CLASPs.....	9
IV. Dab2 is a PTB domain-containing CLASP	12
V. History of Dab2.....	13
VI. Other functions of Dab2	15
VII. Dab2: a complete adaptor?	17
Chapter 2 - FCHO2 organizes clathrin-coated structures and interacts with Dab2 for LDLR endocytosis.....	21
I. Abstract.....	21
II. Introduction	22
III. Results	24
Dab2 interacts with FCHO2.....	24
The Dab2 DPF motifs interact with the μ HD of FCHO2.....	25
The Dab2-FCHO2 binding site is required for normal levels of LDLR endocytosis when AP2 is depleted	28
FCHO2 depletion affects the organization of CCP components and inhibits CME.....	29
Endocytic activity of enlarged clathrin-coated structures.....	31
IV. Discussion.....	33
FCHO2 is a CCS organizing protein	33
Requirement for the Dab2-FCHO2 complex	35
The DPF as a μ HD-interacting motif.....	37
V. Materials and Methods:.....	37
Chapter 3 - The clathrin adaptor Dab2 recruits EH domain scaffold proteins to regulate integrin β 1 endocytosis.....	62
I. Abstract.....	62
II. Introduction	63
III. Results.....	65
The Dab2 NPF sequences mediate binding to endocytic EH domain proteins.	65
EH domain proteins regulate integrin β 1 and TfnR endocytosis.....	66

Internalization of Dab2-dependent cargo requires Dab2 binding to EH domain proteins	69
IV. Discussion.....	71
V. Materials and Methods.....	75
Chapter 4 – A Dab2 conformational change may regulate CCP activity	93
I. Introduction	93
II. Results	95
Part 1: Competition between FCHO2 and AP2 for the Dab2 DPFs	95
Part 2: The Dab2 C-terminus binds its PTB domain	97
III. Materials and Methods.....	100
Chapter 5 - Discussion	110
References	116

List of Figures

Figure 1.1	Summary of CME and Internalization Signals.....	20
Figure 2.1	Dab2 Interacts With FCHO2	49
Figure 2.2	The Dab2 DPF Motifs Interact With the FCHO2 μ HD	50
Figure 2.3	Localization of T7-Dab2 Mutants	51
Figure 2.4	The μ HD of FCHO2 is Required for CCP Localization	52
Figure 2.5	Depletion of EH Domain Proteins Does Not Affect Dab2-FCHO2 Binding.....	53
Figure 2.6	Disruption of Dab2-FCHO2 Inhibits Dab2-Dependent LDLR Endocytosis	54
Figure 2.7	FCHO2 Depletion Affects CCP Component Organization and Inhibits CME	55
Figure 2.8	FCHO2 Depletion Does Not Affect Total Levels of TfnR or LDLR.....	56
Figure 2.9	Effect of FCHO1+2 siRNA on LDLR and TfnR Endocytosis at 37°C.....	57
Figure 2.10	Endocytic activity of enlarged clathrin-coated structures	58
Figure 2.11	Effect of FCHO1+2 siRNA on Endocytosis with a 4°C pre-incubation.....	59
Figure 2.12	Effect of Depletion of Dab2 or AP2 and FCHO1+2 on Endocytosis.....	60
Figure 2.13	Dab2-DPF* is Deficient for LDLR Endocytosis With a 4°C Pre-incubation.	61
Figure 3.1	The Dab2 NPFs are Required for Binding Eps15 and ITSN.....	84
Figure 3.2	Dab2 Binds and Colocalizes With Eps15 and HA-ITSN.....	85
Figure 3.3	The Dab2 NPFs are Not Required for Localization to CCSs.....	86
Figure 3.4	EH Domain Protein Depletion by siRNA.	86
Figure 3.5	EH Domain Proteins Regulate Integrin β 1 and TfnR Endocytosis.	87
Figure 3.6	Effect of EH Protein Depletion on Clathrin, AP2, Dab2 and Cargo Localization..	88
Figure 3.7	Disruption of Dab2-EH Protein Slows Dab2-Dependent β 1 Internalization.	89
Figure 3.8	Lifetime Distribution for CCSs.	90
Figure 3.9	Disruption of Dab2-EH Protein Does Not Affect TfnR Endocytosis.	91
Figure 3.10	Summary of Results and Proposed Model.	92
Figure 4.1	Potential Competition Between AP2 and FCHO2 for Dab2 Binding	102
Figure 4.2	AP2 Outcompetes FCHO2 for Dab2 Binding	103
Figure 4.3	Removing the FCHO2 F-BAR Domain Does Not Affect Competition Results...	104
Figure 4.4	The C-terminus of Dab2 Binds to Its PTB Domain	105
Figure 4.5	The Very C-terminal End of Dab2 is Required to Bind the PTB Domain.....	106
Figure 4.6	The C-terminus Still Binds a PTB Mutant That Does Not Bind Cargo	107
Figure 4.7	Binding of Cargo to the PTB Domain Inhibits C-terminal Binding	108
Figure 4.8	Proposed Model for a Dab2 Conformational Change Upon Cargo Binding.....	109

List of Tables

Table 2.1	FCHO2 Depletion Affects the Number and Size of Clathrin Structures	48
Table 3.1	Effect of EH Domain Protein Depletion on Clathrin Structures	82
Table 3.2	Effect of Dab2 on the Size, Number, and Composition of CCS	83

Acknowledgements

I am grateful to so many people both in the Cooper lab and around the Hutch who have helped make my time in graduate school successful.

First, thanks to Jon. I expect that I've been frustrating at times for him, but he's had a good sense of when to push me and when to back off, and I appreciate that. Thanks, Jon, for putting up with me and guiding me through this to the end.

My labmates are always there to brighten a bad day and celebrate a success. I am hugely indebted to Anjali Teckchandani, who has been thinking about Dab2 with me the whole way and has worn many hats for me over the years: friend, mentor, technical advisor, therapist, and now collaborator. Thanks to Sergi Simo for bringing life into the lab and keeping everyone laughing. Thanks to George Laszlo for forcing me to think about what to do with my life. Moham Ansari has made hundreds of liters of PBS for me and never complained. Thanks also to Khyati Shah, Esther Jhingan, and Natalie Toida for "L" and "C". Rylie Hightower, an undergraduate intern from New Mexico State University, was my hands for Dab2 binding experiments while I was writing.

Thanks to my committee members, Bob Eisenman, Paul Lampe, Chris Kemp, and Merrill Hille for offering useful suggestions.

Thanks to Stephanie Busch for reading the FCHO2 paper and offering suggestions, and for many hours of stress relief.

Thanks to all of my family, who haven't seen us for a major holiday in several years. We'll try to visit more now!

And finally, thanks to my husband Chris. I wouldn't have thought to go to grad school without him, and I doubt I would have made it through without him either. He encouraged me and believed in me more than I believed in myself.

Chapter 1 – Introduction

I. Clathrin-mediated endocytosis: mechanism and hub proteins

For a cell to survive, it must be able to remove transmembrane proteins from the cell surface, either to downregulate proliferative signaling, internalize nutrients, or to reorganize cell-cell or cell-matrix connections. The major mechanism for the internalization of such receptors is clathrin-mediated endocytosis (CME), a process where transmembrane proteins are specifically sorted into areas where the coat protein clathrin and other membrane-bending proteins deform the membrane to create invaginations. All of the proteins in a clathrin-coated pit (CCP) must work together in a tightly spatially and temporally controlled environment for the successful internalization of their cargo.

CME begins with the clustering of receptors, adaptors, and clathrin together in an area of the plasma membrane (Figure 1.1A, reviewed in [1-7]). This membrane begins curving inward with the help of membrane-bending proteins. The nascent CCP continues to grow and mature, accumulating additional cargo, clathrin, and other proteins. Eventually the pit ceases growing and begins membrane fission. After the newly-formed vesicle is released from the membrane, the clathrin coat and many associated proteins are removed. These endosomes then fuse with sorting endosomes, a type of early endosome (reviewed in [8-11]). These compartments have an internal pH of 6.0, which causes most ligands, including LDL, to dissociate from their receptors. An exception to this is transferrin (Tfn); acidic conditions cause bound iron to dissociate from the Tfn ligand, but Tfn itself remains bound to the receptor until the surrounding pH becomes neutral. Proteins and lipids present in the sorting endosome can be trafficked in at least three

directions: they are either recycled directly to the plasma membrane, moved to the endocytic recycling compartment where additional sorting occurs, or remain in the sorting endosome as it matures into a late endosome and delivers its cargo to lysosomes. Fast recycling of membrane receptors is generally the default pathway and this process is made efficient by the budding of thin, tubular structures from the sorting endosome's membrane. Compared to a sphere, the surface area of a tubule relative to its luminal volume is much greater, and this selects for membrane proteins rather than their soluble ligands. Receptors which fail to be recycled in this manner are trafficked to the endocytic recycling compartment, a longer-lived structure. This compartment also recycles transmembrane proteins to the plasma membrane, but using two separate pathways, one fast and one slow. This slow pathway may allow the cell to maintain an intracellular pool of receptors which are ready to be returned to the plasma membrane upon some stimulus. Transmembrane proteins can also be trafficked to the trans-Golgi network from the endocytic recycling compartment. Certain receptors, such as signaling receptors, often need to be more permanently downregulated. The addition of ubiquitin to their cytoplasmic tail is commonly used as a sorting signal for these receptors to remain in the sorting endosome during maturation into a late endosome, and they are then delivered to lysosomes for degradation. ESCRT proteins likely play a role in the recognition of this ubiquitin signal. This late endosome to lysosome path is also followed by most ligands, although some, as mentioned earlier regarding Tfn, are returned to the plasma membrane.

Clathrin, the protein which makes up the coat of coated pits, is so named because of its lattice-like formation around clathrin-coated vesicles (CCVs) [12]. Electron microscopy of clathrin monomers revealed its unique architecture: three legs, all curved in the same direction,

radiate out from a central hub; this structure is termed a triskelion [13]. Each leg is composed of one heavy chain molecule and one light chain molecule [13]. The heavy chain is the major lattice assembly unit, while the light chain regulates this assembly [14, 15]. Dissociated clathrin triskelia are able to reassemble into cages at low pH in vitro [16], but addition of clathrin-assembling adaptor proteins allows assembly at physiological conditions [17]. Clathrin binding sites on other endocytic proteins are fairly degenerate but are often classified into two main types, the type I clathrin box, with the consensus sequence $L\Phi x\Phi[DE]$, where Φ is a bulky, hydrophobic amino acid, and the type II clathrin box, consensus sequence $PWxxW$ [18-20].

The prototypical endocytic adaptor protein, AP2, is found predominantly at the plasma membrane and is one of the most abundant proteins found among the clathrin coat [21, 22]. AP originally stood for “assembly protein,” for its ability to assemble clathrin cages [23], but is now generally understood to mean “adaptor protein” [24]. There are four described AP complexes. AP1 exists as two forms; AP1A is associated with vesicles found at the trans-Golgi network (TGN) and endosomes and plays a role in trafficking between them, while AP1B is expressed in polarized epithelial cells and targets proteins to the basolateral membrane [25, 26]. AP2 localizes to the plasma membrane and traffics from plasma membrane to endosomes [22, 27]. The roles of AP3 and AP4 are not as well-described, but AP3 seems to play a role in the sorting of proteins from endosomes or the Golgi to lysosomes [28-30] and AP4 may also be involved in the sorting of receptors from the TGN to endosomes [31]. Just recently a fifth AP complex was discovered; the colocalization of this AP5 with the late endosomal and lysosomal marker LAMP1 suggest a role in endosomal-lysosomal trafficking [27]. Interestingly, phylogenetic analysis of the AP complexes indicated that AP3 is the ancestral AP complex, while the better

characterized AP1 and AP2 are more recently evolved [27].

AP2, like each of the AP complexes, is a heterotetrameric complex made up of two large subunits, α -adaptin (the α -subunit) and β -adaptin (β 2), one medium subunit, μ 2, and the small subunit σ 2 [32-34]. The alpha and beta subunits are composed of two domains, the “trunk” region, which, along with μ 2 and σ 2, form the core of the AP2 complex, and the appendage domains, which extend out from the core of the complex and are free to interact with other endocytic proteins [35, 36]. AP2 binds clathrin on at least two separate sites: on the globular β subunit appendage and also on the hinge that connects the β appendage to the complex core [37-39]. The presence of multiple binding sites for clathrin is an important element to the ability of AP2 to assemble clathrin lattices, presumably because it allows the adaptor to properly orient two clathrin molecules for binding [38, 39].

Other important functions of adaptor proteins are linkage of clathrin to the plasma membrane and recruitment of receptor cargo into CCPs. Clathrin itself has no ability to bind phospholipids, so it relies on adaptors for membrane recruitment [24]. The α -subunit core domain of AP2 binds membrane phosphatidylinositol-4,5-bisphosphate (PIP₂) and phosphatidylinositol-3,4,5-trisphosphate (PIP₃) [40-42], although PIP₂ is found in higher abundance at the plasma membrane and is thought to be the major phospholipid involved in CME [43]. An additional binding site for phospholipids is found on the μ 2 subunit, but this site is not constitutively accessible for membrane binding [42].

For receptors to be efficiently recruited into CCPs, adaptor proteins must bind to internalization signals on their cytoplasmic tails (Figure 1.1B). AP2 directly recruits cargo with two types of internalization signals to CCPs: the tyrosine-based Yxx Φ motif, where Φ is a bulky, hydrophobic amino acid [44, 45], and the dileucine [DE]XXXL[LI] motif [46]. The Yxx Φ motif, as found in the transferrin receptor (TfnR) and many other receptors, binds to the AP2 μ 2 subunit [47]. However, experiments showed that dileucine and Yxx Φ motifs do not compete for AP2 binding, suggesting they bind to different sites on the adaptor protein [48]. Dileucine motifs were found to interact with the AP2 σ 2 subunit, which was thought to be mostly structural previous to the identification of this cargo-binding motif [3, 42, 49]. Additional adaptors exist in cells that allow the recruitment of cargo containing other internalization signals that cannot bind directly to AP2.

II. Accessory proteins in CME

AP2 functions not only as a cargo adaptor to link receptors to clathrin and membrane phospholipids, but also as a hub for protein recruitment to the growing CCP. Over 60 proteins with a role in the formation, growth, budding, or uncoating of a clathrin coat have been identified [50-52]. Of those, many interact with either the α appendage or β appendage of AP2, often through a canonical AP2-binding DP[FW] motif [53-55]. The majority of proteins involved in endocytosis can be categorized into five main groups based on the dynamics of their recruitment and release from CCPs: clathrin and adaptor proteins, actin regulators, membrane curving proteins, the scission protein dynamin, and uncoating factors [51]. However, additional proteins also act during endocytosis which do not fit easily into one of these classes; these proteins are often responsible for modifying an endocytic protein in some way to permit its interaction with

others [50, 51].

Clathrin and adaptors are among the earliest arriving proteins to a nascent CCP [51]. This is not unexpected, since these are thought to be the major structural components of a pit and are required for CCP formation. Additional proteins that arrive at CCPs with clathrin and AP2 include Eps15 and epsin, both of which have cargo recruitment functions as well as additional functions [56-58]. Eps15 contains binding sites for many endocytic proteins and can act as a scaffold to assemble them [59, 60]. Epsin is able to bend membranes with its ENTH domain [61]. While this group of proteins are all recruited during the early steps of CCP formation, it remains controversial which proteins are responsible for the nucleation event. One exciting recent study implicated the F-BAR proteins FCHO1 and 2, which also arrive early with AP2 and clathrin [51], in CCP nucleation [62]. BAR domains are common in endocytic proteins; these curved bundles of helices bind to membranes and induce their curvature in vitro [63]. When FCHO proteins were depleted from cells with siRNA, AP2 no longer localized to CCPs and the rate of CCP nucleation dropped to near zero [62]. However, other reports disagree with a nucleating role for the FCHO proteins [64], including work shown in Chapter 2 [65], and thus a definitive CCP initiator remains to be identified.

While FCHO proteins arrive early to a CCP with clathrin and adaptors, other membrane-bending proteins are also involved in CCP formation. Curvature of the plasma membrane is an obvious need during endocytosis, and clathrin itself is not sufficient to produce membrane invagination as it can assemble as both curved and flat lattices [66, 67]. Chief among the membrane bending proteins found at CCPs are the BAR domain proteins amphiphysin and

endophilin [51]. BAR domains typically exist as dimers; each protein molecule contributes α -helices which together form a curved, positively charged surface (sometimes described as banana or boomerang shaped [68, 69]) which can interact with negatively charged phospholipids [70, 71]. BAR domain proteins are able to induce curvature of liposomes in vitro ([63, 72-74], among many others), although it is still debated whether they induce or stabilize curvature or simply bind to already curved membranes in vivo [68]. BAR domains not only dimerize but are also thought to oligomerize. By assembling end-to-end, a long string of BAR domain proteins is able to wrap around a liposome or invaginated membrane and enforce curvature [75]. There are many subclasses of BAR domains, including F-BAR, N-BAR, I-BAR, BAR-PH, and PX-BAR [68, 76, 77]. Each of these BAR domain types differs mainly in its degree of curvature: an F-BAR, for example, is much less curved than an N-BAR domain and thus tubulates liposomes to a larger diameter [68]. An exception to this is the I-BAR domain; while the majority of BAR domains exhibit concave curvature, I-BAR domains curve convexly, suggesting a role in membrane protrusions rather than invaginations [78, 79]. Additionally, the N-BAR domain, which is found in amphiphysin and endophilin, has an α helix at each end of the BAR domain which inserts in the lipid bilayer and physically causes curvature [76].

Probably the most extensively studied accessory protein is the large GTPase dynamin, which deforms the lipid bilayer to allow vesicle scission. However, the large amount of work on dynamin has not provided answers for some of the main questions about how it functions. Dynamin forms a network of interactions within a CCP, binding to AP2 and many other accessory proteins, some of which also have membrane-bending functions [54, 59, 80]. A role for dynamin in endocytosis was revealed by the *Drosophila shibere* mutant, the fly dynamin

homolog. When temperature-sensitive *shibere* mutants are placed at a non-permissive temperature, synaptic endocytosis is defective and their membranes exhibit an accumulation of “collared pits” [81]. The “collar” of these pits was shown to contain dynamin oligomers, and the GTPase activity of these complexes is essential for endocytosis [82-84]. Dynamin assembles around the neck of a CCP during later steps of endocytosis, and GTP hydrolysis drives a rearrangement of these dynamin assemblies which causes detachment of the vesicle from the plasma membrane (reviewed in [85]). However, how GTP hydrolysis drives a conformational change in the dynamin oligomers and the mechanism of how this change breaks the lipid bilayer are still not well-understood.

A subset of actin-binding proteins are recruited and released from a growing CCP both along with dynamin and as a separate actin-regulatory protein module [51]. Both actin assembly and actin filament turnover are required for CME in yeast [86-88], and actin dynamics are a tantalizing model for both generating force for membrane scission as well as vesicle movement away from the plasma membrane. Many mammalian CCP proteins regulate actin dynamics, including dynamin, syndapin, intersectin, and HIP1R [89-92]. Additionally, actin and actin regulatory proteins such as the nucleator Arp2/3 and its activator N-WASP have also been shown to localize to CCPs [93]. However, studies using inhibitors of actin polymerization or depolymerization demonstrated variable effects on endocytosis [94]. The development of high-resolution live-cell imaging techniques, particularly TIRF-based systems which allow illumination of the membrane of a cell to a depth of only ~100 – 200 nm, has shed more light on the subject. Multiple studies have visualized fluorescent actin and actin-binding proteins during CME and seen these proteins recruited during the growth of the CCP with an actin burst

occurring with scission, which is similar to the recruitment pattern of dynamin [51, 95-97].

Along with the localization of actin and actin-regulating proteins in CCPs, these real-time images of protein recruitment during endocytosis suggest that the actin cytoskeleton does play a role in endocytosis, even if some CME may proceed without it.

Uncoating and endosomal proteins, as expected, are among the last to arrive at an area of internalization [51]. In order for a newly internalized vesicle to fuse with early endosomes, the clathrin coat must be removed. At least two proteins are required for the uncoating of CCVs: the chaperone and ATPase heat-shock cognate-70 (hsc70) and its co-factor auxilin [98-102]. Auxilin-1 is mainly neuronal, while auxilin-2, more commonly called GAK, for cyclin G-associated kinase, is ubiquitous and contains an additional serine/threonine kinase domain [103-105]. The auxilins each contain a J-domain responsible for recruiting hsc70 to its substrates, in this case assembled clathrin, which is recognized by the central regions of the auxilins [99, 106]. The attachment of hsc70 to the clathrin lattice deforms the structure and leads to dissociation of clathrin from the vesicle [107]. The disassembly of clathrin is likely aided by the phosphatase synaptojanin; dephosphorylation of lipid head groups causes adaptors and clathrin assembly proteins to dissociate from the membrane, destabilizing clathrin polyhedrons [108-110].

III. CLASPs

Many types of transmembrane proteins require internalization, but only a subset contains a dileucine or Yxx Φ motif that will promote AP2-mediated endocytosis. Receptors such as the low-density lipoprotein receptor (LDLR) and epidermal growth factor receptor (EGFR) do not

compete with each other or the TfnR for entry, yet their internalization is still clathrin-dependent, suggesting that each may be internalized by a different adaptor [111, 112]. Additionally, structural studies indicate that it is unlikely that the LDLR internalization motif, FxNPxY, could interact with the cargo-binding region of AP2 [113]. How, then, are these cargoes which do not bind to AP2 brought into the cell? A variety of monomeric adaptor proteins exists to internalize receptors such as this (Figure 1.1B). These alternate adaptors, or CLASPs (CLathrin Associated Sorting Proteins), interact directly with receptors using other internalization signals and also with AP2 and other CCP components, greatly expanding the range of proteins internalized by CME. They function not only as cargo-sorting molecules but may also play a role in organizing the interactions within a CCP.

A cargo-specific adaptor for G-protein coupled receptors (GPCRs) was the first described case of a protein other than AP2 which selectively shuttles a specific receptor into CCPs. β -arrestins, also termed the non-visual arrestins, are essential for the endocytosis of GPCRs upon their activation [114-116]. β -arrestins bind to the phosphorylated tails of GPCRs, both directing them to CCPs as well as blocking their interaction with downstream signaling partners [115, 116]. This ability to direct GPCRs to CCPs depends on β -arrestins' ability to bind concomitantly to four things: phosphorylated cargo, phospholipids, clathrin, and AP2 [117-120]. This suggests that these may be four defining characteristics of clathrin sorting proteins [3, 121].

Receptor ubiquitination can also act as an internalization signal, and polyubiquitin chains are recognized by the adaptor proteins epsin and Eps15 [121, 122]. Ubiquitin is also a commonly used internalization signal during CME in the yeast *S. cerevisiae* [123]. The EGF

receptor, like many monomeric receptor tyrosine kinases (RTKs), is a cargo which is directed for internalization by ubiquitination (reviewed in [124]). The adaptor protein Grb2 binds to phosphorylated tyrosine residues on activated RTKs and then binds the E3 ubiquitin ligase c-Cbl, which ubiquitinates the receptor. Both Eps15 and epsin contain ubiquitin-interacting motifs (UIMs) which can bind to this ubiquitin and complex the cargo with CME machinery (reviewed in [34]). Receptors can be either mono- or polyubiquitinated; epsin and Eps15 appear to prefer to bind to polyubiquitin chains on the EGFR, although this is still debated [121].

Another group of CLASPs is the phosphotyrosine binding domain (PTB)-containing family, which contains the proteins ARH, Dab2, and Numb. Patients with autosomal recessive hypercholesterolemia (ARH) are unable to clear cholesterol from the blood and develop deposits of lipid-rich material on various parts of the body, including in coronary arteries (reviewed in [125, 126]). Surprisingly, however, unlike in familial hypercholesterolemia, a dominant disorder caused by mutation of the LDL receptor itself, the LDLR protein in ARH patients is unmutated and able to bind LDL normally [127-129]. These patients actually have increased levels of plasma membrane-localized LDLR, suggesting a receptor internalization defect [129]. A mutation was found in ARH patients in a novel gene that encodes a protein with a PTB domain, which was named *ARH* after the syndrome [127]. Because of the known interaction of PTB domains with LDLR family members, it was proposed that ARH may act as an adaptor protein to direct LDLR internalization [127]. Further work has shown that ARH is in fact an endocytic adaptor protein for LDLR, and homology between the ARH PTB domain and those of Numb and Disabled-2 (Dab2) suggested that these proteins may also function for internalization of LDLR and similar receptors [130].

IV. Dab2 is a PTB domain-containing CLASP

The punctate localization of endogenous Dab2 and the ability of the Dab1 PTB domain to bind to membrane phospholipids and NPxY internalization sequences on LDLR family members suggested Dab2 might play a role in receptor internalization [131, 132]. Indeed, Dab2 colocalizes with many CCP components, including clathrin, AP2, Eps15 and epsin as well as the LDL and LDLR related protein (LRP) families of receptors [131, 133, 134]. Dab2 and the other PTB domain-containing CLASPs, ARH and Numb, bind to receptors containing NPxY motifs, such as found on members of the LDLR family, including the LDLR and LRPs, β -integrins, and the β -amyloid precursor protein (APP) [130, 131, 135]. Unlike the canonical domain, the Dab2 PTB domain preferentially interacts with unphosphorylated tyrosine signals, making “PTB” something of a misnomer in its case [131]. The Numb PTB, however, is able to bind both phosphorylated and unphosphorylated tyrosine residues [136]. The PTB domain of each protein interacts with both cargo and PIP₂ [130, 131, 137, 138]. Dab2, Numb, and ARH each interact with AP-2, while ARH and Dab2 also have regions that bind to clathrin [130, 131, 133, 137], and Dab2 and Numb both have NPF motifs, which interact with EH domain-containing proteins like Eps15 and Intersectin [139]. Interestingly, Dab2, like AP2, can bind clathrin at two distinct sites, allowing it to drive assembly of clathrin cages [133]. Dab2 exhibits more complexity overall compared to the other PTB domain-containing adaptors; along with its two clathrin boxes, it has three AP2 binding sites, five NPF motifs, three proline-rich sequences, and other potential interaction domains. The central region of the protein, which contains the clathrin binding sites, two of the AP2 binding sites, and two of its NPF motifs, is alternatively spliced. The p96 isoform contains this region while the p67 isoform has it removed [140].

The PTB domain CLASPs exhibit redundancy in some, but not all, situations. ARH was identified as an adaptor for LDLR, but, while hepatic cells from ARH patients are unable to internalize LDL, fibroblasts from these patients internalize LDL normally [141]. Later it was discovered that Dab2 is also able to internalize LDLR but is not expressed in liver cells, suggesting that Dab2 and ARH share a role for LDLR uptake [142, 143]. Depletion of either Dab2 or ARH has no effect on cells that express both adaptors, but siRNA-mediated knockdown of the two together blocks LDLR internalization [142, 143]. There is also some redundancy between Dab2 and Numb for the internalization of integrin $\beta 1$, but the two adaptors appear to act at different areas of the cell. Numb localizes to focal adhesions, suggesting it plays a role in the uptake of extracellular matrix-attached integrin $\beta 1$ [144]. Conversely, Dab2 colocalizes with integrin $\beta 1$ on the top surface of the cell and not at adhesion sites and thus appears to be important for the uptake of free surface integrin [145]. This is thought to be essential for maintaining the free pool of intracellular integrin ready to be deposited at new contacts as a cell migrates. More work is required to fully understand in which situations each of the PTB domain sorting proteins acts.

V. History of Dab2

Dab2 was first identified in 1994 from a screen for transcripts which were downregulated in ovarian cancer, giving it its first name, DOC-2 (deleted in ovarian cancer-2) [146]. Subsequent work detected two splice forms of the protein, p96 and p67, and its N-terminal homology to the *Drosophila* Dab PTB domain [140]. Early work on mammalian Dab2 focused almost exclusively on its role as a potential tumor suppressor. Dab2 has been shown to be downregulated in samples from ovarian [146, 147], prostate [148], breast [149, 150], bladder,

[151], hepatic [152], nasopharyngeal [153], colorectal [154], lung [155], squamous cell [156], and esophageal [157] cancers and upregulated in pancreatic cancer but decreased in its metastases [158]. The mechanism for the loss of Dab2 protein in tumors is not completely understood. Of six breast cancer cell lines negative for Dab2 expression, two showed methylation of the promoter region for the *Dab2* gene [150], suggesting that in some cell types, this may be a cause of Dab2 downregulation. Loss of GATA transcription factors, several of which are able to induce Dab2 expression [159-161], could be an alternative mechanism. Finally, little is known about Dab2 protein turnover, but aberrant regulation of degradation could also play a role in loss of Dab2 protein.

Drosophila disabled is so named due to the enhancer effect its knockout has on *Abl* tyrosine kinase mutants, which exhibit axonal guidance defects [162, 163] as well as non-neuronal epithelial morphogenesis defects [164, 165]. *Dab* mutants have similar phenotypes to *Abl* mutants, and Dab is required for proper localization of Abl, suggesting that it acts upstream of Abl in developmental signaling [164]. Recently, the first evidence that dDab might function in membrane trafficking appeared; dDab colocalizes with clathrin at synapses and *Dab* mutant flies are defective at synaptic vesicle endocytosis [166].

Of the two mammalian homologs of dDab, Dab1 and Dab2, each appears to modulate one of the two reported functions for dDab. Dab1 is expressed in the brain and plays a role in neuronal migration, while Dab2 is expressed in non-neuronal tissues and plays a role in membrane trafficking. Dab1 was discovered as a protein which binds to the tyrosine kinase src [167]. *Dab1* mutant mice have inverted cortical patterning of neurons, suggesting that Dab1 is

essential for proper migration of neurons during development [168]. This inverted patterning is similar to what is seen in animals mutant for the reelin protein, a ligand for the apolipoprotein E receptor-2 (ApoER2) and very low-density lipoprotein receptor (VLDLR) [168, 169]. Reelin binds to ApoER-2 or VLDLR on neuronal membranes, and the receptor cytoplasmic tail then interacts with the Dab1 PTB domain (reviewed in [170]). Although Dab1 is not thought to be involved in receptor endocytosis, this interaction occurs through the NPxY internalization signals of the receptors [132]. This stimulates Dab1 phosphorylation by src family kinases (SFKs). Phosphorylated Dab1 then binds to various cellular proteins, activating Akt and Rap1 through Crk/CrkL and C3G [171]. The exact mechanism of how these signaling pathways activate neuronal migration is not known, but proper control of phosphorylated Dab1 levels is essential, as depletion of its E3-ubiquitin ligase Cullin 5 also produces defects in neuronal migration [172, 173].

VI. Other functions of Dab2

Several mechanisms for the putative tumor suppressive role of Dab2 have been proposed. One of these involves interruption of the mitogen-activated protein kinase (MAPK) signaling cascade. To activate MAPK, receptor tyrosine kinase (RTK) dimers autophosphorylate upon ligand binding. The SH2 domain of growth factor receptor-bound protein-2 (Grb2) binds to phosphotyrosine residues on the RTK and activates son of sevenless (SOS), which then acts as a guanine nucleotide exchange factor (GEF) for Ras. Activated Ras then initiates a kinase cascade that ultimately activates MAPK, which plays a role in many cellular processes, including proliferation, differentiation, and motility (reviewed in [174, 175]). MAPK signaling is misregulated in many, perhaps even all, cancer cells [176]. The C-terminus of Dab2, which

contains at least three SH3-binding, proline-rich sequences, competes with SOS for Grb2 binding, effectively inhibiting Grb2-mediated MAPK activation [177, 178]. However, re-expression of Dab2 in Dab2-negative breast cancer cell lines did not decrease the amount of active MAPK in those cells [179], suggesting that in these cells, even though they lack Dab2 protein, MAPK is being activated through an alternate pathway.

Dab2 also regulates the Wnt signaling pathway, another pathway often misregulated during tumorigenesis [180]. Canonical Wnt signaling stabilizes the transcriptional coactivator β -catenin and allows it to enter the nucleus (reviewed in [181-183]). In the absence of Wnt signaling, β -catenin exists in adherens junctions, but cytoplasmic levels of the protein are low, due to its interaction with a “destruction complex” containing axin and adenomatous polyposis coli (APC), which allows β -catenin to be phosphorylated by glycogen synthase kinase 3 (GSK-3) and ultimately degraded. Upon binding of the Wnt ligand to its coreceptors Frizzled and the low-density lipoprotein-related proteins 5 and 6 (LRP5/6), both GSK-3 and axin are recruited to the cytoplasmic tail of the receptors via the protein Dishevelled (Dsh), causing dissociation of the destruction complex and stabilizing β -catenin. Dab2 binds to both Dsh and axin, interfering with their ability to interact and thereby stabilize β -catenin [184, 185]. The Dab2-axin interaction also inhibits axin degradation, further stabilizing the destruction complex and inhibiting transcription of β -catenin target genes [186]. It remains unclear to what extent the endocytic function of Dab2 has in inhibiting these signaling pathways; however, recently Dab2 was shown to internalize the Wnt coreceptor LRP5/6, suggesting that, at least for Wnt signaling, receptor internalization may be an underlying mechanism of Dab2-mediated tumor suppression [187].

Dab2 also plays an essential role during development. The *Dab2* gene is required during mouse embryonic development; *Dab2* knockout mice do not undergo gastrulation and die before embryonic day 11.5 [188]. However, Dab2 is not essential in the cells of the embryo proper but in the visceral endoderm (VE), an extraembryonic tissue that surrounds the embryo. Early in development, any proteins which need to pass from mother to embryo, such as nutrients and growth factors, must pass through the VE, and VE cells in Dab2 mutant mice are deficient at uptake of several receptors [189]. The lethality of *dab2*^{-/-} mice was rescued by re-expression of the p96 isoform, which contains most of the interaction regions for endocytic components, and only partially rescued by the p67 form, indicating that the developmental defect caused by Dab2 knockout is primarily a defect in endocytosis.

VII. Dab2: a complete adaptor?

As mentioned earlier, the ability of a CLASP to bind to AP2 has been suggested as one of the defining characteristics of such a sorting protein [3]. However, whether AP2, and therefore its interactions with CLASPs, is necessarily required for all CME has been controversial. In 2003, three surprising reports suggested that AP2 was not required for CME of all receptors. Disruption of the AP2 complex with siRNA against the α or μ 2 subunit blocked TfnR but not LDLR or EGFR endocytosis, yet LDLR and EGFR internalization was still clathrin-dependent [190, 191]. Similarly, overexpression of the AP2 kinase AAK1, which sequesters AP2 away from CCPs, inhibited TfnR but not EGFR or LDLR internalization [192]. Together these data cast doubt on the canonical model of AP2 as an essential CCP organizing component and protein interaction hub. The interaction of LDLR with the PTB domain CLASPs suggested that perhaps one of those was sufficient for its internalization in the absence of functional AP2 complexes

[127, 131, 142]. Indeed, Dab2, but not ARH, was able to internalize LDLR when AP2 was depleted with siRNA [142, 143]. Subsequent live-cell imaging studies have intensified the debate about the requirements for AP2. Many studies have reported similar recruitment dynamics of clathrin and AP2 during CCP formation, and some assert that AP2 is associated with almost 100% of CCPs [51, 95, 97]. However, another report suggests that not all clathrin structures within a cell contain AP2, and, in fact, it is actually the more static of these clathrin complexes that mostly colocalize with AP2 and not those actively being internalized [193].

Dab2 appears to be the most likely candidate for a CLASP that can function in the absence of AP2, because of its higher degree of complexity compared to ARH and Numb and AP2-independent internalization of its cargo LDLR. For this to be possible, Dab2 or another protein would then need to fulfill the CCP organizing and accessory protein recruitment functions of AP2. Because Dab2 is able to assemble clathrin and link it to receptors and the membrane via PIP₂, it could theoretically initiate the formation of a CCP. Here I show two types of accessory proteins, FCHO2 (Chapter 2) and the EH domain proteins Eps15 and Intersectin (ITSN) (Chapter 3), which interact directly with Dab2 and can potentially act as indirect links to a multitude of other endocytic accessory proteins. These accessory proteins and their interactions with Dab2 are essential for CME of Dab2 cargo. Depletion of either FCHO2 or Eps15/ITSN also affects the size of CCPs. While EH domain-containing proteins like Eps15 seem to have dedicated interaction sites on Dab2, FCHO2 occupies the same region of Dab2 as AP2, suggesting competitive binding between FCHO2 and AP2 for Dab2. Additionally, I show in Chapter 4 that the binding of cargo to Dab2 may regulate the conformation and potentially the accessory protein binding activity of the protein, indicating that cargo-adaptor binding may act as

a master regulator of CME.

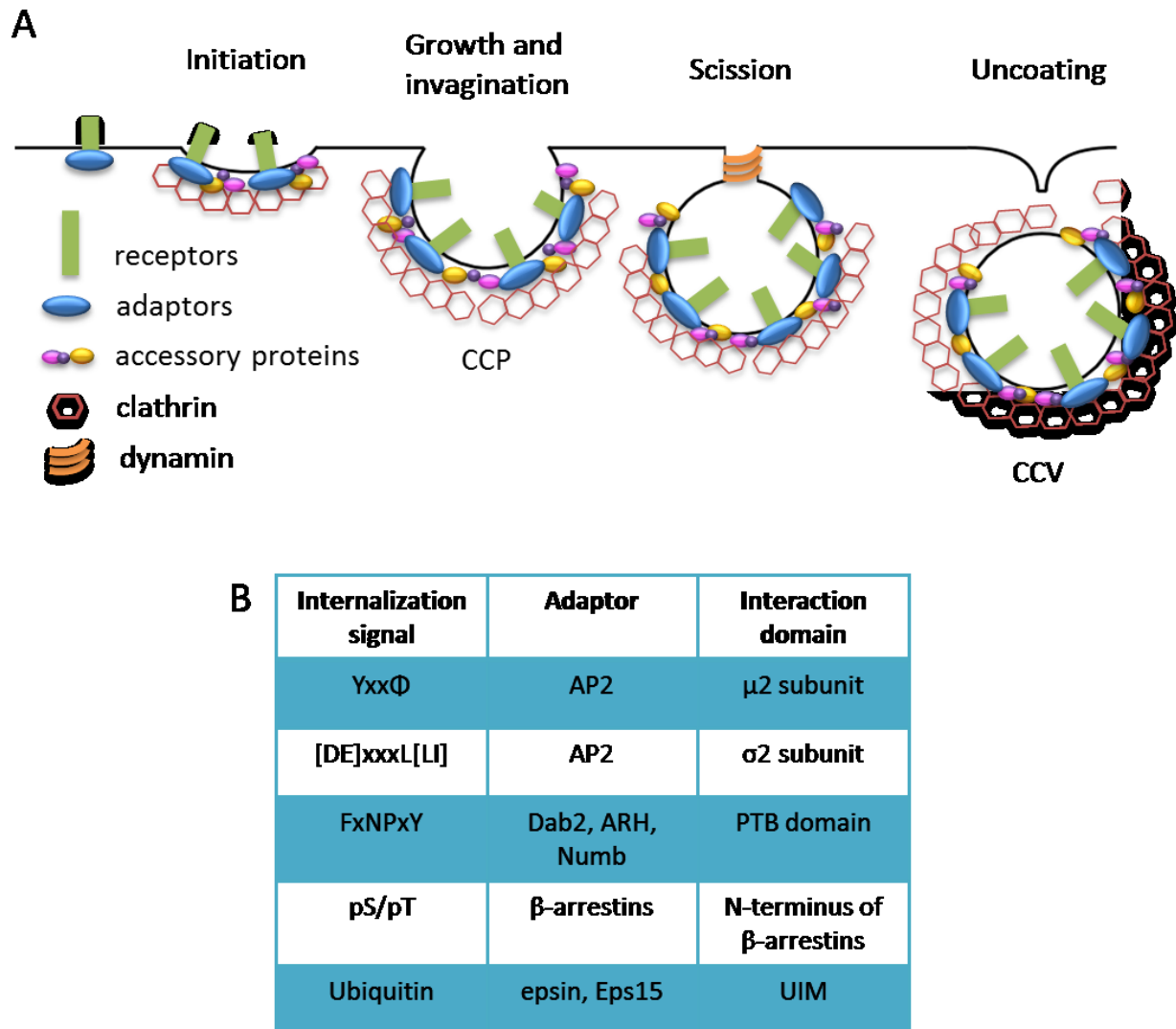


Figure 1.1

Summary of CME and internalization signals

(A) Adaptor proteins concentrate receptors into areas of clathrin enrichment. Additional receptor-adaptor complexes are recruited and the membrane continues to invaginate into a CCP. Accessory proteins are involved which are important for membrane bending and protein recruitment. The GTPase dynamin is required for membrane scission. Additional accessory proteins also play a role in scission and uncoating of the vesicle after budding. (B) Summary of known internalization signals and the specific region of adaptor protein they bind to. (B) is adapted from [2]. CCP, clathrin-coated pit; CCV, clathrin-coated vesicle.

Chapter 2 - FCHO2 organizes clathrin-coated structures and interacts with Dab2 for LDLR endocytosis

Adapted from an article published in *Molecular Biology of the Cell*:

Mulkearns EE, Cooper JA. FCH domain only-2 organizes clathrin-coated structures and interacts with Disabled-2 for low-density lipoprotein receptor endocytosis. *Mol Biol Cell*. 2012 Apr;23(7):1330-42. doi: 10.1091/mbc.E11-09-0812.

I. Abstract

Clathrin-mediated endocytosis regulates the internalization of many nutrient and signaling receptors. Clathrin and endocytic accessory proteins are recruited to receptors by specific adaptors. The adaptor Disabled-2 (Dab2) recruits its cargoes, including the low density lipoprotein receptor (LDLR), and mediates endocytosis even when the major adaptor protein AP2 is depleted. We hypothesized that the accessory proteins that are normally recruited by AP2 may be recruited by Dab2 if AP2 is absent. We identified one such accessory protein, the F-BAR protein FCHO2, as a major Dab2-interacting protein. The μ -homology domain (μ HD) of FCHO2 binds directly to DPF sequences in Dab2 that also bind AP2. Disrupting the Dab2-FCHO2 interaction inhibited Dab2-mediated LDLR endocytosis in AP2-depleted cells. Depleting FCHO2 reduced the number but increased the size of clathrin structures on the adherent surface of HeLa cells and inhibited LDLR and TfnR clustering. However, LDLR was internalized efficiently by FCHO2-deficient cells if additional time was provided for LDLR to enter the enlarged structures before budding, suggesting that later steps of endocytosis are normal under these conditions. These results indicate that FCHO2 regulates the size of clathrin structures and its interaction with Dab2 is needed for LDLR endocytosis under conditions of low AP2.

II. Introduction

Clathrin-mediated endocytosis is a major mechanism by which cells internalize nutrients, reorganize receptors, and regulate signaling (reviewed in [2-6]). Receptors bind to endocytic adaptor proteins that also interact with clathrin and membrane phospholipids. These complexes then aggregate into small membrane areas of clathrin enrichment. As the patches grow, accessory proteins responsible for membrane bending deform the lipid bilayer and the membrane begins to invaginate into a structure called a clathrin coated pit (CCP). The CCP then grows and buds from the membrane forming a sealed clathrin-coated vesicle (CCV), an event requiring the large GTPase dynamin and other accessory proteins. Coat and adaptor proteins are removed from the newly formed vesicle soon after internalization.

The adaptor protein AP2, historically considered a major “hub” for CCP assembly, binds to receptors containing dileucine or YxxΦ motifs, such as the transferrin receptor (TfnR) [3, 5, 53]. It also interacts with clathrin, the membrane phospholipid PtdIns(4,5)P₂, and many other accessory factors needed to form a functional CCP. Some of the accessory proteins known to interact with AP2 include the scaffolding proteins Eps15 and ITSN [194, 195], the membrane-bending BAR-domain protein amphiphysin [80], dynamin [80], and the uncoating factor hsc70 [53]. In addition, AP2 binds to additional receptor-binding proteins, termed CLASPs, for clathrin-associated sorting proteins, to allow internalization of cargo with which AP2 cannot directly associate [196].

Disabled-2 (Dab2) is a CLASP that interacts with AP2 and recruits cargo to CCPs via its N-terminal phosphotyrosine binding (PTB) domain [131]. Other members of the PTB-domain adaptor family include ARH and Numb. These adaptors bind FxNPxY motifs contained in receptors such as the low density lipoprotein receptor (LDLR) [130, 131, 142, 143, 197] and integrin β 1 [135, 144, 145]. Dab2 can bind and assemble clathrin [143] and also associates with the motor protein myosin VI [198] and the signaling adaptor Grb2 [177].

LDLR internalization occurs through two partially redundant pathways utilizing either Dab2 or ARH. ARH requires AP2 to link to clathrin, but Dab2, at least under some conditions, can function in AP2-depleted cells [142, 143, 190]. It seems surprising that Dab2 can function in the absence of AP2 given the multitude of accessory proteins that are recruited by AP2 [53, 54]. We reasoned that for Dab2 to function independently of AP2, Dab2 might be able to also recruit some of the same accessory proteins that are normally recruited by AP2.

Here we report that Dab2 directly binds one such accessory protein, FCHO2. FCHO2 and its close relative FCHO1 contain F-BAR domains which bind to and tubulate membranes in vitro [72, 199, 200]. The C-termini of FCHO proteins contain μ -homology domains (μ HDs), which are similar to the AP2 μ 2 subunit [199]. We detected FCHO2 in an unbiased screen for Dab2 binding partners and found that the Dab2-FCHO2 interaction site is needed for efficient endocytosis of LDLR when AP2-dependent endocytosis is inhibited. Depletion of FCHO2 inhibits endocytosis of the Dab2 cargo LDLR. FCHO2 depletion also inhibits assembly of clathrin-coated pits and induces aggregates of CCP components that appear similar to clathrin

plaques. Additional results suggest that FCHO2 is important for the early steps of endocytosis of Dab2-dependent and independent cargoes.

III. Results

Dab2 interacts with FCHO2

To identify Dab2-binding proteins, we employed a mass spectrometry-based proteomics approach. The p96 form of mouse Dab2 was cloned onto the C-terminus of a His-biotin tag (HBT)-containing vector [201] and introduced into a line of HeLa cells in which Dab2 expression is stably inhibited with shRNA [145]. Cells infected with virus expressing only the HBT tag were used as a control. HBT and HBT-Dab2 protein were sequentially purified over nickel and streptavidin beads and then subjected to SDS-PAGE. Proteins in sections of the gel were then analyzed by LC-MS/MS. Twenty-nine proteins were detected in the Dab2 sample but not the HBT sample in two separate experiments (Figure 2.1A). Strikingly, FCHO2 was the fourth most abundant protein detected. FCHO1 was not detected. We also found six proteins already known to interact with Dab2: four subunits of the AP2 complex ($\alpha 1$, $\alpha 2$, $\beta 1$ and $\mu 1$) [131], myosin VI [198], clathrin heavy chain [133], and Grb2 [177]. Thus the proteomics screen detected known and novel Dab2-binding proteins.

To confirm that Dab2 and FCHO2 interact in cells, we tested whether FCHO2 and Dab2 co-immunoprecipitated. FCHO2 and Dab2 were epitope tagged with GFP and T7, respectively, and transiently expressed in HeLa cells. Cells were lysed and subjected to immunoprecipitation with antibody to T7. Immunoblotting revealed an approximately 130 kD band that corresponded

to the expected size for GFP-FCHO2 (Figure 2.1B). This confirms that FCHO2 and Dab2 interact in cells. Accordingly, immunofluorescence showed GFP-FCHO2 located in distinct cell surface puncta that colocalized with both Dab2 and AP2, indicating that FCHO2 localizes to clathrin-coated structures containing Dab2 and AP2 (Figure 2.1C). This localization pattern suggested that FCHO2 and its interaction with Dab2 were likely involved in some step of clathrin-mediated endocytosis.

The Dab2 DPF motifs interact with the μ HD of FCHO2.

The N-terminus of Dab2 contains a PTB domain, which interacts with PtdIns(4,5)P₂ and receptors containing the FxNPxY sequence [131, 133] (Figure 2.2A). The central region of Dab2 is alternatively spliced; it is present in the p96 form but absent from a p67 splice form [140]. This p96-specific central region contains two clathrin boxes [133]; two NPF motifs, which interact with EH domains [202, 203]; and two DPF sequences, which bind to AP2 [131]. The remainder of the protein, contained in both p67 and p96, includes another AP2-binding sequence, FLDLF [55, 133], a site that binds myosin VI [198], three additional NPF motifs, and binding sites for SH3 domain proteins [140, 177, 204, 205].

To map the region of Dab2 that binds FCHO2, we utilized wildtype p96, p67, and various p96 point and deletion mutants (Figure 2.2A). p96 and the NPF*, AP2*, DPF*, and FLDLF* mutants colocalized with AP2 in CCPs, whereas p67 and p96- Δ C were diffuse (Figure 2.3, [131]). T7-tagged Dab2 constructs were transfected into cells along with GFP-FCHO2 and immunoprecipitated with anti-T7 antibody (Figure 2.2B). FCHO2 bound efficiently to p96 and

to p96-ΔC but not to p67, suggesting that FCHO2 binding requires the p96 central region but not the C-terminus. Mutating all five NPFs to NPV (NPF*) also did not affect binding. However, FCHO2 binding to Dab2 was disrupted by mutating the AP2-binding DPF sequences (DPF*, Figure 2.2B), but not by mutating the AP2-binding FLDLF sequence (FLDLF*, Figure 2.2B). Consistently, a compound mutant containing the DPF* and FLDLF* mutations also failed to bind FCHO2 (AP2*, Figure 2.2B). Previous studies suggested that the DPF and FLDLF sequences may be functionally redundant for binding AP2 [131, 133]. Indeed, we found that wildtype, DPF* and FLDLF* mutants of p96 bound to a GST-tagged AP2 α -appendage ear domain in vitro (Figure 2.2C). These results suggest that the DPF motifs in Dab2 are required for binding to FCHO2 but not for binding AP2, provided that the FLDLF sequence is intact. Thus the DPF* mutant provides a tool for examining the importance of Dab2-FCHO2 interactions for endocytosis of Dab2-specific cargoes.

To determine which region of FCHO2 interacts with Dab2, deletion constructs of FCHO2 were created. GFP was fused to the N-terminus of the F-BAR domain (construct “A”), F-BAR and central region (“B”), central region alone (“C”), central and μ HD (“D”), and μ HD (“E”). Immunofluorescence showed that the μ HD was necessary and sufficient for punctate localization and colocalization with AP2 in clathrin coated pits (Figure 2.4). The μ HD was also necessary and sufficient for co-immunoprecipitation with T7-p96 (Figure 2.2D). While these experiments were underway, Dab2 was detected in a screen for FCHO2 μ HD binding proteins, confirming that Dab2 binds to the μ HD [62]. Together, these data suggest that the μ HD of FCHO2 is responsible for FCHO2 localization to clathrin-coated pits and its interaction with the DPF motifs of Dab2.

A single DPF motif is thought to be sufficient to bind to AP2 [203]. To determine whether this is also the case for FCHO2, we mutated each of the DPF motifs in Dab2 individually, as well as the two amino acids between them. None of the mutations we tested affected FCHO2 binding to Dab2 (Figure 2.2E). Mutation of both DPF motifs (AP2*) was necessary to block FCHO2 binding. This indicates that, like AP2, the motif that interacts with the FCHO2 μ HD is a single DPF. To investigate whether the Dab2-FCHO2 interaction is direct, we produced T7-tagged FCHO2 μ HD and the GST-tagged wildtype and AP2* central regions of Dab2 in bacteria and tested for binding in vitro. The FCHO2 μ HD interacted with the central region of Dab2, and mutation of the AP2-binding sequences decreased binding (Figure 2.2F), indicating a direct interaction (Figure 2.2G).

FCHO2 and the other known μ HD-containing proteins SGIP α , Syp1p, and FCHO1 also bind to the endocytic scaffolding and EH domain-containing protein Eps15 [62, 199, 200, 206]. Because Dab2 is also able to interact with Eps15 and the additional EH domain protein intersectin (ITSN, [207]), Dab2 could potentially also interact with FCHO2 indirectly using Eps15 or ITSN as an intermediate. To determine whether this might be an alternative mechanism for Dab2-FCHO2 interaction, we repeated the Dab2-FCHO2 co-immunoprecipitation in cells that had been transfected with siRNA to four endocytic EH domain proteins: Eps15, Eps15R, ITSN1, and ITSN2. There was no change in the amount of FCHO2 which co-immunoprecipitated with Dab2 from cells depleted of EH-domain proteins (Figure 2.5). Eps15 and ITSN are therefore not required for the FCHO2-Dab2 interaction.

The Dab2-FCHO2 binding site is required for normal levels of LDLR endocytosis when AP2 is depleted

We made use of the DPF* Dab2 mutant to test whether the interaction of Dab2 with FCHO2 is required for Dab2-dependent LDLR endocytosis. We used siRNA to Dab2 and AP2 to block both the Dab2 and ARH-AP2 routes for LDLR endocytosis and assayed rescue by wildtype and mutant Dab2 (Figure 2.6A). These experiments were done in HeLa cells stably expressing an HA-tagged miniLDLR [142, 208]. Anti-HA antibodies were added to the cells at 37°C and uptake was allowed for 2 min. As expected, depletion of Dab2 and AP2 inhibited LDLR endocytosis, which was rescued by wildtype T7-p96 but not by T7-p67 (Figure 2.6B and C). T7-Dab2-DPF* only weakly rescued endocytosis, suggesting that the Dab2-FCHO2 interaction is needed when AP2 levels are low (Figure 2.6A).

We also tested whether the interaction of Dab2 with FCHO2 is required when AP2 is present. We depleted cells of Dab2 and ARH to inactivate both the Dab2 and ARH-AP2 pathways but leave AP2 at normal level (Figure 2.6D, E, [142, 143]). Under these conditions, T7-p96 rescued LDLR endocytosis, but T7-p67 did not, as expected [142]. With AP2 present, T7-Dab2-DPF* also rescued LDLR endocytosis (Figure 2.6D, E). This indicates that AP2 is able to compensate for loss of the interaction between Dab2 and FCHO2. Taken together, these results suggest that the Dab2-FCHO2 interaction is not required for LDLR clustering in CCPs but is required for endocytosis of Dab2-specific cargo when AP2 is absent.

FCHO2 depletion affects the organization of CCP components and inhibits CME

As an alternative approach to understanding the role of FCHO2 in endocytosis, we depleted FCHO2 from HeLa cells using FCHO2 siRNA. Although we were unable to detect endogenous FCHO2 protein using available antibodies, RT-PCR showed that FCHO2 mRNA levels were considerably reduced upon siRNA treatment (Figure 2.7A). FCHO2 siRNA also inhibited expression of transfected GFP-FCHO2 (Figure 2.7A). FCHO2 siRNA induced a striking change in the number and size of clathrin-coated structures (CCSs), particularly on the adherent surface of the cell. There was a noticeable increase in the size of large structures that contained Dab2, AP2, and clathrin light chain-GFP (LcGFP) (Figure 2.7B). These structures appeared similar to the previously described large, flat clathrin arrays, called "clathrin plaques," found on the adherent surface of many cell types [67, 209, 210]. Clathrin plaques are endocytically active [51, 66], although the mechanism is not thoroughly understood [1].

We quantified the numbers and sizes of Dab2-positive CCSs, defining plaques as structures with a diameter greater than 220 nm and pits as structures smaller than 220 nm [1, 211]. Depleting cells of FCHO2 reduced the number of pits and plaques by one-third but significantly increased plaque size (Table 2.1). Although the increase in median plaque size was modest, the distribution of plaque size showed a dramatic increase in the number of plaques greater than $300 \mu\text{m}^2$ (Figure 2.7C). Similar results were obtained using AP2 as a marker for CCSs (data not shown). This suggests that FCHO2 is important for the structural organization of CCS components.

To determine whether FCHO2 depletion affected endocytosis of Dab2 cargo, we measured uptake of HA-miniLDL receptor. Control and FCHO2- or clathrin heavy chain (CHC)-depleted cells were incubated at 37°C for 2 min with HA antibody. Depletion of FCHO2 and CHC inhibited LDLR internalization by 50% and 75%, respectively (Figure 2.7D). The total amount of receptor was not changed by FCHO2 depletion (Figure 2.8). This indicates that FCHO2 is needed for efficient internalization of LDLR, a Dab2 cargo.

To determine whether FCHO2 is also required for Dab2-independent cargo, we measured internalization of TfnR. Depletion of FCHO2 and CHC inhibited TfnR internalization by 60% and 90%, respectively (Figure 2.7E, [200]). Although only a small amount of FCHO1 RNA was detected by RT-PCR (34 cycles against 24 cycles for FCHO2), it was possible that residual internalization of TfnR or LDLR involved FCHO1 (Figure 2.9A). However, cells depleted of FCHO1 and 2 still contained enlarged plaques, and depletion of FCHO1 along with FCHO2 did not additionally inhibit internalization of TfnR or LDLR (Figure 2.9B-D). Together, these data suggest that FCHO2 is involved in the internalization of cargo by Dab2 and other adaptor proteins.

One reason for decreased endocytosis may be reduced receptor clustering in clathrin structures. Indeed, staining of cell surfaces revealed that both LDLR and TfnR were increased on the surface of FCHO2-depleted cells, and were more diffuse and not clustered in pits or plaques (Figure 2.7F and G). There were significant decreases in the percent of surface receptor that colocalized with Dab2 in CCSs when FCHO2 was depleted (Figure 2.7H). Together, these data suggest that FCHO2 plays an important, though not essential, role in CME and may be

involved in both organizing CCSs and recruiting receptor to them.

Endocytic activity of enlarged clathrin-coated structures

Clathrin plaques are reportedly active in endocytosis, either by budding off normal sized CCVs or by bulk internalization of the entire plaque at once, utilizing the same protein components as canonical CCPs [1, 50, 51, 66]. Because FCHO2 depletion increased the size of clathrin structures and prevented receptor entry into them, we suspected this correlated with a defect in the early, receptor recruitment steps of endocytosis. However, we wondered whether FCHO2-deficient plaques could internalize. It is well established that cargo recruitment continues at 4°C even though budding is inhibited [212, 213]. Therefore, we reasoned that incubation at 4°C might provide time for cargo recruitment to FCHO2-deficient CCSs, allowing us to measure internalization after warming to 37°C. Indeed, pre-incubation at 4°C for 1 hr allowed surface LDLR to move from its diffuse localization at 37°C (Figure 2.7F) and become more concentrated in CCPs and plaques (Figure 2.10A). This movement was apparent in both control and FCHO2-depleted cells (Figure 2.7H and Figure 2.10E). Thus pre-incubation at 4°C allows LDLR to accumulate in enlarged clathrin structures in FCHO2-depleted cells and suggests a defect in receptor trapping by enlarged plaques.

We then warmed 4°C pre-incubated cells to 37°C and measured endocytosis. Under these conditions, depletion of FCHO2, or of both FCHO2 and FCHO1, did not significantly inhibit LDLR internalization (Figure 2.10B and Figure 2.11A). Previous results indicated that LDLR endocytosis after 4°C pre-incubation occurs via either the Dab2 or ARH-AP2 pathway

[142]. Accordingly, endocytosis of pre-clustered receptors from enlarged plaques of FCHO2-deficient cells was not greatly affected by depleting AP2 or Dab2 (Figure 2.12). Therefore, LDLR endocytosis occurs efficiently in FCHO2-depleted cells via the AP2 or Dab2 pathways, provided that LDLRs are given time to accumulate in CCSs before internalization is measured.

If FCHO2-deficient plaques are in fact internalizing LDLR, then the quantity of LDLR located in plaques should decrease after warming to 37°C. Cells were incubated with antibody against HA-miniLDLR at 4°C for 1 hr and then either fixed or warmed for 2 min at 37°C. Surface LDLR was visualized using immunofluorescence. Control cells that had been warmed for 2 min had a 24% decrease in LDLR intensity in CCSs on the adherent surface compared to cells that had not been warmed (Figure 2.10F). FCHO2-depleted cells had a 29% decrease in LDLR intensity in CCSs, including the large plaques, after warming. This decrease in intensity suggests that the receptor clustered into clathrin plaques during the 4°C incubation was, in fact, internalized during the 37°C incubation. Indeed, endocytic vesicles containing LDLR co-localized with large clathrin plaques of FCHO2-depleted cells (Figure 2.10F, blue channel). These results indicate that the large CCSs in FCHO2 are endocytically active.

Surprisingly, different results were obtained with the TfnR. 4°C pre-incubation did not increase the colocalization of TfnR with Dab2-positive CCSs (Figure 2.10C and E), and there was still a significant 50% decrease in the amount of TfnR internalized under these conditions (Figure 2.10D). Again we found no change in the amount of TfnR internalized with additional depletion of FCHO1 compared to FCHO2 siRNA alone (Figure 2.11B). This suggests that FCHO-deficient clathrin structures have a defect in clustering and internalizing TfnRs.

Together, these data indicate that the plaque-like structures formed under conditions of depleted FCHO2 are able to internalize but some receptors are recruited inefficiently.

IV. Discussion

We identified the F-BAR protein FCHO2 as a binding partner for the endocytic adaptor Dab2 and found that the Dab2 DPF motifs directly interact with the FCHO2 μ HD. LDLR endocytosis is known to occur by parallel Dab2-dependent and Dab2-independent, ARH-AP2-dependent pathways. Disruption of the Dab2-FCHO2 interaction decreased the uptake of LDLR in AP2-deficient but not ARH-deficient cells, suggesting that Dab2 needs to bind to FCHO2 when AP2 levels are low. Dab2 may provide an alternative to AP2 for recruiting or stabilizing FCHO2 in clathrin-coated structures. We also found that FCHO2 regulates the size and number of CCSs. Depletion of FCHO2 decreased the number of pits but increased the size of larger CCSs that are probably clathrin plaques. These larger plaques contained less of the Dab2 cargo LDLR and of the Dab2-independent cargo TfnR under physiological conditions, and endocytosis of both cargoes was inhibited. However, LDLR endocytosis was restored when FCHO2-deficient cells were pre-incubated at 4°C to accumulate receptor into plaques, suggesting that enlarged, FCHO2-deficient plaques can internalize.

FCHO2 is a CCS organizing protein

Our results suggest that FCHO2 stimulates the formation of clathrin structures and limits the growth of plaques: when FCHO2 is absent, the number of clathrin structures is reduced by approximately one-third and the size of the larger plaques increases dramatically. Clathrin-

dependent endocytosis of LDLR was also inhibited, but was rescued by simply pre-incubating the FCHO2-deficient cells in the cold before assay, suggesting that FCHO2 is not needed for internalization per se. Our HeLa cells contain very little FCHO1 RNA, and results obtained with cells depleted of both FCHO1 and FCHO2 were very similar to those obtained when FCHO2 alone was depleted. Overall, our results suggest that FCHO1/2 limit the size of plaques and/or enforce the curvature of clathrin lattices. It is perhaps not surprising that proteins that bind curved membranes, like FCHO1/2, would regulate lattice curvature. However, our conclusions contrast with a recent study which reported that depletion of FCHO1/2 completely inhibited the initiation of all clathrin structures [62]. The reason for the different results is not clear. Most experiments in the previous report used BSC1 cells, which are unusual in that they lack clathrin plaques. Our HeLa cells, like many other cell types, have plaques on their ventral, adherent surface [66, 67, 97]. Also, HeLa cells express Dab2, while BSC1 cells only have very low levels of the protein [142, 214]. The differences may also be technical. Our inability to detect either endogenous FCHO1 or 2 with available antibodies means that small amounts of FCHO1/2 may have remained. Thus it is possible that low levels of FCHO1/2 reduce the number of pits and plaques and cause larger plaques, while complete absence of FCHO1/2 may completely inhibit clathrin assembly, as reported [62]. Alternatively, another protein that functionally overlaps with FCHO1/2 may be present in our HeLa cells.

In our hands, the absence of FCHO2 also inhibited the recruitment of receptors into clathrin structures. This inhibition could be a relatively trivial consequence of the altered number and size of plaques. When there are fewer, larger structures, there is more distance between them, so receptors freely diffusing on the membrane may have a longer random walk

before being trapped. The ability of FCHO-deficient plaques to accumulate LDLR after pre-incubation in the cold is consistent with this physical explanation. However, a purely physical explanation may not explain why FCHO2-deficient enlarged structures were unable to accumulate TfnR even after pre-incubation at 4°C (Figure 2.10). FCHO2-depleted cells showed a lower ratio of AP2 to Dab2 in enlarged structures than in control CCSs (Figure 2.7B). This could affect recruitment of TfnR, an AP2 cargo. It also suggests that the plaques that grow when FCHO2 is absent somehow incorporate more Dab2 than AP2. A defect in receptor recruitment may explain the absence of all clathrin structures in the experiments of Henne *et al* [62]. Empty CCPs are thought to abort prematurely [215]. If CCPs in FCHO1/2 cells are unable to recruit cargo, they may abort prematurely.

We found that FCHO2-depleted cells internalized LDLR provided that they were pre-incubated in the cold before warming and measuring internalization. This suggests that the enlarged FCHO2-deficient plaques are endocytically active, although we cannot exclude unanticipated effects of the pre-incubation. Temperature shifts were recently reported to induce artifactual membrane scission [216], although this was clathrin-independent and LDLR endocytosis in FCHO2-depleted cells was clathrin dependent (Figure 2.10). Therefore, although we cannot exclude experimental artifacts, we favor the interpretation that FCHO2-deficient plaques can internalize.

Requirement for the Dab2-FCHO2 complex

Mutation of the DPF motifs of Dab2 inhibited LDLR endocytosis when AP2 but not

ARH was depleted from cells (Figure 2.6). This indicates that the interaction between Dab2 and a DPF-interacting protein is essential for Dab2 function when AP2 levels are low. This DPF-interacting protein is likely FCHO2. While this requirement is only revealed under artificial conditions, its discovery adds to the understanding of the complex interactions occurring within a CCP.

Our finding that full-length wildtype Dab2 was able to rescue LDLR endocytosis at physiological conditions in cells depleted of AP2 and Dab2 (Figure 2.6A-B) was surprising because of reports that AP2 is required for CCP formation [217]. AP2 may not be completely absent from our cells, just reduced low enough to inhibit the alternate ARH-AP2 route for LDLR endocytosis. We think it likely that modest over-expression of Dab2 is able to compensate for low levels of AP2 and permit receptor accumulation and endocytosis. Under these conditions, the FCHO2-interacting DPF motifs are needed, suggesting that Dab2 can substitute for AP2 and recruit or stabilize FCHO2 in clathrin structures.

Since pre-incubation in the cold rescued LDLR endocytosis in FCHO2-depleted cells (Figure 2.10 2.10), we wondered whether pre-incubation might rescue LDLR endocytosis by DPF*-mutant Dab2 in AP2-deficient cells. Surprisingly, it did not (Figure 2.13). How can these results be reconciled? The FCHO2-depleted cells have enlarged plaques, whereas Dab2-DPF* was assayed in cells with normal pits and plaques. Perhaps canonical pits and plaques require a Dab2-FCHO2 complex when AP2 levels are low, but enlarged plaques do not. This could suggest a fundamental difference between normal endocytic structures and those created upon

FCHO2 depletion. Enlarged plaques may be a compensation mechanism upon loss of membrane-bending proteins, to prevent a block of CME.

The DPF as a μ HD-interacting motif

DPF motifs have been shown to bind AP2, but we show here that the DPF motifs of Dab2 also interact with the μ HD of FCHO2 (Figure 2.2). DPF motifs exist in many proteins, including Eps15, auxilin, amphiphysin, AP180, synaptojanin, and HIP1 [55]. This raises the possibility that FCHO2 also binds to these other proteins through DPF sequences. In fact, Eps15, which binds to the FCHO2 μ HD [72], contains the sequence DPFKDDPF, which is highly similar to the DPFRDDPF sequence of Dab2. The abundance of proteins containing DPF motifs suggests that many additional proteins may also interact with FCHO2 through their DPF motifs. The μ HD of FCHO2 is a novel binding domain for DPF motifs, and this presents the possibility of competitive binding of DPF proteins by FCHO2 and AP2, thereby regulating interactions within a coated pit. Additionally, sequential binding of FCHO2 and AP2 to DPF sequences could play a role in the advancement of a CCP from one stage to another, for example from pit initiation to cargo recruitment.

V. Materials and Methods:

Cells

HeLa and BSC1 cells were cultured in DMEM, 10% FBS, 1% Pen-Strep in 37°C/5% CO₂. HeLa cells stably expressing Dab2 shRNA have been previously described [145] and were maintained with the addition of 400 μ g/mL Hygromycin B. HeLa cells expressing HA-tagged

mini-LDL receptor have also been described [142] and were cultured with 2 µg/mL puromycin.

Plasmids and transfection

T7-p96 and -p67 have been described [142], as has the C-terminal truncation mutant [131]. Point mutations in the NPF motifs, DPF, and FLDLF motifs were created using site-directed mutagenesis. NPF was mutated to NPV [218], DPF to DAF, and FLDLF to ALALF. FCHO1 (accession #BC028021) and FCHO2 (accession #BC137070) cDNAs were obtained from Open Biosystems and cloned into the EcoRI sites of the pGL1-superC vector, creating an N-terminal GFP fusion product. GFP-FCHO2 constructs of amino acids 1-280, 281-520, 521-810, 1-520, and 281-810 were created by PCR and also cloned into pGL1-superC. GST-Dab2-206-492 has been described, and mutations in the AP2-binding sites were created in the same manner as for T7-p96-AP2*. Individual DPF mutations were created by site-directed mutagenesis of the GST-Dab2-206-492 construct. Each DPF was changed to DAF and the RD sequence between the two DPFs was changed to AA. For bacterial expression, FCHO2 cDNA was cloned into pET21a(+) (Novagen). GST-AP2 α -ear was a gift from Harvey McMahon (MRC Laboratory of Molecular Biology, Cambridge, UK) [203]. pQCXIP-HBT was from Peter Kaiser (University of California, Irvine, CA) [201]. LCa-GFP was a gift from Mark Von Zastrow (University of California, San Francisco, CA) [219]. shRNA resistant p96 was created using site-directed mutagenesis and the following primers: (1)

CAGGGACAACACAAGCAGAGAATATGGGT

CAACATTTCTTGTCTGGCATA and (2) CAACACAAGCAGAGAATATGGGTAAATATA
TCCTTGTCTGGCATAAAAATCATT and reverse complements and inserted C-terminal to the

HBT tag of pQCXIP-HBT. All DNA transfections were performed with Lipofectamine 2000 (Invitrogen) or GeneIn (GlobalStem) according to the manufacturers' protocols.

Antibodies

The following primary antibodies were used: mouse anti-HA.11 (Covance), rabbit anti-GFP (Invitrogen), mouse anti-TfnR (Abcam), rabbit anti-Dab2 (Santa Cruz), mouse anti-p96 (BD Transduction Laboratories), mouse anti-T7 (Novagen), mouse anti- α -adaptin AP6 (Calbiochem and Abcam), mouse anti-ERK (BD Transduction Laboratories), goat anti-actin (Santa Cruz), goat anti-GST (GE Healthcare), and rabbit anti-Eps15 (Santa Cruz). Appropriate Alexa-tagged secondary antibodies were used for immunofluorescence (Invitrogen) and HRP-tagged antibodies for Western blotting (GE Healthcare).

Mass spectrometry

Retroviral particles were produced by transfecting HEK293T cells with pQCXIP-HBT or pQCXIP-HBT-p96-resistant and an amphotropic packaging vector using calcium phosphate. Virus was harvested and used to infect HeLa cells stably expressing Dab2 shRNA. 48 hr after infection, cells were selected with 2 μ g/mL puromycin and cloned. A clonal line that expressed p96 at high levels was isolated. Before lysing for protein purification, cells were treated with 1 μ M biotin in their cell culture media for 24 hr to increase biotinylation levels.

Three 15-cm dishes of cells were lysed for protein purification in lysis buffer (50 mM Tris-HCl pH 8.0, 100 mM NaF, 30 mM sodium pyrophosphate, 2 mM sodium molybdate, 1%

NP-40, 2 mM sodium orthovanadate, and protease inhibitors (Roche)), sonicated, centrifuged 10 min at 14,000xg, and rotated with nickel beads for 1.5 hr at 4°C. Beads were then washed three times in lysis buffer and once in lysis buffer including 20 mM imidazole. Proteins were eluted in elution buffer (0.3 M NaCl, 0.5 M imidazole, 50 mM NaH₂PO₄, 10 mM EDTA, protease inhibitors, pH 7.9) by rotating beads for 10 min at room temperature in 500 µl elution buffer. The elution was repeated and the eluates were combined. The eluate was then added to streptavidin beads washed in lysis buffer and rotated for 1.5 hr at 4°C. Beads were washed five times in lysis buffer and resuspended in 50 µl Laemmli buffer. After SDS-PAGE on 4-12% gradient gels (Bio-Rad), entire gel lanes were excised.

Individual gel slices in 1.5 mL tubes (Eppendorf) were subjected to consecutive 15 min washes with water, 50% acetonitrile, 100% acetonitrile, 100 mM ammonium bicarbonate, and 50% acetonitrile in 50 mM ammonium bicarbonate. After removing the final wash solution, the gel slices were dried thoroughly by vacuum centrifugation. The gel slices were then cooled on ice and an ice-cold solution of 12.5 ng/µL sequencing grade trypsin (Promega) in 50 mM ammonium bicarbonate was added to the gel slices and incubated on ice for one hour. The trypsin solution was discarded and replaced with 50 mM ammonium bicarbonate and incubated overnight at 37°C. Following digestion, the supernatants were collected and the gel slices were washed with 0.1% formic acid followed by washing with 0.1% formic acid in 50% acetonitrile (30 min each wash). The original digestion supernatant and the washes for a single sample were combined into a single tube and dried by vacuum centrifugation. The digestion products were desalted using Ziptips (Millipore) per the manufacturer's instructions and dried by vacuum centrifugation.

Dried peptide mixtures were resuspended in 5 μ L of 0.1% formic acid and analyzed by LC/ESI MS/MS with a nano2D LC (Eksigent) coupled to LTQ-OrbiTrap mass spectrometer (ThermoElectron) using a “vented” instrument configuration as described [220] and a solvent system consisting of 0.1% formic acid in water (A) and 0.1% formic in 100% acetonitrile (B). In-line de-salting was accomplished using an IntegraFrit trap column (100 μ m \times 25 mm; New Objective) packed with reverse phase Magic C18AQ (5 μ m 200 Å resin; Michrom Bioresources) followed by peptide separations on a PicoFrit column (75 μ m \times 200 mm; New Objective) packed with reverse phase Magic C18AQ (5- μ m 100 Å resin; Michrom Bioresources) directly mounted on the electrospray ion source. A linear gradient was used starting at 2% B and proceeding to 40% B in 40 minutes. The acetonitrile percentage was increased to 90% B and held for 5 minutes, and then it was reduced to 2% B and held for 15 minutes. A flow rate of 400 nL/minute was used for chromatographic separations and the mass spectrometer capillary temperature was set to 200 °C. A spray voltage of 2750 V was applied to the electrospray tip and the LTQ-OrbiTrap instrument was operated in the data-dependent mode, switching automatically between MS survey scans in the OrbiTrap (AGC target value 1,000,000, resolution 60,000, and ion time 150 milliseconds) with MS/MS spectra acquisition in the linear ion trap (AGC target value of 10,000 and ion time 100 milliseconds). The 5 most intense ions from the Fourier-transform (FT) full scan were selected in the linear ion trap for fragmentation by collision-induced dissociation with normalized collision energy of 35%. Selected ions were dynamically excluded for 45 seconds.

The protein database search algorithm X!Tandem [221] was used to identify peptides from the human (v3.59) IPI protein databases. Peptide false discovery rates were measured

using Peptide Prophet [222] and results were stored and analyzed in the Computational Proteomics Analysis System (CPAS) [223]. Peptides were filtered with a minimum Peptide Prophet probability that produced a false discovery rate of approximately 5% and the resulting peptides were grouped into proteins.

Immunoprecipitation

Cells were lysed in lysis buffer (150 mM NaCl, 10 mM HEPES pH 7.4, 2 mM EDTA, 50 mM NaF, 1% Triton-X100, protease inhibitors), rotated at 4°C for 30 min, and centrifuged for 10 min at 14,000xg. Protein concentrations were measured and equal amounts of protein were used for immunoprecipitation. Lysate was rotated with primary antibody for 3 hr at 4°C. Protein A+G beads (Amersham) washed in lysis buffer were added to the lysate/antibody mixture and rotated for 1 hr at 4°C. Beads were then washed in lysis buffer three times and resuspended in 5x Laemmli buffer before SDS-PAGE.

Protein purification and binding assays

GST-tagged proteins were induced in BL-21 with 0.1 mM IPTG for 3-4 hr at 30°C with shaking. Cells were collected by centrifugation and resuspended in resuspension buffer (0.5% NP-40 and 1 mM DTT in PBS with protease inhibitors). Lysozyme was added to a concentration of 0.5 mg/mL and cells were lysed 15 min on ice. The lysates were then sonicated and centrifuged at 4,000xg for 20 min. Glutathione sepharose-4B beads (GE Healthcare) were washed twice in resuspension buffer and added to the lysates. After rotation at 4°C for 1.5 hr, beads were washed twice in resuspension buffer with 350 mM NaCl and three times in

resuspension buffer. Beads were aliquoted and snap frozen in resuspension buffer with the addition of 5% glycerol.

His-tagged FCHO2- μ HD was purified similarly [224], with the following changes. Protein expression was induced at 22°C for 3 hr and the bacterial pellet was resuspended in resuspension buffer with the addition of 20 mM imidazole pH 8.0. After incubation of the lysate with Ni²⁺ beads, beads were washed twice in resuspension buffer with 350 mM NaCl and 15 mM imidazole, and then washed three times in resuspension buffer with 15 mM imidazole. Beads were then loaded into an empty Bio-Rad poly-prep column and eluted with increasing concentrations of imidazole ranging from 50 - 200 mM. The majority of T7-FCHO2- μ HD-His was eluted with 100 mM imidazole and protein from this fraction was used for binding experiments.

For Dab2-FCHO2 binding experiments, 150 ng of T7- μ HD-His was mixed with the same amount of glutathione sepharose-bound GST-Dab2 and the volume was increased to 500 μ L with Buffer A (50 mM Tris pH 8.0, 150 mM NaCl, 1 mM EDTA, 0.5% Triton X-100, and protease inhibitors). After 1.5 hr rotating at 4°C, beads were pelleted, washed twice in Buffer A with 500 mM NaCl, washed three times in Buffer A, and resuspended in 120 μ L 5X Laemmli sample buffer. 2 μ L of this volume were used for SDS-PAGE and Western blotting.

For GST- α -ear:Dab2 binding, T7-tagged Dab2 constructs were transiently transfected into HeLa cells which were lysed in 150 mM NaCl, 20 mM HEPES pH 7.2, 5 mM DTT, 0.1%

Triton X-100 and protease inhibitors. Lysates were harvested, cleared by centrifugation, and incubated as above with glutathione sepharose-bound GST- α -ear. Beads were washed twice in Buffer A (50 mM Tris pH 8.0, 150 mM NaCl, 1 mM EDTA, 0.5% Triton X-100, and protease inhibitors) with 500 mM total NaCl, three times in Buffer A, and resuspended as above.

siRNA

Pools of siRNA (siGENOME SMARTpools) against human AP2 μ 2, Dab2, FCHO1, FCHO2, Eps15, Eps15R, ITSN1, and CHC were from Dharmacon/Fisher Scientific. ITSN2 siRNA was from Santa Cruz Biotechnology. For rescue experiments, a single Dab2 siRNA (Dharmacon/Fisher Scientific) that targets human but not mouse Dab2 (AAAGGGTGAAGGCUGGUUCUU) was used so that rescues could be performed using mouse Dab2 sequences. 50 pmol siRNA was transfected into cells using Oligofectamine (Invitrogen) according to the manufacturer's protocol. Cells plated on 2 μ g/mL collagen IV (Sigma-Aldrich) were transfected with siRNA on day 1, transfected again on day 3, and assayed on day 5. For Dab2 rescue experiments and immunoprecipitation from cells treated with siRNA, DNA was transfected on day 4 using Lipofectamine 2000 (Invitrogen). To assay siRNA depletion of GFP-tagged FCHO constructs, cells were transfected with siRNA pools on day 1, transfected with DNA on day 2 using GeneIn (GlobalStem), transfected again with siRNA on day 3, and harvested on day 4.

Endocytosis

Endocytosis assays were performed essentially as described [142], with some

modifications. For assays at 37°C, cells were removed from the 37°C incubator, washed quickly with PBS, and antibody was added in 37°C assay media (DMEM/F12, 0.1% BSA, 10 mM HEPES pH 7.4). The cells were immediately placed into a 37°C waterbath for 2 min. Cells were then moved directly to 4°C, washed with cold PBS, acid stripped (0.5 M NaCl, 0.2 M acetic acid) for 10 min, and fixed in cold 4% paraformaldehyde for 20 min.

For assays including a 4°C pre-incubation, cells were removed from 37°C to 4°C, washed in cold PBS, incubated with primary antibody in assay media for 1 hr, and washed again in cold PBS. Pre-warmed assay media was then added and the cells were moved to a 37°C waterbath for 2 min. Cells were then moved back to 4°C and acid stripped and fixed as above.

Immunofluorescence

Cells grown on collagen IV-coated glass coverslips were fixed in 4% paraformaldehyde for 20 min at room temperature and washed three times in PBS. They were then permeabilized for 10 min in 0.1% Triton-X100 in PBS. Cells were washed in PBS and blocked for 1 hr in 5% normal goat serum/2% BSA in PBS before primary antibody was added in blocking solution. After a 2 hr incubation in primary antibody at room temperature, cells were washed, incubated for 1 hr in Alexa-fluor conjugated secondary antibody (Invitrogen) at room temperature and DAPI for 10 min. After several washes in PBS, coverslips were mounted on slides with Prolong Gold with Anti-fade (Invitrogen).

Cells to be incubated at 4°C were removed from the tissue culture incubator to 4°C, washed in cold PBS, and incubated at 4°C for 1 hr in endocytosis assay media. They were then washed in cold PBS and fixed for 20 min in cold 4% paraformaldehyde. For surface receptor staining, cells were blocked and incubated with appropriate primary and secondary antibodies for surface receptor before permeabilization. If necessary, remaining surface antibody was blocked with goat secondary antibody.

Microscopy and image quantification

Cells were imaged using an Olympus Deltavision IX70 deconvolution microscope or a Deltavision IX71 deconvolution microscope. All images were taken using a 60x NA 1.42 oil objective with a z-slice size of 0.2 μm . Images were acquired and deconvolved using SoftWorx (Applied Precision), and all exposure times and image scaling were equal within an experiment. All quantification was done with ImageJ (NIH).

RT-PCR

RNA was harvested from cells using an RNeasy kit (Qiagen) according to the manufacturer's directions. cDNA was created using random primers (Invitrogen) and Superscript II reverse transcriptase (Invitrogen) according to the manufacturer's instructions. PCR was performed using the primers: (1) GAGCAGATCCCACCAAGTGT and (2) CAAGCTGTGCATTTGGAAGA for FCHO2, and (1) GCGAGAAGATGACCCAGATCATGTT and (2) GCTTCTCCTTAATGTCACGCACGAT for actin. Two sets of primers were used to detect FCHO1 cDNA:

(1) AAGCCATGGAGGAGACACAC and TGACGTTCTCGATGTTCTGC and

(2) ACCATGAAACGCCATTCTTC and TCTTGGACACCTGCTCCTCT.

Table 2.1**FCHO2 depletion decreases the number of CCSs and increases the size of clathrin plaques**

Dab2-positive structures were measured and quantified using ImageJ. Pits were defined as structures with diameters less than 220nm and plaques as structures with diameters larger than 220nm. Shown is mean \pm standard error from 5 fields from at least n experiments. P-values were calculated using Student's t-test.

	Median pit size (μm^2 , n=6)	Median plaque size (μm^2 , n=6)	CCSs per cell (n=5)	CCPs per cell (n=5)	Plaques per cell (n=5)
Control	0.0247 ± 0.0003	0.112 ± 0.019	484 ± 101	159 ± 40	326 ± 34
FCHO2 siRNA	0.0227 ± 0.0020	0.133 ± 0.024	327 ± 48	107 ± 30	220 ± 23
p-value	0.18	0.035	0.036	0.014	0.054

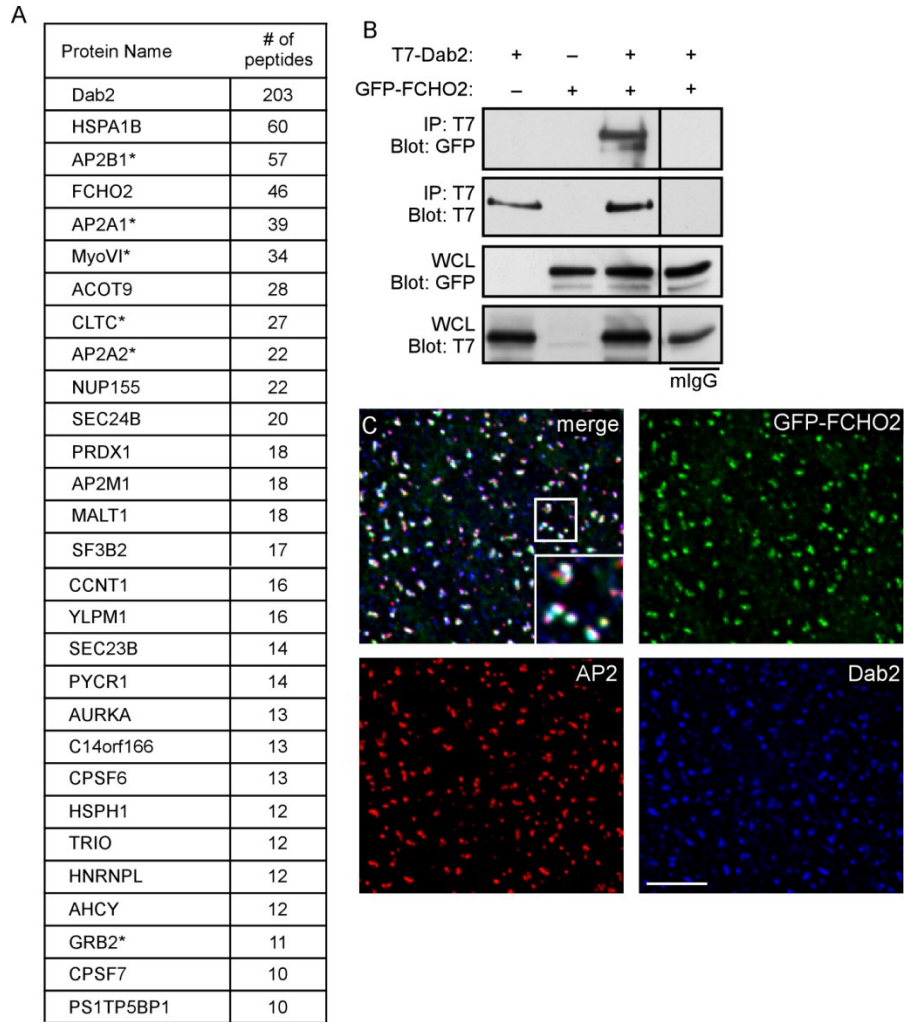


Figure 2.1
Dab2 interacts with FCHO2

(A) Proteins detected by mass spectrometry from HBT-Dab2 purification. The total number of peptides is additive from two experiments. *, previously described interaction with Dab2. (B) Co-immunoprecipitation of GFP-FCHO2 with T7-Dab2 transiently expressed in HeLa cells. HeLa cells were lysed 48 hr after transfection GFP-FCHO2 and T7-Dab2 and subjected to immunoprecipitation with anti-T7. (C) HeLa cells transiently transfected with GFP-FCHO2 were fixed, permeabilized, and stained with antibodies to Dab2 and α -adaptin. White areas in the merge panel are places where all three proteins colocalize. A 0.2 μ m thick section of the adherent surface of the cell is shown. Scale bar is 5 μ m.

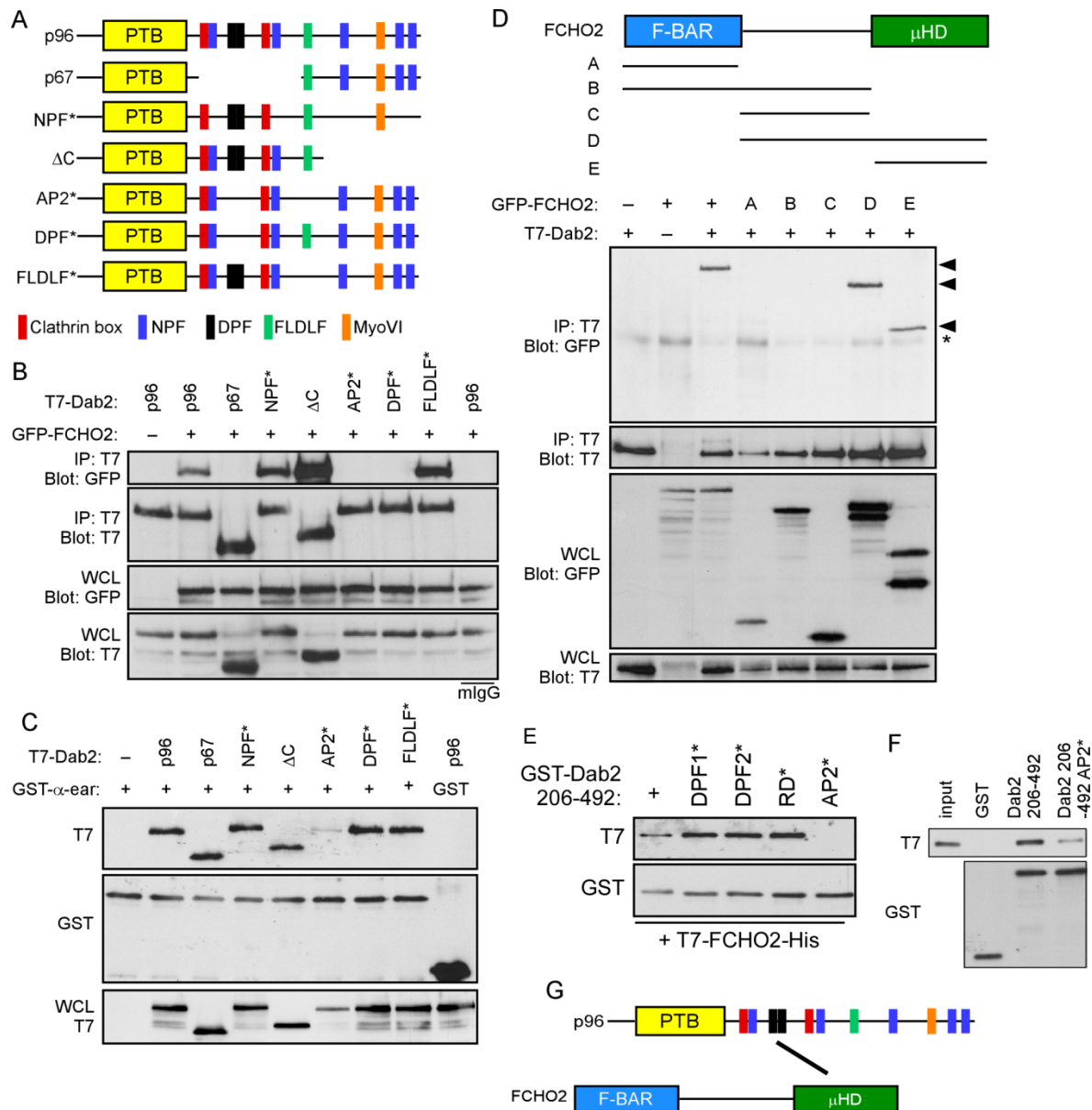


Figure 2.2

The Dab2 DPF motifs interact with the FCHO2 μHD

(A) Schematic of Dab2 structure and mutants. p96: full-length, p67: splice form lacking amino acids 229-447, NPF*: all five NPFs changed to NPV, ΔC: truncation after amino acid 576, AP2*: two DPFs changed to DAF and FLDLF changed to ALALF, DPF*: two DPFs changed to DAF, FLDLF*: FLDLF changed to ALALF. (B) HeLa cells were transiently transfected with full length GFP-FCHO2 and T7-tagged Dab2. Cells were lysed 48 hr after transfection and immunoprecipitated with antibody to T7. (C) Binding of Dab2 mutants to AP2-ear. Cells were transiently transfected with T7-tagged Dab2, lysed, and mixed with purified, glutathione sepharose-bound GST-AP2-ear. (D) (Top) Schematic of FCHO2 structure. FCHO2 contains an N-terminal F-BAR domain (residues 1-280), a central area (residues 281-520), and a C-terminal μHD (residues 521-810). FCHO2 construct A contains amino acids 1-280; B contains 1-520; C, 281-520; D, 281-810; and E, 521-810. (Bottom) HeLa cells were transiently transfected with GFP-FCHO2 and full-length T7-p96. Cells were lysed 48 hr after transfection and immunoprecipitated with antibody to T7. Arrowheads indicate GFP-tagged FCHO2 forms that co-immunoprecipitated with T7-Dab2. *, non-specific band. (E) T7-FCHO2-His was mixed with immobilized GST or mutants of Dab2 206-492. DPF1* is P264A, DPF2* is P299A, RD* is R296A and D297A. (F) Purified, bacterially grown T7-FCHO2 μHD-His was mixed with purified, glutathione sepharose-bound GST Dab2 206-492 and immunoblotted with antibodies against T7 and GST. (G) The Dab2 DPF motifs (black) interact directly with the FCHO2 μHD.

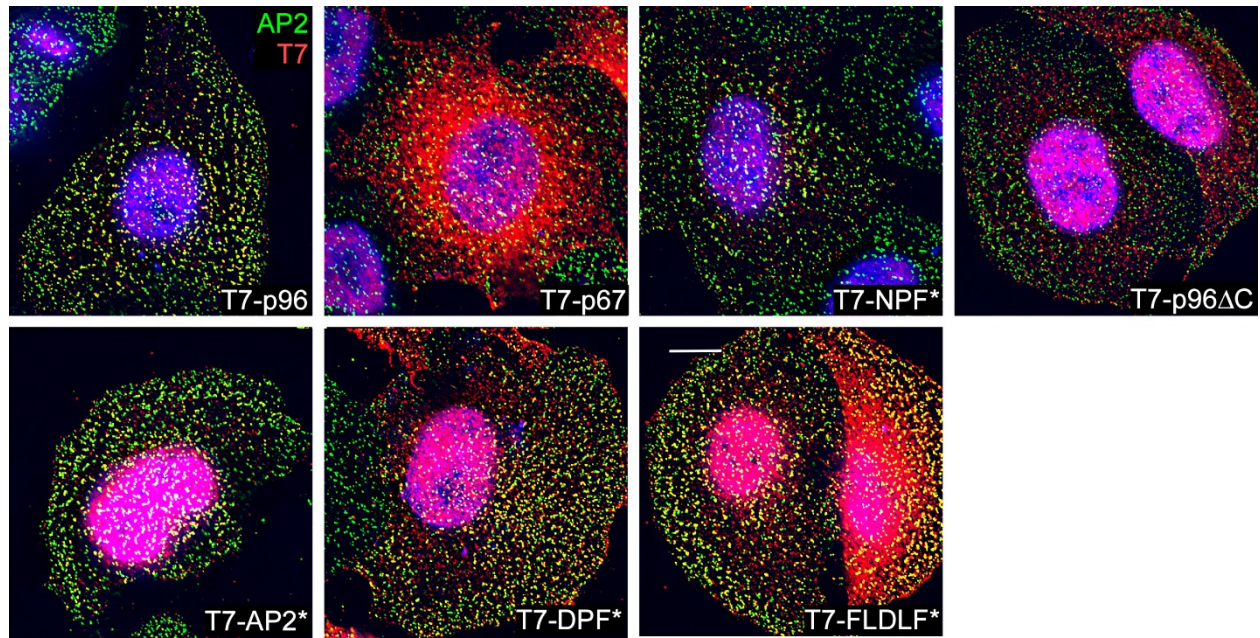


Figure 2.3

Localization of T7-Dab2 mutants

Fixed HeLa cells were permeabilized and stained with antibodies to T7 and α -adaptin. The adherent surface of the cell is shown. Nuclear T7 staining is non-specific background. Scale bar is 10 μ m.

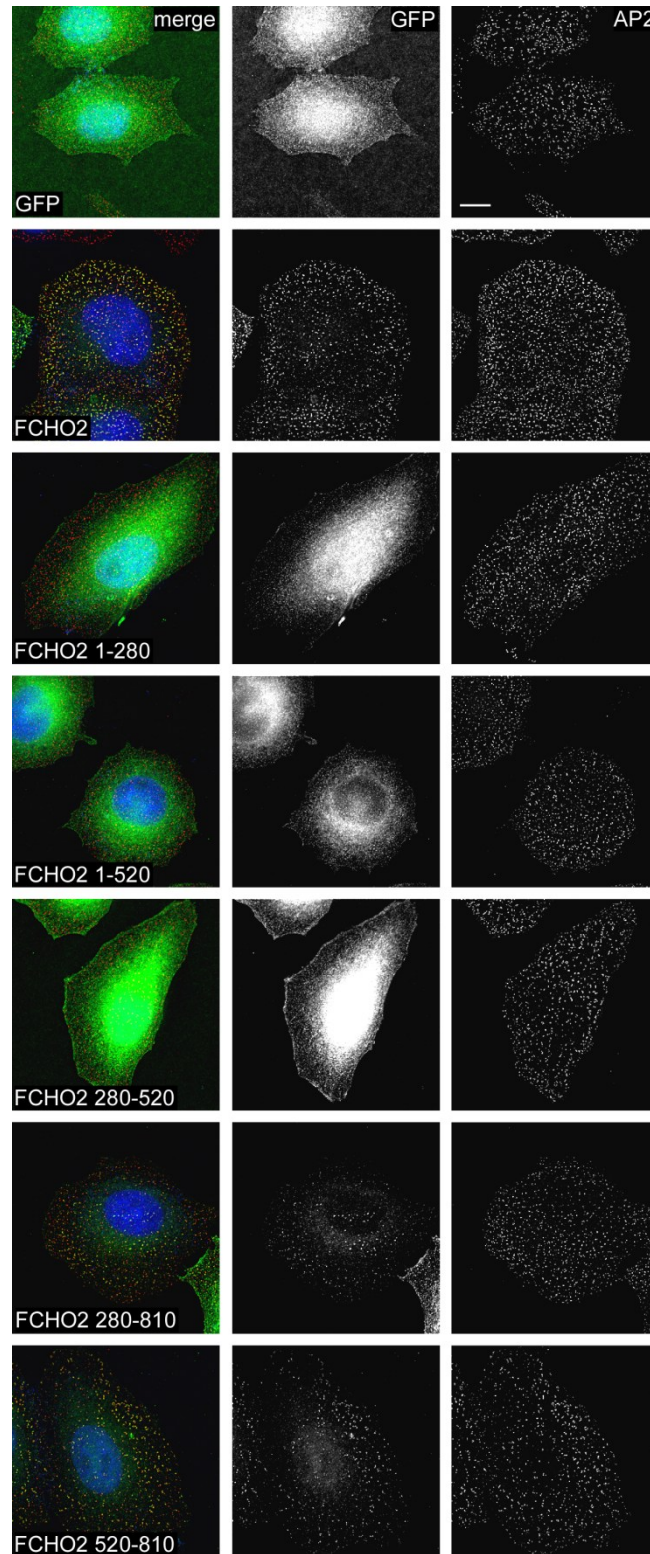


Figure 2.4

The μ HD of FCHO2 is required to direct it to clathrin-coated pits

HeLa cells were transfected with GFP-tagged FCHO2 fragments, permeabilized, and stained for AP2. Shown is the adherent surface of the cell. Scale bar is 10 μ m.

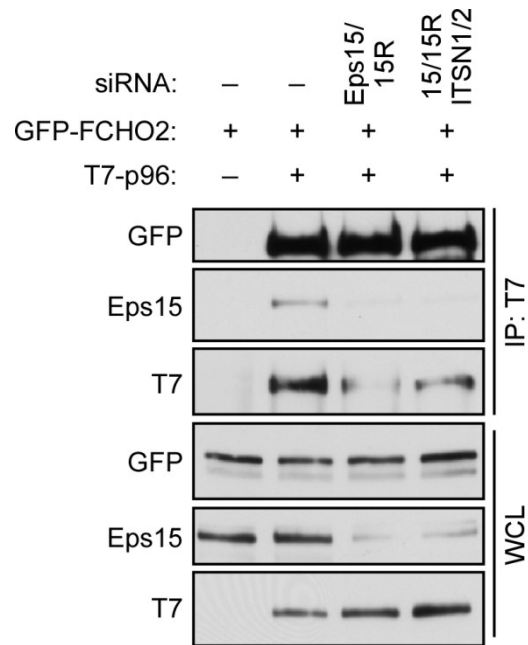


Figure 2.5

Depletion of EH domain proteins does not affect Dab2-FCHO2 binding

HeLa cells were transfected with two rounds of siRNA for Eps15/15R or Eps15/15R+ITSN1/2. Cells were also transiently transfected with DNA for T7-Dab2 and GFP-FCHO2. Cells were lysed and subjected to immunoprecipitation with antibodies to T7.

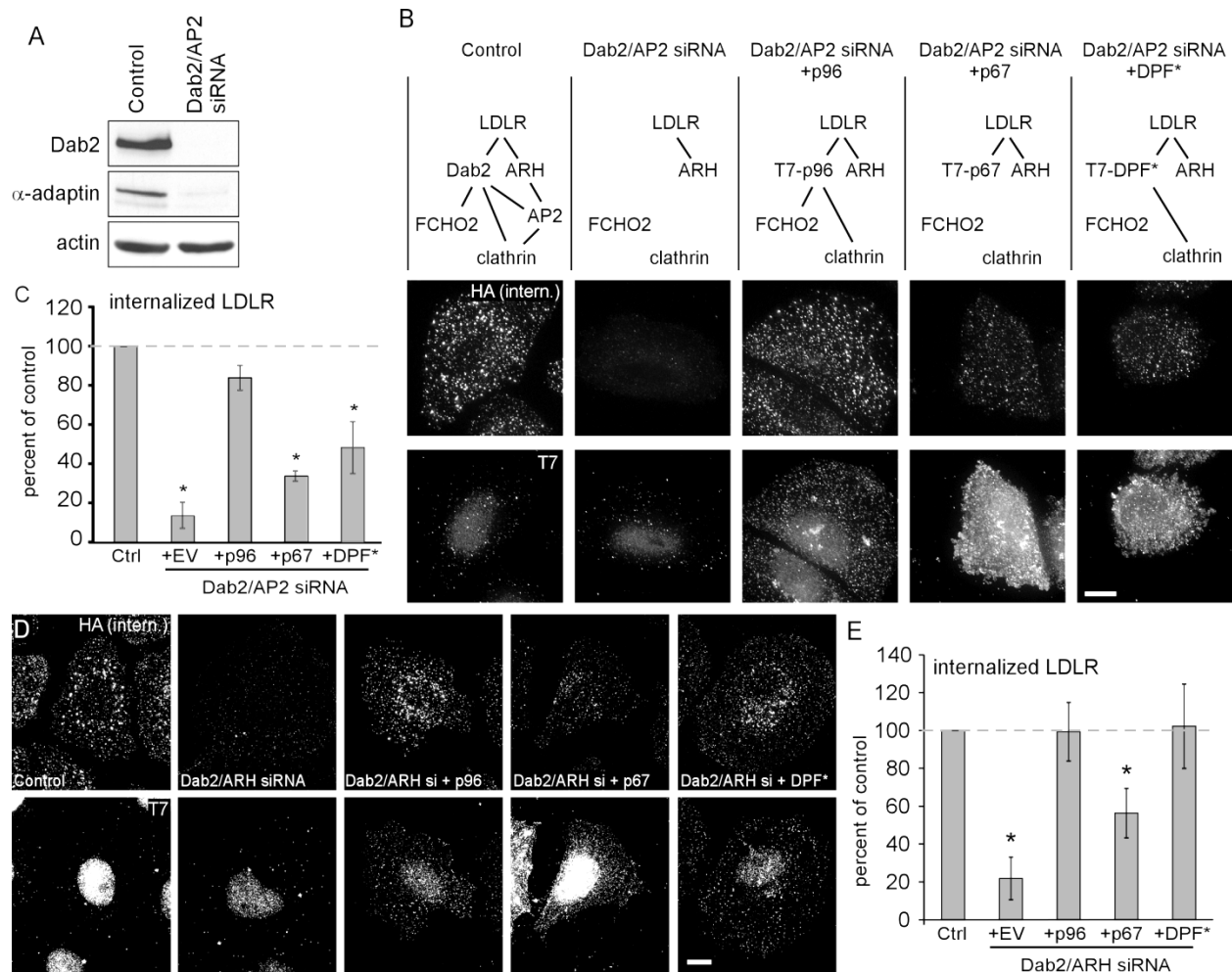


Figure 2.6
Disruption of the Dab2-FCHO2 interaction inhibits Dab2-dependent LDLR endocytosis when AP2 is depleted

(A) Dab2 and AP2 are efficiently depleted from HeLa-miniLDLR cells with siRNA. Cells were transfected with siRNA to Dab2 and AP2 μ 2 on days 1 and 3 and lysed for Western blotting on day 5. (B) Dab2-DPF* does not function for LDLR endocytosis in cells with low AP2 levels. HeLa-miniLDLR cells were transfected with siRNA to Dab2 and AP2 or buffer control. The cells were then transfected with DNA encoding T7-tagged Dab2 p96, p67, or DPF-mutant p96 (DPF*). Antibody to HA-miniLDLR was added for 2 min at 37°C to measure receptor uptake. Fixed and permeabilized cells were stained with anti-T7 and appropriate secondary antibodies for anti-T7 (bottom row) and internalized anti-HA (top row). Only cells which were transfected with T7-Dab2 contain specific T7 staining; nuclear staining is background. Images are z-stack projections and scale bar is 10 μ m. (C) Means and standard errors of fluorescence intensity of at least five cells from three separate experiments are shown. *, $P < 0.05$ by Student's t-test compared to control cells. Dashed line indicates control level, EV: empty vector. (D) Dab2-DPF* functions normally for LDLR endocytosis in cells with normal AP2. HeLa-miniLDLR cells were transfected with siRNA to Dab2 and ARH or buffer control. The cells were then transfected with DNA encoding T7-tagged Dab2 p96, p67, or DPF-mutant (DPF*). Antibody to HA-miniLDLR was added for 2 min at 37°C to measure receptor uptake. Fixed and permeabilized cells were stained with anti-T7 and appropriate secondary antibodies for anti-T7 (bottom row) and internalized anti-HA (top row). Images are z-stack projections and scale bar is 10 μ m. (E) Means and standard errors of fluorescence intensity of at least five cells from three separate experiments are shown. *, $P < 0.05$ by Student's t-test compared to control cells. Dashed line indicates control level, EV: empty vector.

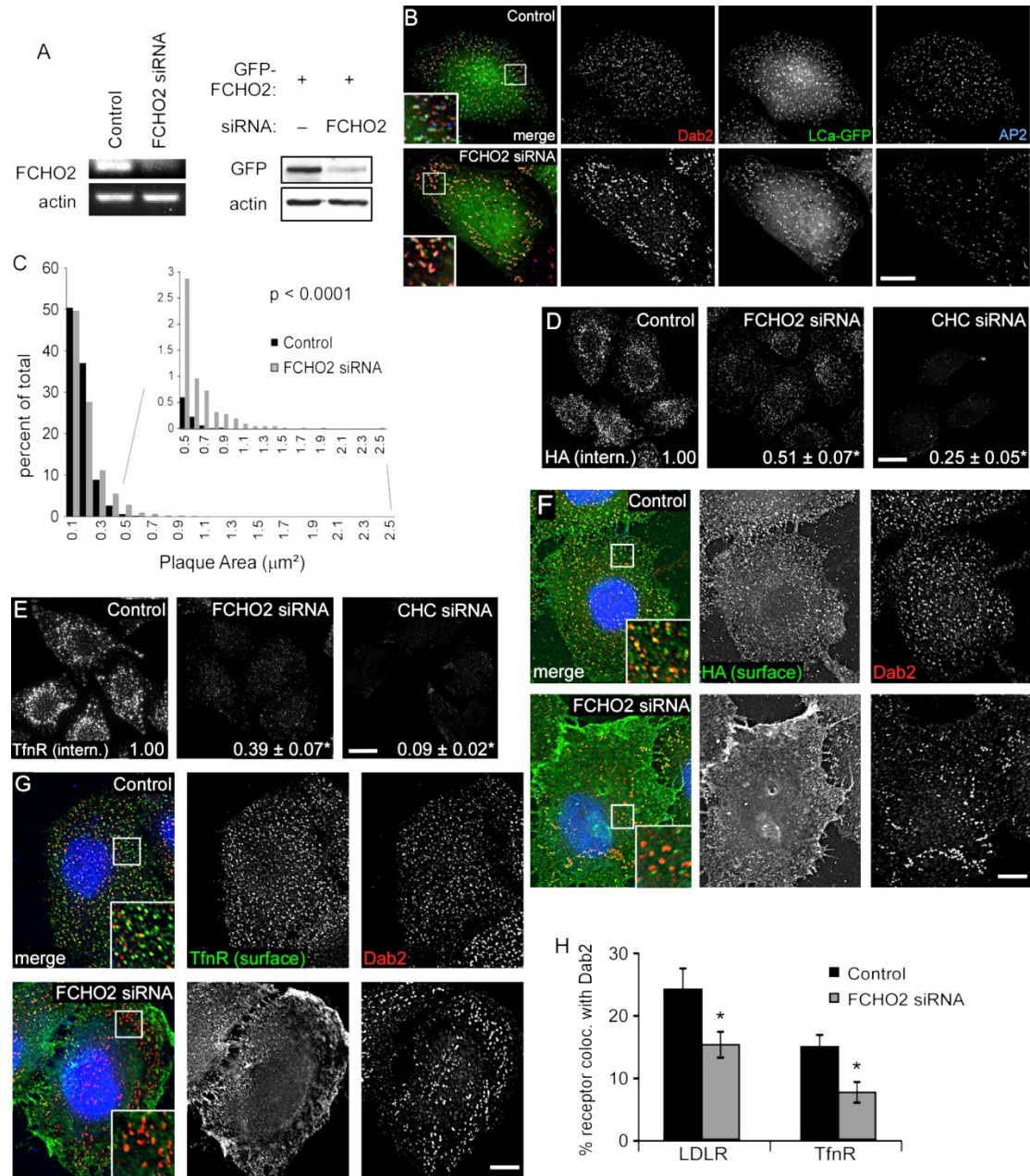


Figure 2.7

FCHO2 depletion affects the organization of CCP components and inhibits CME

(A, Left) HeLa-miniLDLR cells were transiently transfected with siRNA on days 1 and 3 and analyzed for mRNA levels by RT-PCR on day 5. (Right) FCHO2 siRNA depletes GFP-FCHO2 from HeLa cells. Cells were transfected with FCHO2 siRNA on day 1, GFP-FCHO2 DNA on day 2, FCHO2 siRNA again on day 3, and lysed for Western blot on day 4. (B) HeLa cells transiently transfected with FCHO2 siRNA and LCa-GFP were permeabilized and stained with antibodies to Dab2 and AP2. The bottom surface of the cell is shown. Scale bar is 10 μ m. (C) The size of Dab2-positive structures with diameters larger than 220 nm was measured using ImageJ. The data shown is from a representative experiment. P-value was calculated using the Mann-Whitney-U test. (D, E) Cells were given antibody against HA (D) or TfR (E) and allowed to internalize for 2 min at 37°C. Values are mean fluorescent intensity \pm standard error of three experiments. Images are z-stack projections. Scale bars are 20 μ m. *, $P < 0.05$ by Student's t-test compared to control. (F, G) Non-permeabilized cells were stained with antibody to the extracellular domain of HA-miniLDLR (F) and TfR (G), permeabilized, and stained with antibody to Dab2. Images are of the adherent surface of cells. Blue is DAPI staining and scale bars are 10 μ m. (H) Using ImageJ, the percent area of surface receptor which colocalized with Dab2 was measured and mean and standard errors were plotted. *, $P < 0.05$ by Student's t-

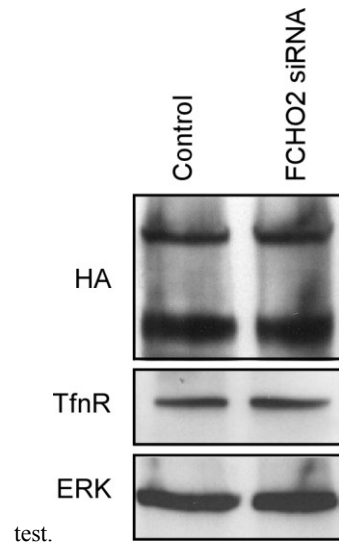


Figure 2.8

FCHO2 depletion does not affect total cellular levels of TfnR or HA-miniLDLR.

HeLa cells transfected with siRNA to FCHO2 were lysed and immunoblotted for either TfnR or HA-miniLDLR. For HA-miniLDLR, the upper band corresponds to the unprocessed, ER form of the protein and the lower is the processed form (Li et al., 2001). ERK was used as a loading control.

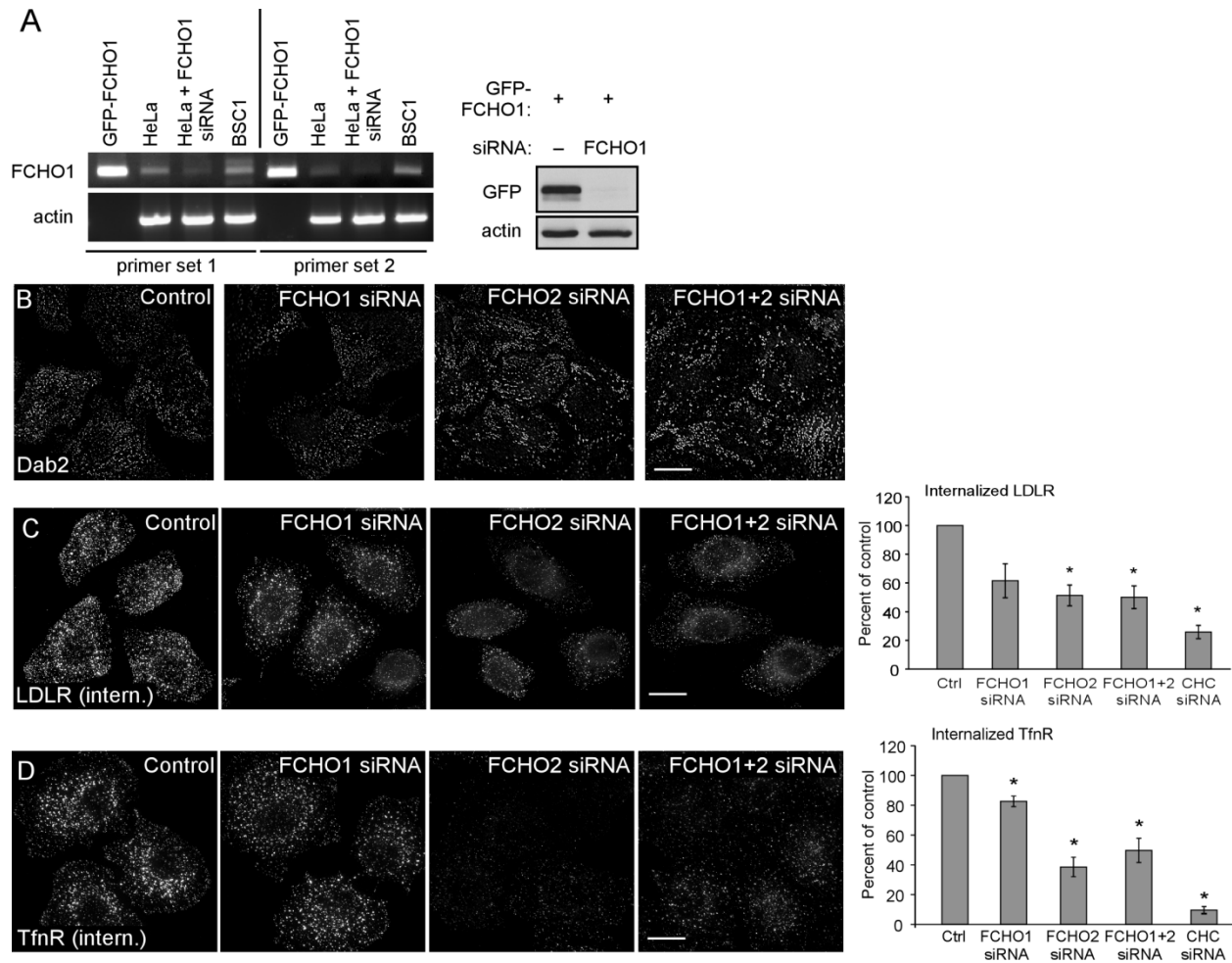


Figure 2.9

Effect of FCHO1+2 siRNA on LDLR and TfnR endocytosis at physiological conditions

(A) (Left) FCHO1 siRNA depletes both FCHO1 mRNA and GFP-FCHO1 protein. HeLa-miniLDLR cells were transfected with FCHO1 siRNA or buffer control on days 1 and 3 and lysed for RNA on day 5. Only low levels of FCHO1 were detected in HeLa cells. BSC1 cells were used as a positive control for FCHO1 expression [62], and GFP-FCHO1 as a positive control for PCR. (Right) HeLa cells were transfected on days 1 and 3 with FCHO1 siRNA or buffer control and GFP-FCHO1 DNA on day 2, lysed, and subjected to Western blotting. (B) CCS size in cells transfected with siRNA for FCHO1, FCHO2, FCHO1+2, or buffer control. Cells were fixed and stained with anti-Dab2 antibody. Images are the adherent surface of a field of cells. Scale bar is 20 μ m. (C, D) Cells were transfected with FCHO1, FCHO2, FCHO1+2, or CHC siRNA or buffer control on days 1 and 3, and endocytosis was measured on day 5. Cells were given antibody against HA (C) or TfnR (D) and allowed to internalize for 2 min at 37°C. Values shown are means \pm standard error for at least three experiments. Images are z-stack projections of the entire cell height. Scale bars are 20 μ m. *, P-value < 0.05 by Student's t-test. In neither case were FCHO2 and FCHO1+2 cells significantly different from one another.

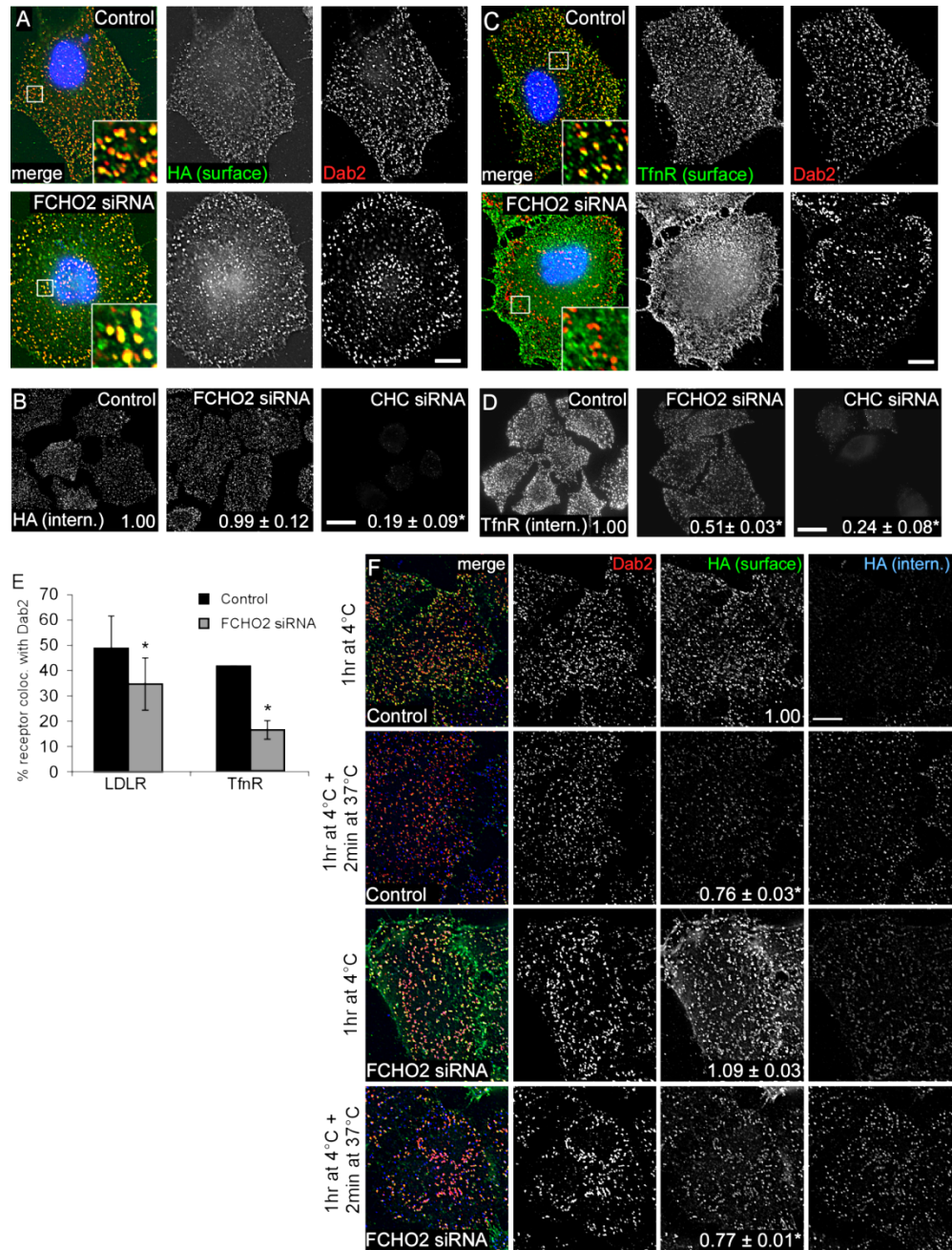


Figure 2.10

Endocytic activity of enlarged clathrin-coated structures

(A) Control or FCHO2 siRNA-treated miniLDLR cells were fixed, stained with antibody to HA (A) or TfnR (C), permeabilized, and then stained with antibody to Dab2. Images are adherent surface of cells and scale bar is 10 μ m. (B, D) miniLDLR cells were incubated with antibody to HA (B) or TfnR (D) for 1 hr at 4°C, washed, warmed to 37°C for 2 min, then cooled, acid stripped, permeabilized, and receptor uptake was visualized using immunofluorescence. Values are mean fluorescent intensity \pm standard error of three experiments. Images are z-stack projections and scale bar is 20 μ m. *, $P < 0.05$ by Student's t-test. (E) Using ImageJ, the percent of surface receptor area which colocalized with Dab2 area was measured and mean and standard errors were plotted. *, $P < 0.05$ by Student's t-test. (F) HeLa miniLDLR cells were given antibody to HA-miniLDLR for 1 hr at 4°C, washed, and either fixed ("1 hr at 4°C") or warmed to 37°C for 2 min and fixed. Non-permeabilized cells were stained with secondary antibody to surface HA-labeled receptor and then permeabilized and stained with anti-Dab2 and secondary antibodies for anti-Dab2 and internalized anti-HA-labeled receptor. Numbers on surface HA panels are mean fluorescent intensity \pm standard error of surface HA which colocalized with Dab2. Scale bar is 10 μ m. *, $P < 0.05$ by Student's t-test, compared to control after 1 hr at 4°C.

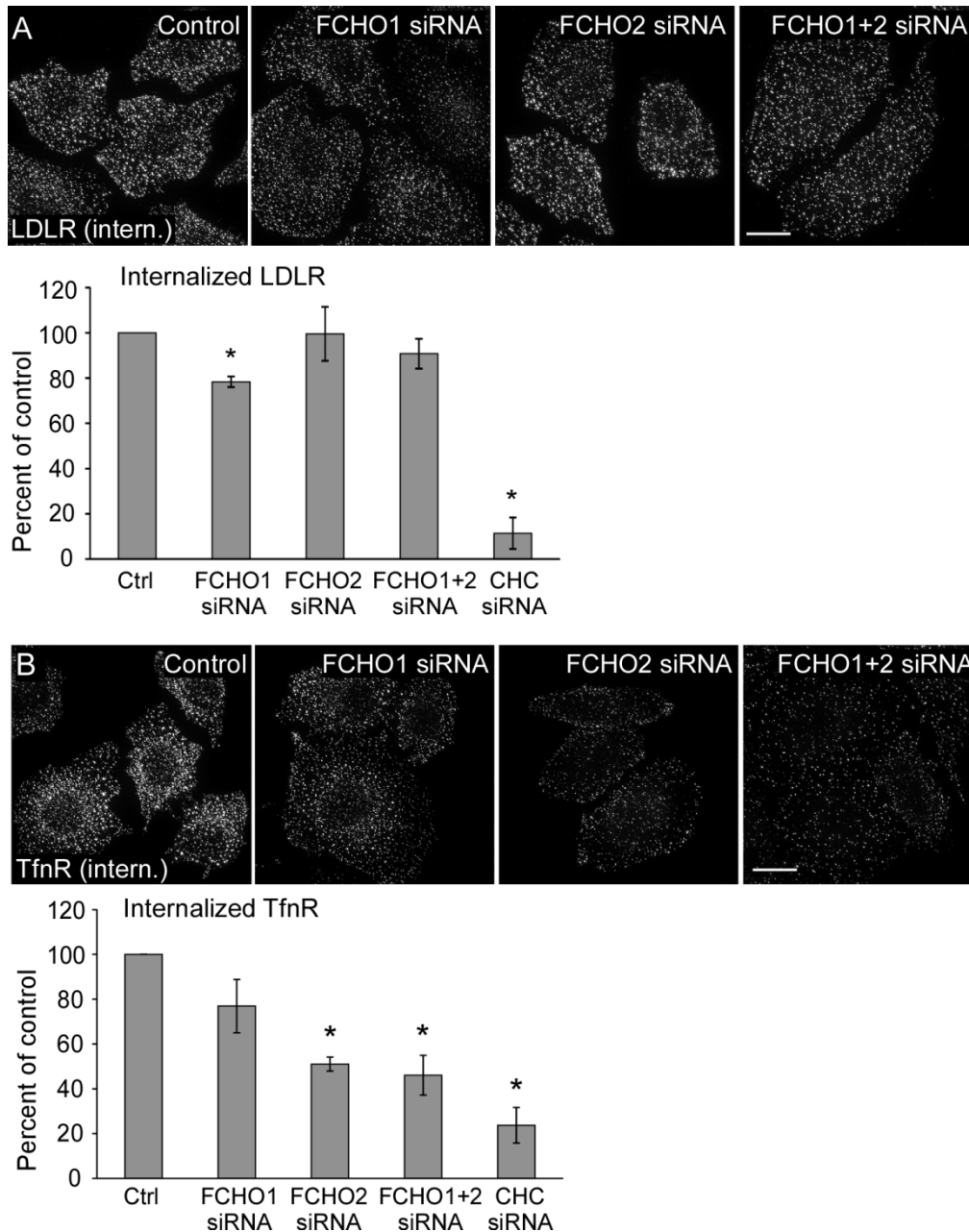


Figure 2.11

Effect of FCHO1+2 siRNA on LDLR and TfnR endocytosis with a 4°C pre-incubation

HeLa-miniLDLR cells were transfected with FCHO1, FCHO2, FCHO1+2, or CHC siRNA or buffer control on days 1 and 3, and endocytosis was measured on day 5. Cells were given antibody against HA (A) or TfnR (B) and incubated for 1 hr at 4°C. Cells were then placed in a 37°C waterbath and allowed to internalize for 2 min. Values shown are means \pm standard error for at least three experiments. Images are z-stack projections. Scale bars are 20 μ m. *, P-value < 0.05 by Student's t-test. In neither case were FCHO2 and FCHO1+2 cells significantly different from one another.

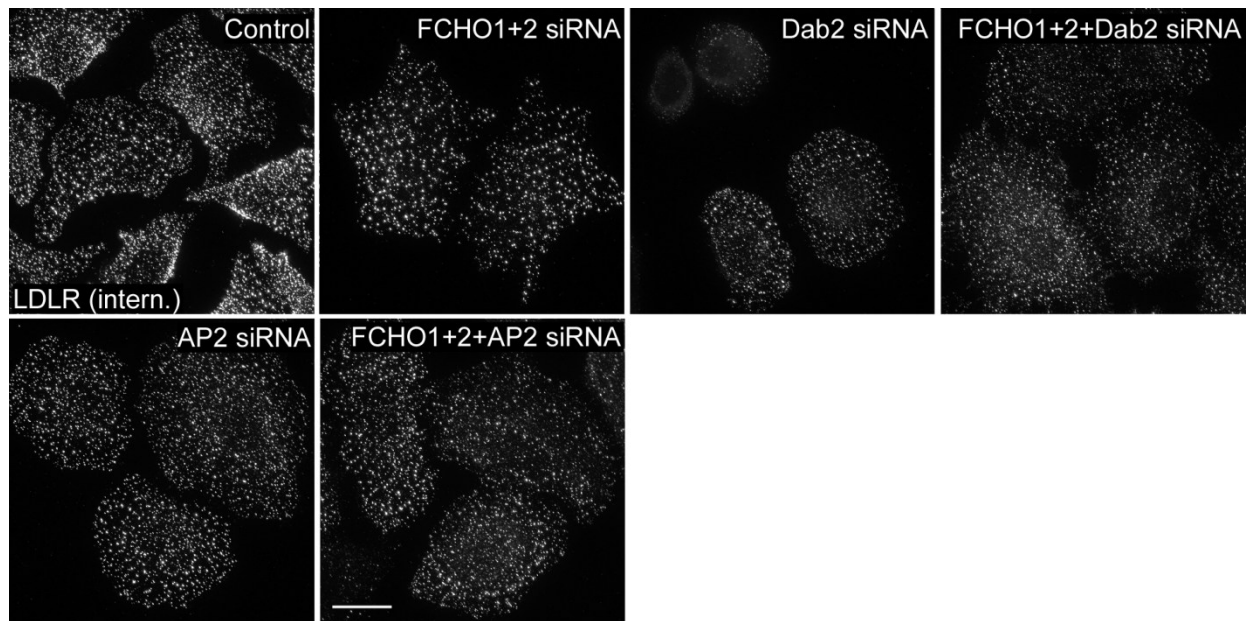


Figure 2.12

Additional depletion of Dab2 or AP2 with FCHO1+2 does not further decrease LDLR endocytosis with a 4°C pre-incubation

HeLa-miniLDLR cells were transfected with combinations of FCHO1, FCHO2, Dab2, and AP2 siRNA or buffer control. Cells were given antibody against HA and incubated for 1 hr at 4°C. Cells were then placed in a 37°C waterbath and allowed to internalize for 2 min. Images are z-stack projections. Scale bar is 20 μ m.

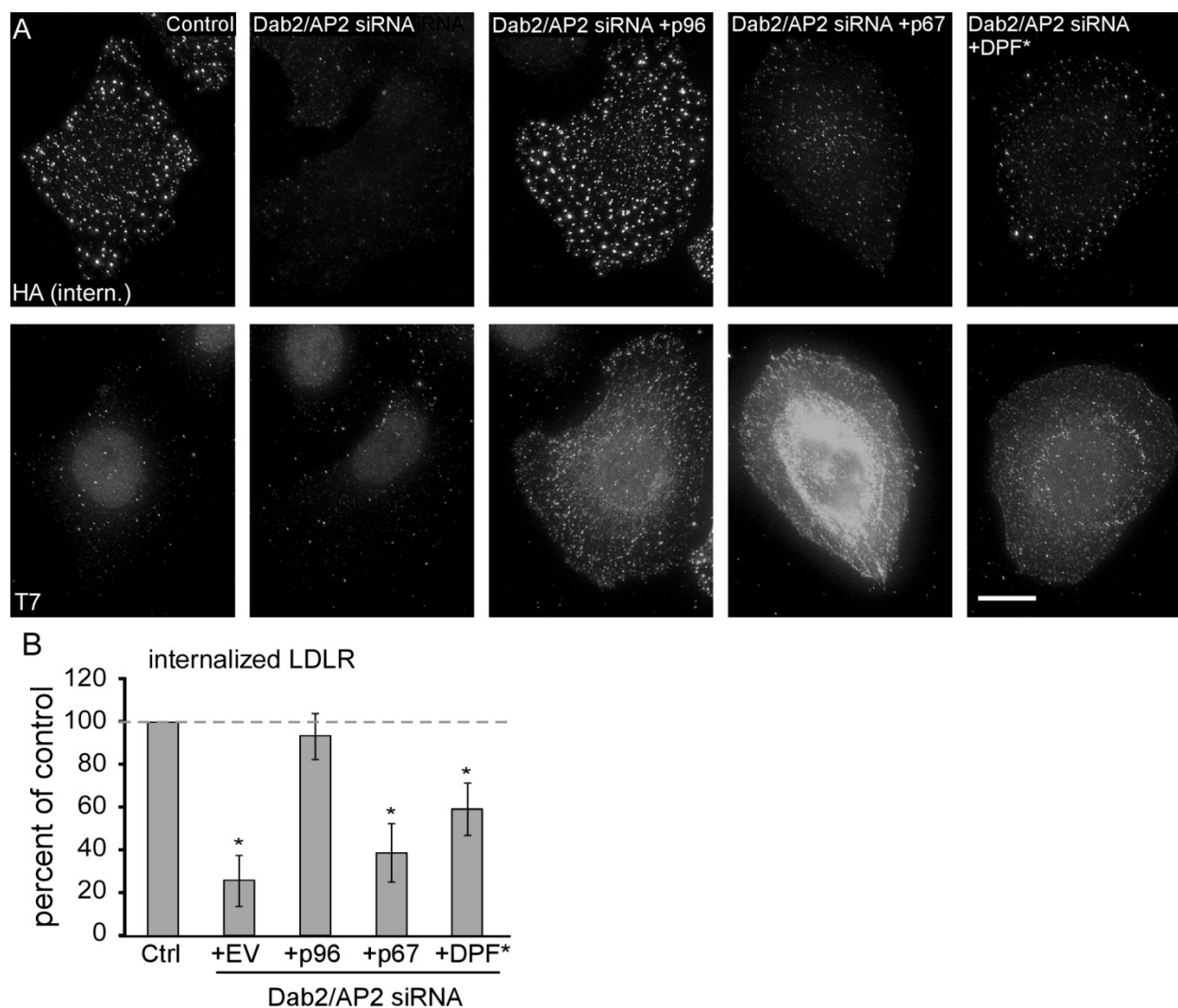


Figure 2.13

Dab2-DPF* is deficient for LDLR endocytosis even when cells are given a 4°C pre-incubation.

(A) HeLa-miniLDLR cells were transfected with siRNA to Dab2 and AP2 and DNA for T7-tagged Dab2 forms. Cells were incubated at 4°C for 1 hr with anti-HA, warmed to 37°C for 2 min, and then stained with antibodies to internalized HA and T7. Images are z-stack projections of the entire cell. Bar, 10µm. (B) Means and standard errors of fluorescence intensity of at least five cells from three separate experiments are shown. *, $P < 0.05$ by Student's t-test compared to control cells. Dashed line indicates control level, EV: empty vector.

Chapter 3 - The clathrin adaptor Dab2 recruits EH domain scaffold proteins to regulate integrin β 1 endocytosis.

Adapted from an article published in *Molecular Biology of the Cell*:

Teckchandani A, Mulkearns EE, Randolph TW, Toida N, Cooper JA. The clathrin adaptor Dab2 recruits EH domain scaffold proteins to regulate integrin β 1 endocytosis. *Mol Biol Cell*. 2012 Aug;23(15):2905-16.

I. Abstract

Endocytic adaptor proteins facilitate cargo recruitment and clathrin-coated pit nucleation. The prototypical clathrin adaptor AP2 mediates cargo recruitment, maturation and scission of the pit by binding cargo, clathrin and accessory proteins, including the EH domain proteins Eps15 and Intersectin. However, clathrin-mediated endocytosis of some cargoes proceeds efficiently in AP2-depleted cells. We found that Dab2, another endocytic adaptor, also binds to Eps15 and Intersectin. Depletion of EH domain proteins altered the number and size of clathrin structures and impaired the endocytosis of the Dab2- and AP2-dependent cargoes, integrin β 1 and transferrin receptor, respectively. To test the importance of Dab2 binding to EH domain proteins for endocytosis, we mutated the EH domain binding sites. This mutant localized to clathrin structures with integrin β 1, AP2 and reduced amounts of Eps15. Interestingly, although integrin β 1 endocytosis was impaired, transferrin receptor internalization was unaffected. Surprisingly, while clathrin structures contain both Dab2 and AP2, integrin β 1 and transferrin localize in separate pits. These data suggest that Dab2-mediated recruitment of EH domain proteins selectively drives the internalization of the Dab2 cargo, integrin β 1. We propose that adaptors may need to be bound to their cargo to regulate EH domain proteins and internalize efficiently.

II. Introduction

Many plasma membrane receptors and essential macromolecules are internalized by clathrin-mediated endocytosis (CME). Receptors associate with endocytic adaptors, which co-assemble with clathrin to form clathrin-coated pits (CCPs). The endocytic adaptors bind to PtdIns(4,5)P₂, clathrin and internalization signals within the cytoplasmic tails of their cargoes, thus linking cargoes to clathrin and the membrane. Subsequent recruitment of an extensive network of proteins regulates invagination of the pit and internalization. The prototypical clathrin adaptor AP2 is a tetrameric complex comprising a core of small (σ 2), medium (μ 2) and large (α and β 2) subunits [3, 225, 226]. The μ 2 subunit recognizes PtdIns(4,5)P₂ and the Yxx Φ sorting signal in the transferrin receptor (TfnR, [47]. The μ 2 subunit binds to the acidic dileucine internalization signal, [DE]XXXL[LI] [227]. The α and β 2 subunits bind to endocytic accessory proteins that regulate assembly and budding of CCPs, including scaffolding proteins Eps15 and ITSN, membrane-bending/curvature-sensing proteins epsin, endophilin and FCHO1/2, the phosphoinositide phosphatase synaptojanin, and dynamin, a GTPase implicated in vesicle fission [53, 54, 62]. Thus, AP2 may be thought of as a hub for protein-protein interactions that sequentially and cooperatively regulate two key processes in endocytosis: first, the recruitment of cargo and clathrin to form CCPs and, second, the invagination and eventual budding of the CCP to form a clathrin-coated vesicle.

Some cargoes utilize alternative, monomeric adaptor proteins known as clathrin-associated sorting proteins (CLASPs) [2]. Dab2 is one such CLASP. It contains a PTB (phosphotyrosine binding) domain that recognizes PtdIns(4,5)P₂ and the FxNPxY internalization motif found in Dab2 cargoes LDLR and β -integrin [131, 133, 142, 143, 145, 228, 229]. Dab2

binds clathrin as well as cargoes, and is thus well-suited to recruit cargoes to CCPs. Furthermore, Dab2 can function in AP2-deficient cells [142, 143, 190, 230], implying that Dab2 may also bind accessory proteins that regulate CCP invagination and budding. Indeed, Dab2 contains binding sites for FCHO2, myosin VI, CIN85 and Grb2 [65, 177, 198, 204]. Dab2 also contains NPF (Asparagine Proline Phenylalanine) motifs that potentially bind Eps homology (EH) domains [139, 231].

CCPs contain the EH domain proteins Eps15, Eps15R and Intersectin1 and 2 (ITSN1 and 2) that are important for endocytosis [60, 72, 232]. These EH domain proteins provide binding sites for numerous other accessory proteins including dynamin, synaptojanin, stonin, synaptotagmin, SHIP2, FCHO2 and epsin [62, 232, 233]. Thus, EH domain proteins could assemble many of the same endocytic accessory proteins as are recruited by AP2.

In this paper we report that Dab2 binds to Eps15 and ITSN. Depleting cells of Eps15, ITSN and their close relatives inhibited endocytosis of both Dab2-dependent and -independent cargoes and affected clathrin assembly, causing an increase in size of large clathrin-coated structures (CCSs), probably plaques. To test the role of Dab2-EH domain protein interactions under conditions where the size distribution of clathrin structures was not affected, we reconstituted Dab2-deficient cells with a mutant Dab2 that cannot bind EH domain proteins. Clathrin structures reconstituted with this mutant recruited integrin β 1 normally, but contained less Eps15 and internalized integrin β 1 inefficiently, suggesting that the Dab2-EH domain interaction is important for Dab2-dependent endocytosis. Surprisingly, transferrin receptor endocytosis was unaffected. Integrin β 1 and TfnR do not colocalize on the cell surface, even

though most clathrin structures contain both Dab2 and AP2. We propose that cargo regulates adaptor-dependent EH domain protein recruitment or activation for efficient internalization.

III. Results

The Dab2 NPF sequences mediate binding to endocytic EH domain proteins.

The major endocytic splice form of Dab2, p96, contains five NPF sequences (Figure 3.1), suggesting that it may interact with the endocytic EH domain-containing proteins, Eps15 and ITSN. We tested for co-immunoprecipitation of T7-tagged Dab2 p96 with HA-tagged ITSN and endogenous Eps15. Dab2 p96 co-immunoprecipitated with both Eps15 and HA-ITSN (Figure 3.1B and C) and localized to clathrin structures that also contained Eps15 and HA-ITSN (Figure 3.2A). Moreover, endogenous Eps15 and Dab2 co-immunoprecipitated (Figure 3.2B). Another splice form of Dab2, p67, does not associate with CCPs (Figure 3.3) [131]. p67 did not bind to Eps15, and only weakly to HA-ITSN (Figure 3.1B,C). To test whether the NPF sequences in Dab2 were required for binding Eps15 and ITSN, we made point mutations in p96. Point mutations in all five NPFs completely blocked Dab2 interaction with both Eps15 and ITSN (Figure 3.1B and C). Mutating the three C-terminal NPFs strongly inhibited Eps15 binding and partially inhibited ITSN binding, whereas mutating the two central NPFs, which are absent from p67, did not inhibit binding of either Eps15 or ITSN (Figure 3.1B,C). These mutant forms of p96 were all localized in CCSs (Figure 3.3Figure 3.3). This suggests that the Dab2 NPF sequences are not required for Dab2 localization to CCSs but are required for binding Eps15 and ITSN. Additionally, the C-terminal NPF sequences play predominant roles in these interactions.

We tested whether Dab2 binds Eps15 directly by use of purified His-tagged fragments of Dab2 and GST-tagged EH domains of Eps15 in vitro (Figure 3.1D). The Eps15 EH domains bound more strongly to a Dab2 fragment containing the 3 C-terminal NPFs than to a central fragment containing the 2 central NPFs (Figure 3.1D), consistent with the co-immunoprecipitation results (Figure 3.1B,C). Previous studies have suggested that some EH domains recognize NPF_X_{COOH} or NPF_{XX}_{COOH} [234, 235]. The fifth NPF of Dab2 lies in the sequence NPF_A_{COOH}. This may contribute to the stronger binding of the C-terminal region of Dab2 to Eps15 because placing an epitope tag after the fifth NPF sequence slightly inhibited binding (Figure 3.1D). Similar results were obtained with EH domains from Eps15R (Figure 3.1D).

Taken together, these results suggest that Eps15 and ITSN bind to Dab2 p96 in cells, probably directly, principally via the C-terminal three NPF sequences. They do not bind significantly to the non-endocytic Dab2 p67 splice form, even though the relevant NPF sequences are present, possibly because p67 is not in coated pits.

EH domain proteins regulate integrin β 1 and TfnR endocytosis.

We tested whether endocytic EH domain proteins are important for Dab2-dependent and -independent endocytosis using siRNA. We first evaluated which endocytic EH domain proteins are expressed in HeLa cells using antibodies and RT-PCR (Figure 3.4). We detected Eps15, Eps15R, ITSN1S and ITSN2 but not the neuronal form, ITSN1L [194]. We found that all four

gene products could be depleted using a mixture of siRNAs (Figure 3.4). We call cells depleted of all four EH domain proteins "EH-depleted" or "EH-deficient" cells.

We measured endocytosis of integrin $\beta 1$, a Dab2-dependent cargo, and TfnR, a Dab2-independent cargo, in EH-deficient cells. Cell surface receptors were labeled at 4°C with antibodies to the extracellular domain of integrin $\beta 1$ or TfnR. Cells were then warmed to 37°C to allow internalization. Surface antibody was removed by a low pH wash and internalized antibody was detected by indirect immunofluorescence. ~ 40% less integrin $\beta 1$ and TfnR was detected inside Eps15+15R- and ITSN1+2-depleted cells (Figure 3.5A-C). Depleting all 4 EH domain proteins showed a further decrease in internalized integrin $\beta 1$ and TfnR levels, although this was not as low as with clathrin depletion (Figure 3.5A-C). To confirm that the decreased content of internalized receptor was due to defective internalization and not accelerated recycling we followed the uptake of integrin $\beta 1$ and TfnR in the presence of Primaquine, an inhibitor of recycling. Control cells internalized both receptors more rapidly than EH-deficient cells (Figure 3.5D-G). Taken together, the results suggest that Eps15/15R and ITSN1/2 play partially overlapping roles in CME of Dab2-dependent and -independent cargoes.

To determine whether EH domain proteins regulate CCS nucleation or assembly, we analyzed clathrin structures in EH-deficient HeLa cells by immunofluorescence using antibodies to clathrin, AP2 and Dab2. We designate CCSs with diameter 100-200 nm as CCPs, and CCSs with diameters >200 nm as plaques [66]. As reported, the ventral surface of HeLa cells has CCPs and plaques while the dorsal surface has only CCPs (Figure 3.6C-D', Table 3.1)[66]. Clathrin, AP2 and Dab2 were still recruited to pits and plaques in EH-depleted cells (Figure

3.6A, B). The number and size of CCPs on the dorsal surface and the size of CCPs on the ventral surface were unchanged (Table 3.1). However, EH-depleted cells had decreased numbers of CCPs and plaques on the ventral surface and the median plaque size significantly increased (Figure 3.6A-D, Table 3.1). The larger plaques were particularly strongly affected (Figure 3.6C', Table 3.1). The overall result of EH domain protein deficiency is that cell surface area occupied by CCPs was decreased while area occupied by large plaques was dramatically increased (Figure 3.6C').

Changes in CCP and plaque number and plaque size could conceivably contribute to decreased endocytosis of integrin $\beta 1$ and TfnR in EH-deficient cells. We tested whether recruitment of receptors to CCPs and plaques was affected in EH-deficient cells by immunofluorescence. Dab2 co-localizes with integrin $\beta 1$ predominantly on the dorsal surface of HeLa cells [145], and this colocalization was not altered when EH domain proteins were depleted (Figure 3.6E). Although Dab2 is not an adaptor for TfnR internalization, TfnR, AP2 and Dab2 are found together in many clathrin structures [143]. The fraction of TfnR co-localizing with Dab2 was also unaffected when EH domain proteins were depleted (Figure 3.6F). Therefore, EH domain proteins are not needed for recruitment of Dab2-dependent or -independent cargoes to CCSs. These results suggest that EH domain proteins regulate CCP/plaque nucleation, growth and internalization, but not the collection of Dab2-dependent or -independent cargoes into CCPs and plaques.

Internalization of Dab2-dependent cargo requires Dab2 binding to EH domain proteins

To determine the importance of Dab2 binding to EH domain proteins in Dab2-mediated endocytosis without the complication of altered CCP/plaque nucleation and growth, we made use of the p96 NPF1-5* mutant, which does not bind EH domain proteins (Figure 3.1B,C). Dab2-deficient HeLa cells were reconstituted with wild type or mutant Dab2. We first confirmed that the number and size of CCSs were not altered (Table 3.2). We then measured the uptake of integrin β 1 (Figure 3.7A, B). As expected, integrin β 1 internalization was inhibited in Dab2-deficient cells and rescued by p96 but not p67 or vector [145]. Interestingly, p96 NPF1-5* did not rescue integrin β 1 endocytosis (Figure 3.7A,B), even though it localized correctly and recruited integrin β 1 to CCSs (Figure 3.3 and Figure 3.7C). These results suggest that Dab2-mediated integrin β 1 internalization requires binding of Dab2 to EH domain proteins.

We tested whether reduced integrin β 1 internalization by p96 NPF1-5* correlates with reduced recruitment of EH domain proteins to CCSs. We measured Eps15 and AP2 levels in CCSs in control, Dab2 depleted, wildtype p96 rescued and p96 NPF1-5* reconstituted cells. Similar amounts of Eps15 were recruited to CCSs in control and Dab2-depleted cells but approximately 25% less Eps15 ($P < 0.001$) was recruited to CCSs in cells reconstituted with p96 NPF1-5* (Table 3.2). AP2 content was similar in CCSs of control cells and cells reconstituted with either wildtype p96 or p96 NPF1-5*, but was increased approximately 75% ($P < 0.001$) in cells depleted of Dab2 (Table 3.2). This suggests that Dab2 normally competes with AP2 for incorporation into CCSs. When Dab2 is absent, EH domain proteins can be recruited by AP2 [53], but when p96 NPF1-5* replaces wildtype Dab2, fewer EH domain proteins are recruited.

Since p96 NPF1-5* recruits but does not internalize integrin β 1 (Figure 3.7A-C), we suspected that CCS invagination or budding is defective. This would be consistent with a report that CCP half-life is increased when Eps15 or ITSN is depleted from BSC1 cells [236]. Therefore we used live microscopy and automated tracking software to measure CCS lifetimes in HeLa cells transfected with EGFP-tagged clathrin light chain [215, 237]. CCSs on the ventral surface of control HeLa cells exhibited a broad range of lifetimes, with a preponderance of short-lived structures (Figure 3.8). These may correspond to early aborting CCPs observed in BSC1 cells [215]. When Dab2 was absent, there was a noticeable decrease in the proportion of structures with short lives (Figure 3.8). The defect was rescued by re-expressing wild type p96, but not mutant p96 NPF1-5* (Figure 3.8). Thus, removing Dab2 or replacing Dab2 with a mutant that cannot bind EH domain proteins reduces the number of short-lived CCSs. These results suggest that the linkage of wildtype Dab2 to EH domain proteins has a unique role in determining whether short-lived clathrin structures grow or disappear.

Since CCSs reconstituted with the Dab2 NPF1-5* mutant have less Eps15 (Table 3.2) and altered dynamics (Figure 3.8), we wondered if all CME was impaired. To test this, we measured TfnR endocytosis. As expected, TfnR internalization was unaltered in Dab2-deficient, p96-expressing or p67-expressing cells (Figure 3.9A,B) [142, 145]. Surprisingly, TfnR endocytosis was also unaffected in p96 NPF1-5* re-expressing cells. This suggests that enough Eps15 is recruited to CCSs to support internalization of a Dab2-independent cargo. Given that Dab2 and AP2 extensively co-localize in CCSs (Figure 3.3 and Figure 3.9C)[131, 143], why isn't integrin β 1 co-internalized with TfnR? We considered the possibility that integrin β 1 and TfnR may sort to separate CCSs. Previous reports have shown that different receptors may localize to

distinct CCP subsets [219, 238-240]. We performed immunofluorescence for surface integrin $\beta 1$ and Tfn. Both integrin $\beta 1$ and Tfn puncta were widely distributed over both surfaces (Figure 3.6F, Figure 3.7C, Figure 3.9C)[145]. However, very few integrin $\beta 1$ puncta contained Tfn (Figure 3.9C). Thus, p96 NPF1-5* may affect internalization of CCSs containing integrin $\beta 1$ but have no effect on structures containing TfnR.

These data show that recruitment of EH domain proteins to Dab2 is critical for endocytosis of CCSs containing the Dab2 cargo integrin $\beta 1$ but not CCSs containing TfnR. Proteins besides Dab2 in integrin $\beta 1$ CCSs do recruit EH domain proteins but seemingly do not mediate internalization. We propose that receptors may only internalize if they are bound to the cognate adaptor and the adaptor can recruit EH domain proteins.

IV. Discussion

Our results are summarized in Figure 3.10 and suggest the following model: EH domain proteins regulate the number and size of CCSs and the internalization, but not recruitment, of Dab2-dependent and -independent cargoes integrin $\beta 1$ and TfnR. EH domain proteins are recruited to CCSs by AP2, the NPF sequences in Dab2, and other accessory proteins. If Dab2 is absent, more AP2 enters CCSs and the content of EH domain proteins is unaffected. However, cargo internalization may depend on specific adaptor-EH domain protein interactions. A Dab2 mutant that cannot bind EH domain proteins (p96 NPF1-5*) acts as a dominant negative, slightly reducing the recruitment of EH domain proteins to CCSs and inhibiting integrin $\beta 1$ internalization. Internalization of TfnR from a different set of CCSs was unaffected. We propose that specific receptor-adaptor-EH domain protein complexes are required for efficient

endocytosis. In addition, the number of clathrin structures with short half-life is reduced in Dab2-deficient cells or cells reconstituted with the p96 NPF1-5* mutant. We speculate that the Dab2-EH domain protein complex may also have a role in determining whether short-lived clathrin structures grow or abort.

We found that Eps15 and ITSN bind to NPF sequences in Dab2 (Figure 3.1). While NPF is the core of most EH-binding peptides, individual EH domains prefer specific surrounding sequences. For example, the second EH domain of Eps15 shows a slight preference for Alanine at +1 (NPFA) and the first EH domain of ITSN is specific for NPF_X_{COOH} or NPF_{XX}_{COOH} at the C terminus of a protein [234, 235]. The fifth NPF motif of Dab2 is the most highly conserved across evolution and fits both these requirements; it lies in the sequence NPFA_{COOH}. This may explain why the C-terminal region of Dab2 binds Eps15 and ITSN more strongly than the central region (Figure 3.1B-D). In addition, Eps15 and ITSN form heterodimers, so they may bind cooperatively or competitively [233].

EH domain proteins in CCSs may act as scaffolds to bring in additional endocytic accessory proteins including dynamin, synaptojanin, stonin, synaptotagmin, SHIP2, FCHO2 and epsin [232]. We found that depleting EH domain proteins from HeLa cells had no effect on CCPs on the dorsal surface but significantly decreased the number of pits and plaques on the ventral surface. The median size of plaques, but not pits, increased significantly, suggesting a role in CCS nucleation and growth (Table 3.1). It is possible that EH domain proteins help recruit membrane curvature sensing proteins, like FCHO2, epsin and endophilin, to form CCPs.

In the absence of EH domain proteins, clathrin structures still form, but they tend to be flat plaques rather than curved CCPs.

Our results differ from a report that depletion of EH domain proteins inhibited all clathrin-coated structures [62]. However, these authors used BSC1 cells, and the functions of EH domain proteins may depend on the cell type. Unlike HeLa cells, BSC1 cells have neither Dab2 nor plaques, so the presence of Dab2 in HeLa cells may permit CCS nucleation in the absence of EH domain proteins [66, 97, 214]. Alternatively, HeLa cells may express additional EH domain proteins, besides Eps15, Eps15R, ITSN1 and ITSN2, that can also nucleate CCSs. It is possible that complete removal of the entire suite of endocytic EH domain proteins from HeLa cells would abolish all clathrin-containing structures, as reported in BSC1 cells.

Internalization of Dab2-dependent and -independent cargoes (integrin β 1 and TfnR respectively) was inhibited in EH-depleted HeLa cells (Figure 3.5). Decreased internalization of TfnR may be an indirect consequence of the decreased numbers of pits and plaques and the increased plaque size on the ventral surface of the cell (Table 3.1, Figure 3.6). Plaques have longer lifetimes (2-16 min) compared to CCPs (~60 s) [66], so internalization from the larger structures may be inhibited. However, this explanation is unlikely to account for the decreased internalization of integrin β 1, since integrin β 1 is internalized from the dorsal surface where the number and size of CCPs was unaltered (Table 3.1) [145]. Therefore, it is possible that EH domain proteins may directly regulate internalization of integrin β 1. This conclusion is supported by use of a Dab2 mutant that does not bind EH proteins. This mutant fails to support integrin β 1 internalization but TfnR internalization is normal (Figure 3.7 and Figure 3.9).

Separate regulation may be possible because integrin $\beta 1$ and TfnR do not significantly co-localize, suggesting that they internalize from different CCSs (Figure 3.10). This separation may have arisen because integrin $\beta 1$ and TfnR follow different endocytic routes following internalization [241-243]. Segregation of cargoes has been reported before: the EGF and Tfn receptors also sort to different CCP populations [239] and different GPCRs localize to distinct CCP subsets [219, 238, 240]. However, many other receptors are found in the same CCSs. For example, the LDL and Tfn receptors are predominantly found in the same CCSs [143]. So some receptors enter through shared pits, and some through different pits.

Even though integrin $\beta 1$ and TfnR appear to internalize through different CCSs, both cargoes co-localize with both adaptors Dab2 and AP2 as well as EH domain proteins. These commonalities make it difficult to explain how the Dab2 NPF mutant inhibits internalization of integrin $\beta 1$ but not TfnR. One possibility is that integrin $\beta 1$ internalization requires integrin $\beta 1$ -Dab2-EH domain complexes and TfnR internalization requires TfnR-AP2-EH domain complexes (Figure 3.10). This model implies that cargo regulates EH domain protein function. Several studies suggest that cargo regulates internalization [214, 215, 219, 244, 245]. Information on cargo occupancy may be relayed to the EH proteins by conformational changes in the adaptors. For example, AP2 undergoes conformation changes that enhance the affinity between AP2 and membranes following phosphorylation of AP2 by AAK1. In the new conformation, the Yxx Φ -sorting signal and PtdIns(4,5)P₂ binding sites are both exposed. The simultaneous binding of AP2 to multiple sites on the plasma membrane stabilizes the adaptor-membrane complex such that it can mediate clathrin assembly [246, 247]. In principle, cargo-adaptor complexes could then regulate the affinity of EH domain proteins for downstream

accessory proteins, thus allowing for efficient internalization. Further experiments will be needed to understand if and how EH domain protein function may be regulated by cargoes.

Why would adaptors need to bind both cargo and EH domain proteins for efficient endocytosis? One reason may be to ensure that only clathrin structures ‘fully loaded’ with receptors are internalized. Clathrin pits with less than their full receptor capacity may not have enough functional EH domain proteins for internalization and may need to wait to recruit additional receptors. The lifetime of productive CCPs (not including plaques) ranges from 30 to >120 s [215]. It is tempting to speculate that CCPs with longer lifetimes wait on the cell surface until they have their ‘full’ receptor load and therefore sufficient functional EH domain proteins for internalization. Communication between receptors and EH domain proteins, mediated by endocytic adaptors like Dab2, may be important for regulating the endocytic checkpoint [215, 236]. In the absence of Dab2 or Dab2-associated EH domain proteins, the checkpoint may be incomplete and CCSs may escape past the checkpoint instead of being aborted, perhaps explaining the decrease in short life time events (Figure 3.8). However, there are other possible explanations and more experiments will be required to determine the role of EH domain proteins in CCP dynamics and to fully understand the composition and regulation of the checkpoint.

V. Materials and Methods

Cells and DNA constructs:

HeLa cells and HEK 293s were cultured in DME supplemented with 10% FBS and 1% penicillin-streptomycin at 37°C with 5% CO₂. HeLa cells stably expressing Dab2 shRNA have been previously described [145] and were grown in the presence of 250 µg/ml hygromycin B.

T7-tagged mouse p96 and p67 have been previously described [142]. The NPF motifs were mutated to NPV by site-directed mutagenesis (TTC/TTT to GTC/GTT). shRNA resistant p96 was created using site-directed mutagenesis using the following primers and their reverse complements:

5'CAGGGACAACACAAGCAGAGAATATGGGTCAACATTTTCCTTGTCTGGCATA 3' and
5'CAACACAAGCAGAGAATATGGGTTAATATATCCTTGTCTGGCATAAAAATCATT3'.

LCa-GFP was a gift from M. Von Zastrow (UCSF). HA-tagged ITSN was a gift from J. O'Bryan (University of Illinois, Chicago).

T7-mDab2-206-492-His, T7-His-mDab2-493-766, and T7-mDab2-493-766-His were created by cloning of the Dab2 insert from GST-Dab2-206-492 [65, 131] or amino acids 493-766 of full-length protein into PET21a(+) (EMD Biosciences, Darmstadt, Germany). To create the N-terminal His fusion protein of 493-766, sequence for the His tag was included in the 5' PCR primer, and a stop codon was introduced at the end of the Dab2 insert. GST-Eps15-EH and GST-Eps15R-EH were from S. Confalonieri [139].

Antibodies:

The following antibodies were used: mouse anti-T7 (Novagen), mouse anti-HA.11 (Covance), rabbit anti-Eps15 (Santa Cruz), mouse anti-Eps15 (kind gift from S. Polo, Istituto FIRC di Oncologia Molecolare, Milan, Italy), rabbit anti-Dab2 (Santa Cruz), mouse anti-integrin β 1, P5D2 (provided by E. Wayner, Fred Hutchinson Cancer Research Center), mouse anti-TfnR (Abcam), mouse anti-ERK (BD Transduction Laboratories), mouse anti-clathrin (Abcam) and mouse anti-adaptin (Calbiochem).

Protein purification and binding:

GST-EH domains were purified as described [65]. His-tagged Dab2 fragments were purified similar to [224]. DNA was introduced into NiCo21(DE3) *E. coli* and a 20 mL starter culture was grown overnight at 37°C. The starter was added to 200 mL LB and grown for 2 hr at 30°C in the presence of protease inhibitors (20 mM benzamidine, 1 mM PMSF, 5 mM EDTA). Protein expression was induced at 22°C overnight with 300 mM IPTG. After centrifugation, the bacterial pellet was resuspended in resuspension buffer (0.5% NP-40, 1 mM DTT, 20 mM imidazole pH 8.0 in PBS with protease inhibitors). Lysozyme was added to a concentration of 0.5 mg/mL and cells were lysed 15 min on ice. The lysates were then sonicated and centrifuged at 4,000xg for 20 min. Lysate was incubated for 1.5 hr with Ni²⁺ beads (Qiagen, Valencia, CA) at 4°C. Beads were washed twice in resuspension buffer with 350 mM NaCl and 15 mM imidazole, and then washed three times in resuspension buffer with 15 mM imidazole. Beads were then loaded into an empty Bio-Rad poly-prep column and eluted with increasing concentrations of imidazole ranging from 50-200 mM in PBS with 1 mM DTT and 5% glycerol.

Equal amounts of glutathione-Sepharose-immobilized GST, GST-Eps15-EH and GST-Eps15R-EH were mixed with eluted His-tagged Dab2 fragments overnight at 4°C in Buffer A (50 mM Tris pH 8.0, 150 mM NaCl, 1 mM EDTA, 0.5% Triton X-100). Beads were washed five times in Buffer A and resuspended in 5X Laemmli buffer for SDS-PAGE.

Immunoprecipitation:

For co-immunoprecipitation experiments, T7-tagged p96, p67, p96 NPF mutants and HA-tagged ITSN were transfected into HEK 293s using Lipofectamine2000 according to the

manufacturer's protocols. After 48 hours, cells were lysed at 4°C in buffer containing 150 mM NaCl, 10 mM HEPES pH 7.4, 2 mM EDTA, 50 mM NaF, 1% Triton-X-100 and protease inhibitors followed by centrifugation for 15 minutes at 14,000xg. Lysate was rotated with primary antibody for 3 hours at 4°C. Protein A+G beads were added to the lysate/antibody mix for 1 hour at 4°C. After centrifugation, the protein/antibody/bead complex was washed 3 times in lysis buffer, resuspended in 5x Laemmli buffer, then resolved by SDS-PAGE.

To determine whether endogenous Dab2 and Eps15 co-immunoprecipitate, lysates were prepared in the presence of a reversible cross linking agent, Dithiobis succinimidyl propionate (DSP, Pierce Biotechnology).

siRNA transfection:

Knockdown experiments were performed as described previously (Maurer and Cooper, 2006). Cells were transfected with 50 pmol of a pool of four siRNA oligonucleotides specific for Eps15, Eps15R, ITSN1 (Thermo Fisher Scientific) and ITSN2 (Santa Cruz), using Oligofectamine (Invitrogen) on days 1 and 3 and analyzed on day 5. The siRNA to ITSN1 and 2 knock down both the long and short ITSN isoforms.

RT-PCR:

Total RNA was extracted using an RNeasy kit (Qiagen) according to the manufacturer's directions. Total RNA was reverse transcribed using SuperScript II reverse transcription and random primers (Invitrogen). PCR was performed using Taq polymerase and the following primers:

Eps15R: 5'-TGGGAAGATATGGGACTTGG-3' and 5'-CCTTTTCTTCCACCCTCACA-3'

ITSN1 pan: 5'-CTCAGGAAAGGGACAAGCAG-3' and 5'-CTGGCTTAGCTGGTTCTTGG-3'

ITSN2 pan: 5'-CTCAGAGTGGGCAGTTCCTC-3' and 5'-CAGCTTTGGCCATGTCAGTA-3'

Actin: 5'-GCGAGAAGATGACCCAGATCATGTT-3' and 5'-

GCTTCTCCTTAATGTCACGCACGAT-3'

Antibody internalization assay:

Antibody uptake assays were performed essentially as described (Roberts et al., 2001) with some modifications. Cells were plated on coverslips coated with 4 µg/ml collagen IV and then incubated with anti-integrin β1 antibody (P5D2) or anti-TfnR diluted in assay media (DME, 10 mM Hepes, pH 7.4, and 0.1% BSA) for 30 min at 4°C. After washing off unbound antibody with cold DME, cells were warmed to 37°C in DME with 10% FBS for the appropriate time and fixed with cold formalin for 20 minutes. To visualize internalized receptors, surface-bound antibody was removed by acid stripping for 5 min on ice (0.5 M NaCl and 0.2 M acetic acid) before fixing with cold formalin. To inhibit recycling, 2 µM Primaquine (Sigma) was used.

To detect surface receptors, anti-integrin β1 antibody (P5D2) or Alexa fluor 488-conjugated human Tfn was added to cells in assay media (DME, 10 mM Hepes, pH 7.4, and 0.1% BSA) for 60 min at 4°C. After washing off unbound antibody/Tfn with cold DME, cells were fixed with cold formalin for 20 minutes.

Immunofluorescence:

To visualize surface receptors, non-permeabilized cells were fixed and stained with antibodies to extracellular epitopes. To detect intracellular proteins, cells were fixed and permeabilized with 0.1% Triton X-100 in PBS for 5 min at 25°C. Cells were washed in PBS and blocked for 30 minutes in 5% normal goat serum + 2% BSA in PBS before primary antibody was added for 3–4 h at 25°C or overnight at 4°C. Coverslips were rinsed in PBS before the addition of Alexa Fluor 488– or Alexa Fluor 568–secondary antibodies, diluted 1:1,000 (all from Invitrogen), for 1 h at 25°C. Secondary antibodies included goat anti–mouse, IgG2b-isotype–specific antibodies, and goat anti–rabbit. After several PBS rinses, coverslips were mounted in ProLong Gold solution (Invitrogen).

Imaging:

Fixed cells were visualized using a 100× NA 1.4 oil objective on a DeltaVision IX70 microscope (Olympus). Images were recorded using fixed camera settings (IX-HLSH100; Olympus). Images were acquired and deconvolved using SoftWorx (Applied Precision), and all exposure times and image scaling were equal within an experiment. Deconvolved images from single planes corresponding to the ventral surfaces of the cells or flattened Z-projections were analyzed using ImageJ (National Institutes of Health). Figures were assembled using Photoshop (Adobe) and Canvas (Deneba) software.

To measure CCS lifetimes, control and Dab2 shRNA HeLa cells expressing Clathrin-LCa-EGFP and pCGT, T7-p96, or T7-p96 NPF1-5* were plated in 35 mm dishes containing a glass coverslip a day before imaging. Images were acquired on a confocal Nikon LiveScan

(Prairie technologies swept field) system, equipped with a 37°C chamber and a Photometrics QuantEM 512x512 pixel EMCCD camera. A 100x NA 1.4 oil objective was used. Images were recorded every 2s for 4 minutes. CCS lifetimes were analyzed using the uTrack software package described in [215, 237]. The mean lifetime of CCPs in BSC1 cells is 39 s [215], comparable to the median lifetimes of 34 - 36 s that we obtain.

Table 3.1**Effect of EH domain protein depletion on size and number of CCPs and clathrin plaques**

Control and siRNA-treated HeLa cells grown on collagen IV-coated coverslips were fixed, permeabilized and stained with anti-AP2 to detect clathrin-coated structures. CCP, structures with diameter ~100-200 nm; plaques, structures with diameter > 217 nm. EH domain protein depletion significantly decreased the numbers of AP2-containing pits and plaques. #, $P < 0.05$; **, $P < 0.001$ by *t* test. The median size of pits on both surfaces was unaltered. However, there was a significant increase in the median size of plaques on the ventral surface of the cell. ***, $P < 0.001$ by the Mann-Whitney test. This test was used because the data follow a non-parametric distribution. 4,000 structures were analyzed for each condition, from three experiments. ImageJ was used to obtain measurements.

siRNA	-	Eps15+15R	ITSN1+2	Eps15+15R +ITSN1+2
CCPs, ventral				
number/cell	221 \pm 50	110 \pm 8 #	106 \pm 18 #	78 \pm 17 #
median diameter (nm)	151	151	156	151
mean intensity	46 \pm 3	47 \pm 1	47 \pm 1	47 \pm 1
Plaques, ventral				
number/cell	335 \pm 18	286 \pm 35	240 \pm 48	186 \pm 20 **
median diameter (nm)	310	383 ***	327	429 ***
mean intensity	66 \pm 5	77 \pm 3	68 \pm 3	74 \pm 1
CCPs, dorsal				
number/cell	610 \pm 23	641 \pm 19	626 \pm 16	715 \pm 39
median diameter (nm)	151	151	151	151
mean intensity	48 \pm 1	45 \pm 1	45 \pm 1	48 \pm 1

Table 3.2**The effect of Dab2 on the size, number, and composition of CCS**

Control and Dab2-deficient HeLa cells re-expressing vector alone, T7-p96 or T7-p96 NPF1-5* and clathrin light chain (LCa)-EGFP were grown on collagen-coated coverslips and fixed, permeabilized and stained with anti-Eps15 or Anti-AP2 antibody. Clathrin structures on the ventral surface were characterized. No difference in the median size, number of CCSs or clathrin content (area x mean intensity) was detected. However, the Eps15 content per clathrin structure was decreased in cells expressing the T7-p96 NPF1-5* mutant and the AP2 content was increased in Dab2 deficient cells. The Eps15 content in clathrin structures was obtained by multiplying binary images of clathrin and Eps15 (to obtain area of 'colocalized' Eps15), and superimposing onto the raw Eps15 image (to obtain intensity). ***, $P < 0.001$ by the Mann-Whitney test. This test was used because the data follow a non-parametric distribution. ~2000 structures were analyzed for each condition. ImageJ was used to obtain measurements.

	Control + pCGT	Dab2 shRNA + pCGT	Dab2 shRNA + T7-p96	Dab2 shRNA +T7-p96NPF 1-5*
median diameter of CCS (nm)	242	224	240	252
number of CCS	588 ± 41	521 ± 31	557 ± 63	569 ± 59
relative level clathrin/CCS	1	0.91	1.03	1.04
relative level Eps15/CCS	1	1.07	0.96	0.76***
relative level AP2/CCS	1	1.74***	1.23	1.09

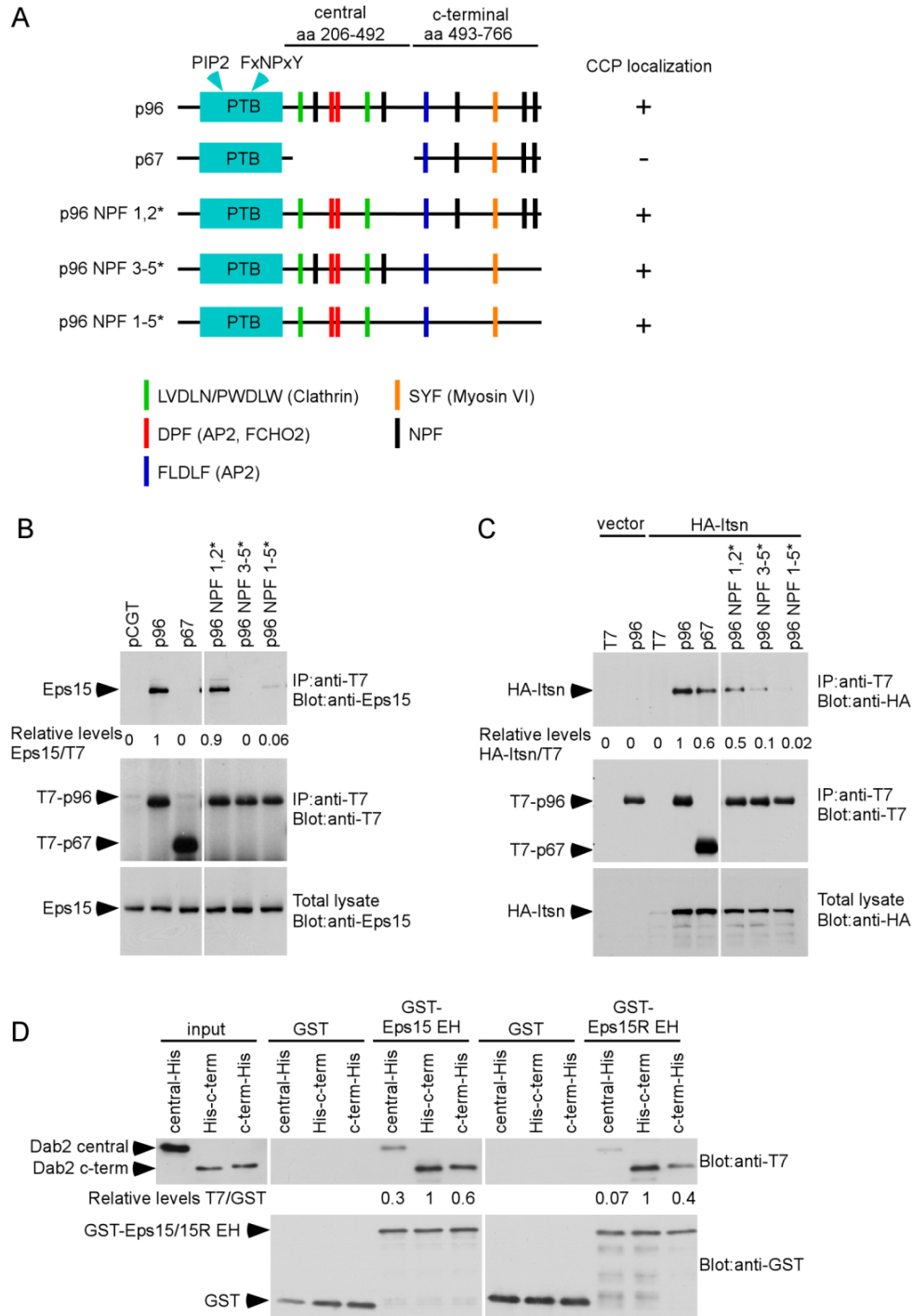


Figure 3.1

The Dab2 NPFs are required for binding Eps15 and ITSN.

(A) Drawing of T7-p96, T7-p67 or T7-p96 NPF mutants showing binding sites. The Dab2 central and C-terminal fragments used for in vitro binding are also shown. (B,C) HEK 293 cells were transfected with control vector, T7-p96, T7-p67 or T7-p96 NPF mutants and HA-ITSN. Cell lysates were immunoprecipitated with anti-T7 antibody and immunoblotted with either anti-Eps15 (B) or anti-HA (C). Representative blots from one of four independent experiments are shown. Pixel intensities were measured by ImageJ. (D) Binding of purified Dab2 and Eps15/15R EH domain. Purified, bacterially grown T7-mDab2-206-492-His (central fragment), T7-mDab2-493-766-His (C-terminus of Dab2) and T7-His-mDab2-493-766 (C-terminus of Dab2 with N-terminal tag) were mixed with purified, glutathione Sepharose-bound GST-EH domain of Eps15 or Eps15R. Pixel intensities were measured by ImageJ. (Experiments performed by AMT, EEM, and NT)

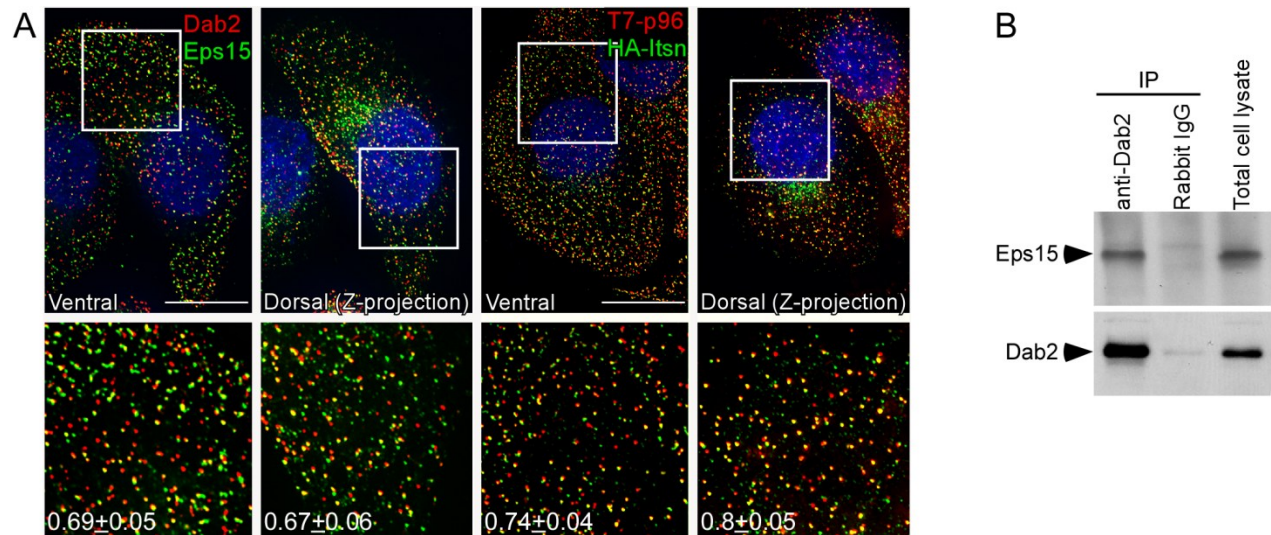


Figure 3.2

Dab2 binds and colocalizes with Eps15 and HA-ITSN.

(A) Untransfected or T7-p96 + HA-ITSN-expressing HeLa cells were grown on collagen IV-coated coverslips, fixed, permeabilized and stained with either anti-Dab2 and anti-Eps15 or anti-T7 and anti-HA. Single 0.2 μ m sections at the ventral surface or Z-projections of the dorsal surface are shown. The white boxes indicate the enlarged images shown in the insets. The fraction of Dab2 that colocalizes with Eps15 or HA-ITSN at both surfaces was determined by ImageJ (Manders colocalization coefficient). In all cases random colocalization, obtained by flipping the red channel (Dab2), was <0.10 . ~10 cells/condition from two independent experiments were analyzed. Bar, 10 μ m. (B) HeLa cell lysates containing the cross-linking agent DSP were immunoprecipitated with anti-Dab2 antibody or rabbit IgG and immunoblotted with anti-Eps15. (Experiments performed by AMT and NT)

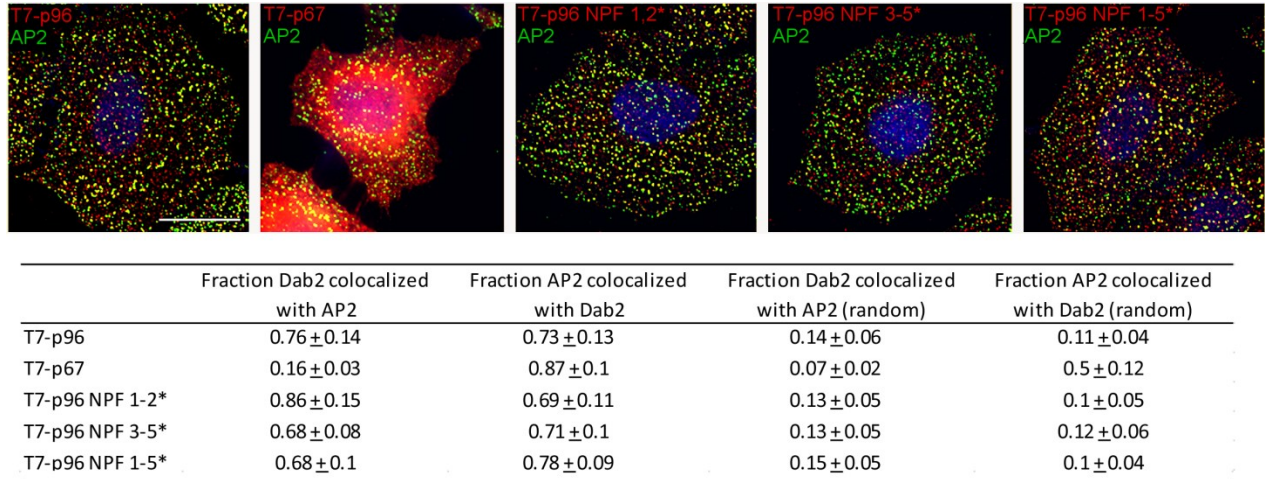


Figure 3.3

The Dab2 NPFs are not required for localization to CCSs.

HeLa cells were transfected with T7-p96, T7-p67 or T7-p96 NPF mutants. Cells were grown on collagen IV-coated coverslips, fixed, permeabilized and stained with anti-T7 and anti-AP2. Single 0.2 μ m sections at the ventral surface are shown. The fraction of T7-Dab2 that colocalized with AP2 (Manders colocalization co-efficient, M1) and the fraction of AP2 that colocalized with T7-Dab2 (Manders colocalization co-efficient, M2) were determined with ImageJ. The red channel (T7-Dab2) was flipped to determine random colocalization. Mean values and standard errors are shown for ~5 cells/treatment. Bar, 10 μ m. (Experiments performed by AMT and NT)

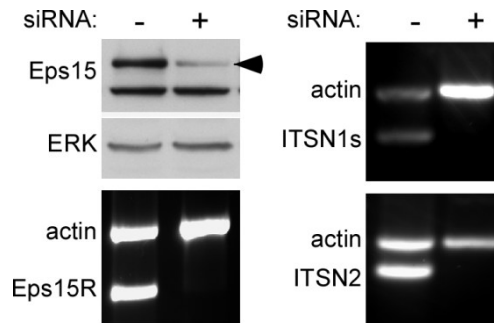


Figure 3.4

EH domain protein depletion by siRNA.

EH domain proteins were efficiently depleted from HeLa cells following 2 rounds of transfection with siRNA. Eps15 protein levels were analyzed by Western blot. The arrow indicates the Eps15 band. Eps15R and ITSN mRNA levels were analyzed by RTPCR. (Experiments performed by AMT and NT)

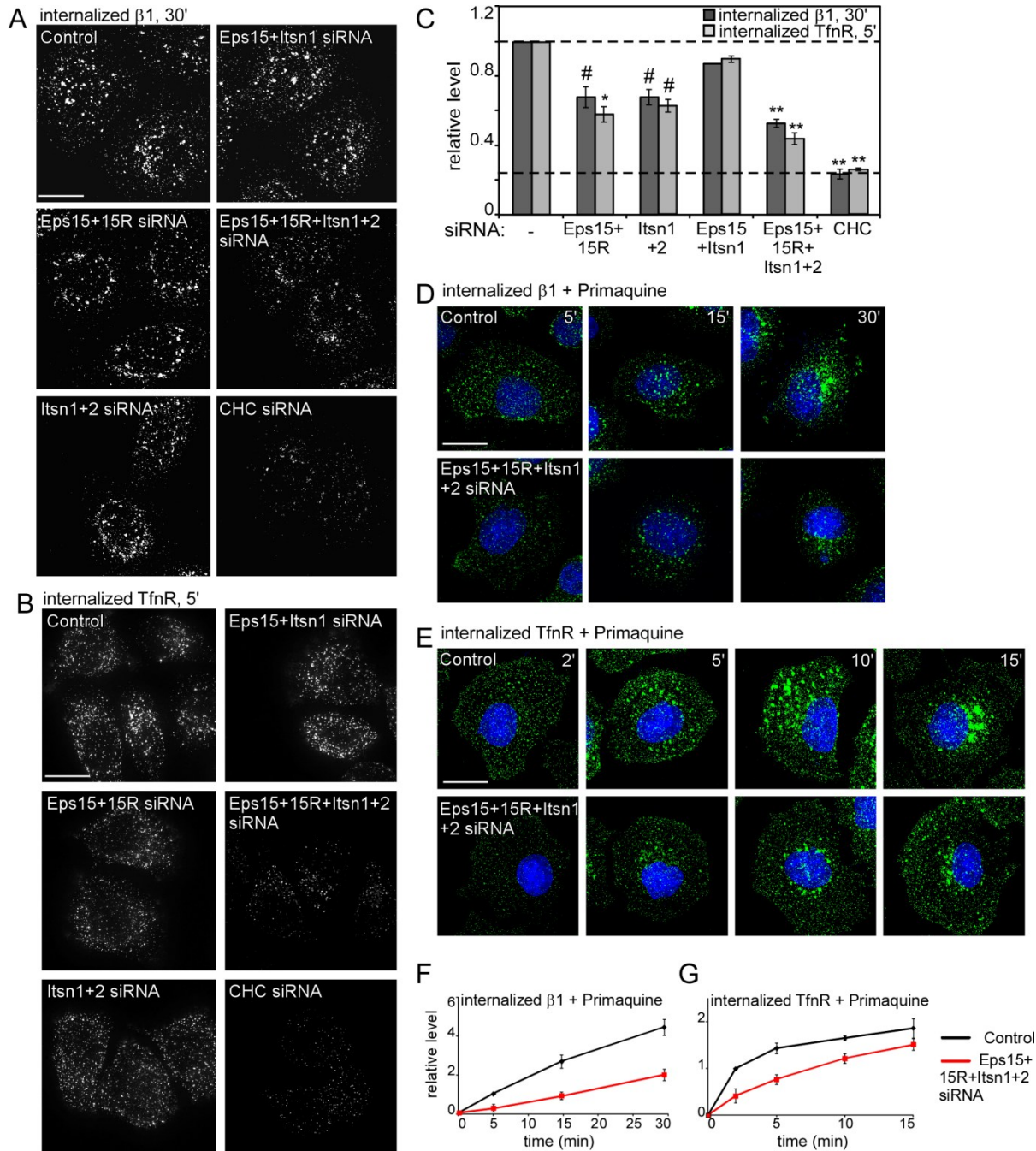


Figure 3.5

EH domain proteins regulate integrin $\beta 1$ and TfnR endocytosis.

(A-C) Control and siRNA-treated HeLa cells were incubated with anti-integrin $\beta 1$ (A) or anti-TfnR antibody (B) for 30 min at 4°C followed by warming at 37°C for 30 ($\beta 1$) or 5 min (TfnR). (D-G) Control and EH domain-deficient HeLa cells were incubated with anti-integrin $\beta 1$ (D) or anti-TfnR antibody (E) for 30 min at 4°C, and then warmed to 37°C for the indicated times in the presence of 2 μ M Primaquine. Surface antibody was removed by acid stripping and internalized antibody was detected. (A,B,D,E) Z-projections of the entire cell are shown. (C,F,G) Pixel intensities were measured by ImageJ. Mean values and standard errors of internalized receptor after normalizing with surface receptor at time = 0 are shown. ~15 cells/treatment from three independent experiments were analyzed. #, $P < 0.05$, *, $P < 0.01$, **, $P < 0.001$ by t test. Bar, 10 μ m. (Experiments performed by AMT and NT)

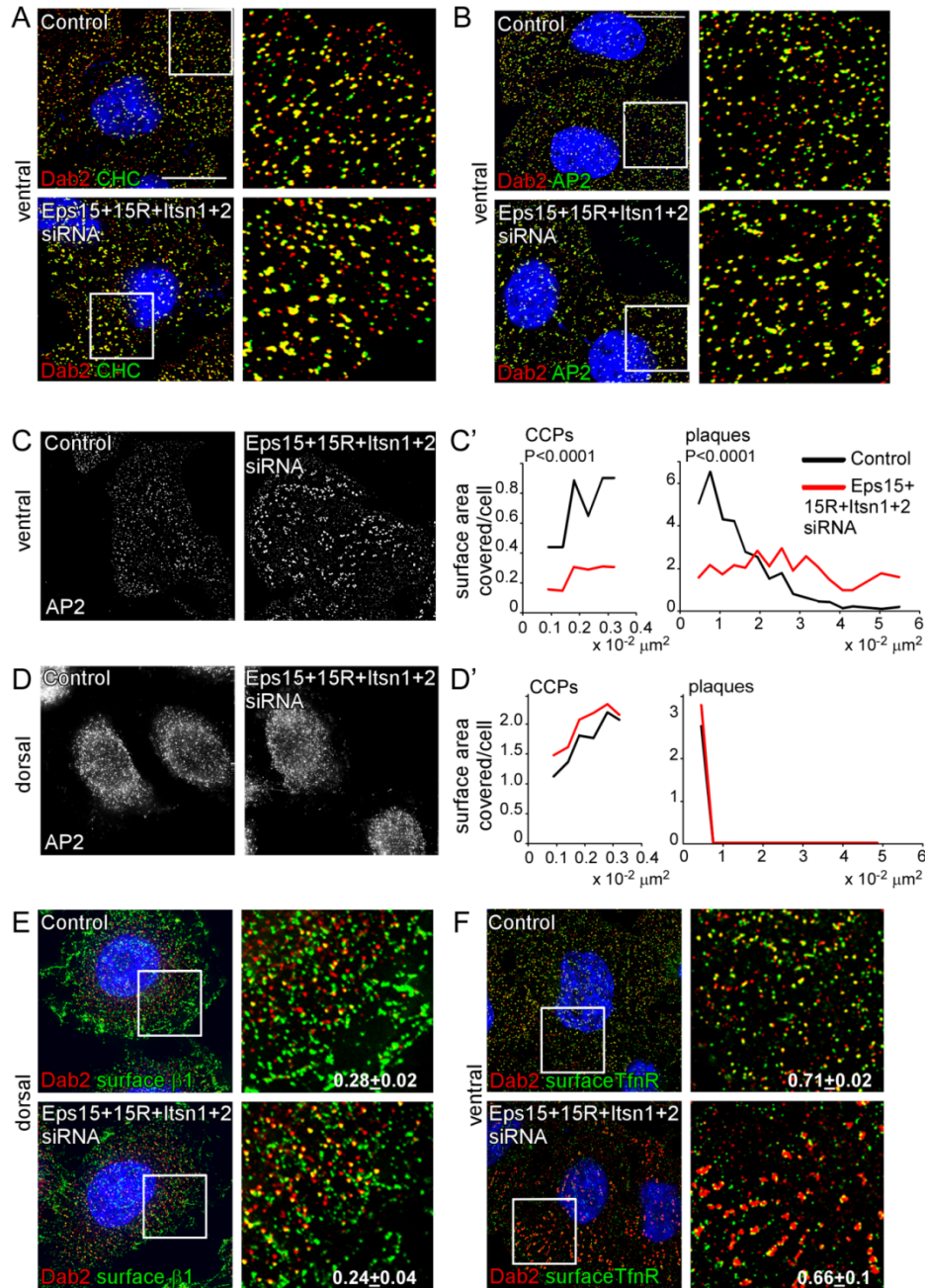


Figure 3.6

Effect of EH domain protein depletion on clathrin, AP2, Dab2 and receptor localization.

Control and EH domain-deficient HeLa cells grown on collagen IV-coated coverslips were fixed, permeabilized and stained with anti-Dab2 and anti-CHC (A) or anti-AP2 (B) to detect clathrin-coated structures. (C) AP2 staining alone on the ventral and dorsal surface is shown. AP2 staining was used to calculate the surface area covered by CCPs (size $0.009 \mu m^2 - 0.032 \mu m^2$ which corresponds to structures with diameters 107nm – 202nm) or plaques (size $> 0.032 \mu m^2$) by ImageJ. ~ 2000 puncta/treatment from three independent experiments were used. P values were calculated using the Mann-Whitney test, a non-parametric test. (E,F) Cells were stained with either anti-integrin $\beta 1$ (E) or anti-TfnR (F) antibody before permeabilizing to detect surface receptor. 0.2 μm sections of the ventral or dorsal surface are shown. The white boxes indicate the enlarged images shown in the insets. The fraction of surface integrin $\beta 1$ or TfnR that colocalized with Dab2 was measured by ImageJ (Manders colocalization coefficient). In all cases random colocalization, obtained by flipping the red channel (Dab2), was < 0.08 . ~10 cells/treatment from three separate experiments were analyzed. Bar, 10 μm . (Experiments performed by AMT and NT)

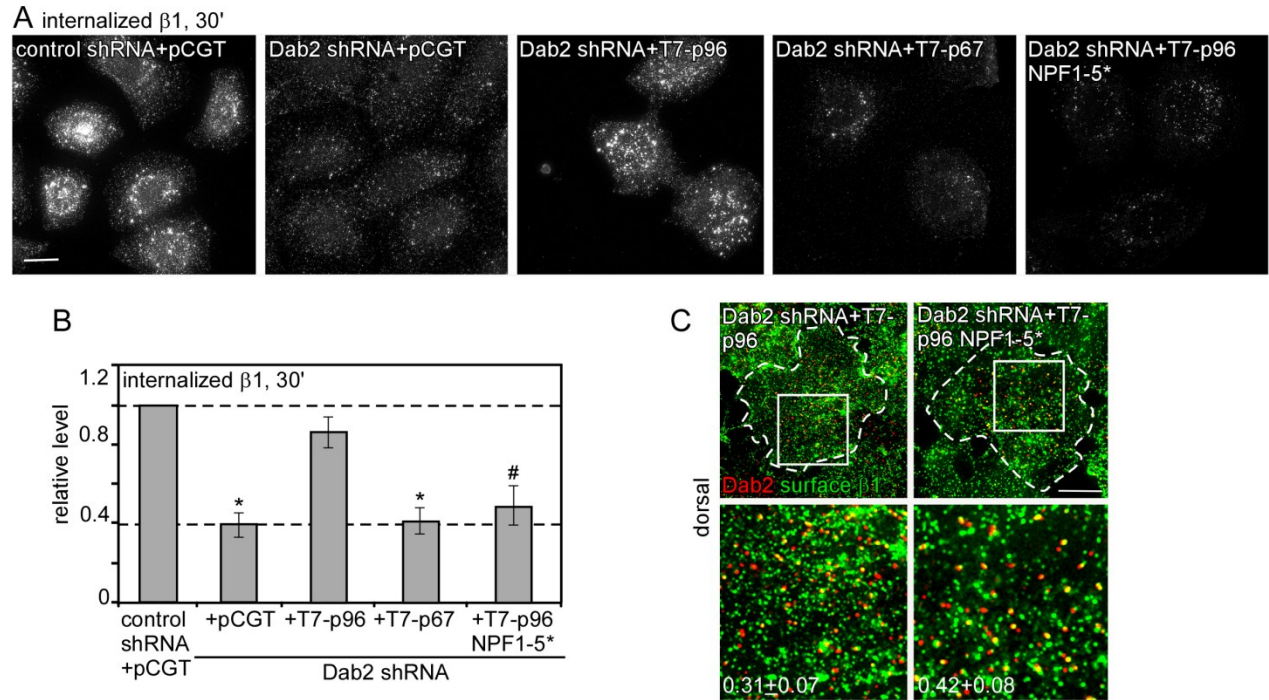


Figure 3.7

Disruption of the Dab2-EH domain protein interaction slows Dab2-dependent integrin $\beta 1$ internalization.

(A-C) Control and Dab2-deficient HeLa cells re-expressing vector alone, T7-p96, T7-p67 or T7-p96 NPF 1-5* were incubated with anti-integrin $\beta 1$ antibody for 30 min at 4°C followed by warming at 37°C for 30 min. (A,B) Surface antibody was removed by acid stripping and internalized antibody was detected. (A) Z-projections of the entire cell showing internalized integrin $\beta 1$ antibody. (B) Pixel intensities were measured by ImageJ. Mean values and standard errors are shown for ~30 cells/treatment from three independent experiments. #, $P < 0.05$, *, $P < 0.01$, by t test. (C) Cells were stained with anti-integrin $\beta 1$ antibody before permeabilizing to detect surface receptor. Z-projections of the dorsal surface are shown. The white boxes indicate the enlarged images shown in the insets. Bar, 10 μm . The fraction of surface integrin $\beta 1$ that co-localized with Dab2 in T7-p96 or T7-p96 NPF 1-5* expressing cells was calculated using ImageJ (Manders colocalization coefficient). In all cases random colocalization, obtained by flipping the red channel (Dab2), was < 0.07 . ~5 cells/treatment were analyzed. (Experiments performed by AMT and NT)

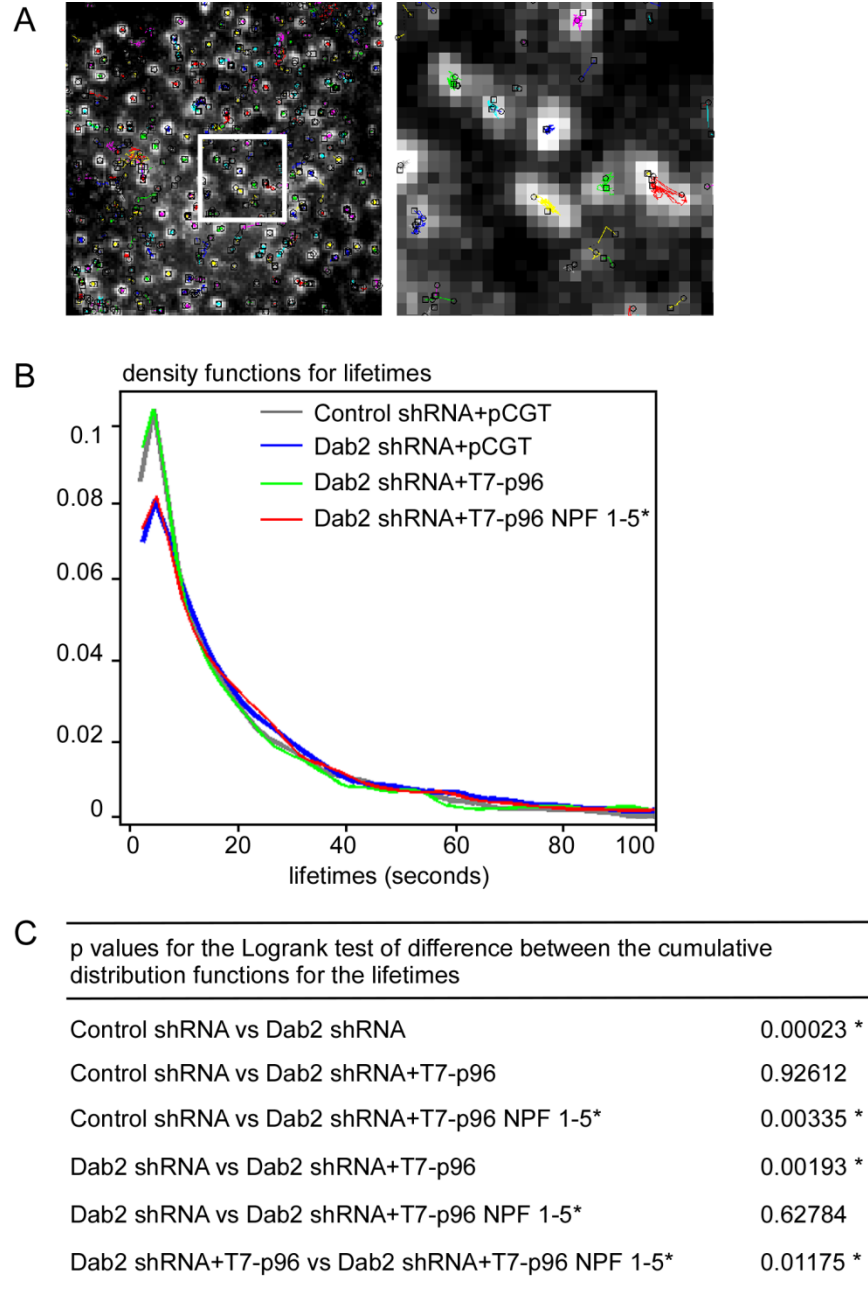


Figure 3.8
Lifetime distribution for CCSs.

To track CCSs, ventral surfaces of control and Dab2-deficient HeLa cells re-expressing vector alone, T7-p96 or T7-p96 NPF1-5* and LCa-EGFP were imaged every 2 s for 4 min. (A) A single frame from a video overlaid with all observed trajectories. The white box indicates the enlarged image shown in the inset. (B) Lifetime distribution for CCSs was determined from the elapsed time between the appearance and disappearance of LCa-EGFP puncta. All structures appearing after the first frame and disappearing before the last frame are included. ~80% of larger clathrin structures (size $> 0.032\mu\text{m}^2$) persisted for longer than 4 min so were excluded. Also highly motile clathrin structures were not used to calculate lifetimes. (C) P values calculated by log-rank test. ~2000 puncta from two independent experiments were analyzed for each condition. (Experiments performed by AMT and TR)

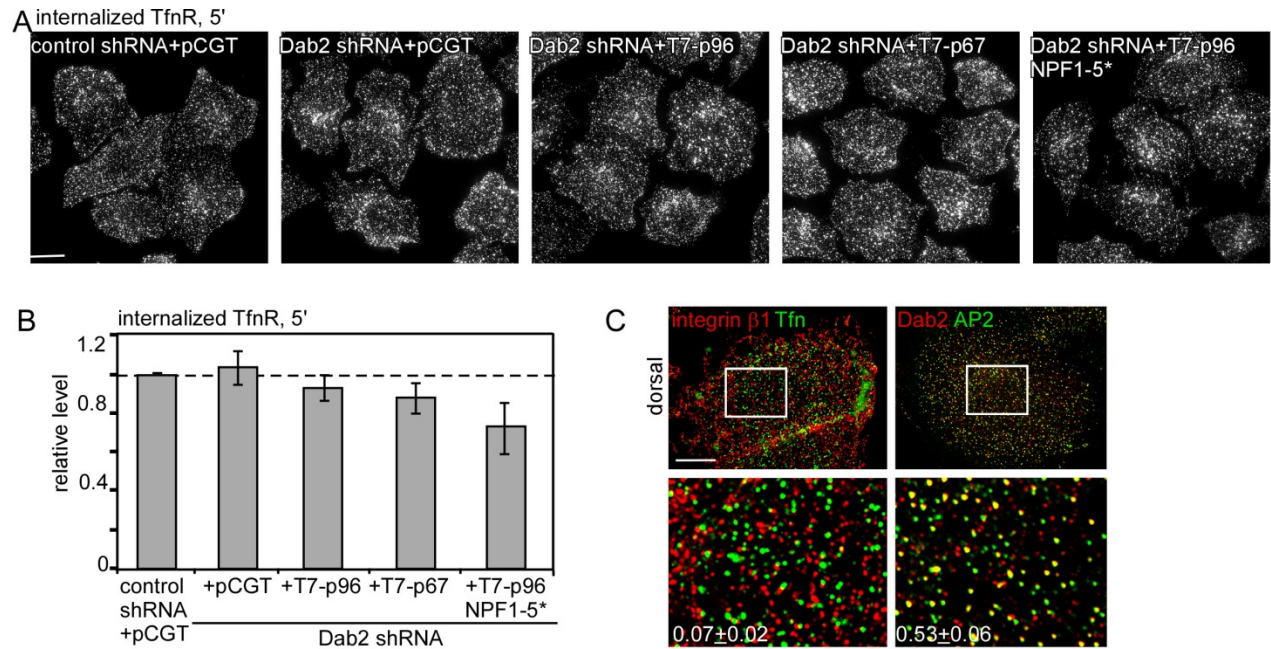


Figure 3.9

Disruption of the Dab2-EH domain protein interaction does not affect TfnR endocytosis.

(A-B) Control and Dab2-deficient HeLa cells re-expressing vector alone, T7-p96, T7-p67 or T7-p96 NPF 1-5* were incubated with anti-TfnR antibody for 30 min at 4°C followed by warming at 37°C for 5 min. (A,B) Surface antibody was removed by acid stripping and internalized antibody was detected. (A) Z-projections of the entire cell showing internalized TfnR antibody. (B) Pixel intensities were measured by ImageJ. Mean values and standard errors are shown for ~30 cells/treatment from three independent experiments. #, $P < 0.05$, *, $P < 0.01$, by t test. (C) Control cells were incubated with anti-integrin $\beta 1$ antibody and Alexa fluor 488-conjugated human Tfn to detect surface $\beta 1$ and TfnR or permeabilized and stained with anti-Dab2 and anti-AP2. Z-projections of the dorsal surface are shown. The white boxes indicate the enlarged images shown in the insets. Bar, 10 μ m. The fraction of CCSs that contain both receptors integrin $\beta 1$ and Tfn or both adaptors Dab2 and AP2 are shown. Random colocalization, obtained by flipping the red channel, was < 0.03 . (Experiments performed by AMT and EEM)

	AP2 in CCS	Dab2 in CCS	EH protein in CCS	receptor in CCS $\beta 1$	TfnR	internalization $\beta 1$	TfnR
control	=	=	=	=	=	=	=
EH-deficient	=	=	↓↓	=	=	↓	↓
Dab2-deficient	↑	↓↓	=	↓	=	↓	=
Dab2-NPF1-5*	=	=	↓	=	=	↓	=
Dab2-p96	=	=	=	=	=	=	=

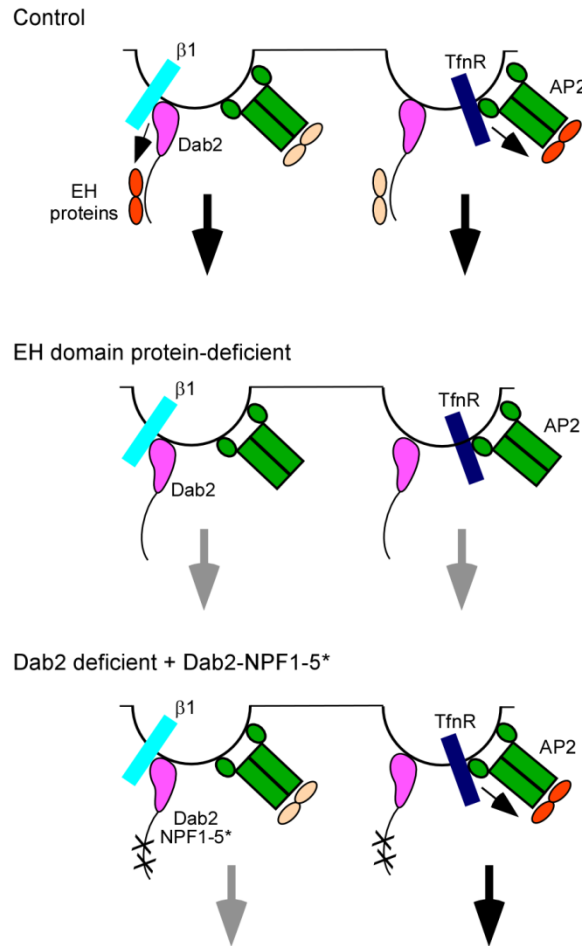


Figure 3.10

Summary of results and proposed model.

(Upper) Summary of results taken from Table 3.2 and Figure 3.3, Figure 3.5, Figure 3.7 and Figure 3.9. =, same as in control; upward arrow, increased; downward arrow, decreased.

(Lower) Model. Dab2 and AP2 are found together in most clathrin-coated structures. However, their receptors integrin $\beta 1$ and TfR do not localize to the same structures. Internalization of a clathrin structure is driven by adaptors bound to both receptor and EH domain proteins (shown in orange). Inactive EH domains are shown in pale yellow. Small black arrows indicate regulation of EH domain proteins by adaptor-receptor complexes. Large black arrows indicate endocytosis. In the absence of EH domain proteins internalization of integrin $\beta 1$ and TfR is impaired (grey arrows). When cells are reconstituted with a Dab2 mutant that does not bind EH domain proteins integrin $\beta 1$ is not internalized efficiently because this Dab2 mutant cannot bind EH domain proteins. However, TfR endocytosis proceeds normally because its adaptor AP2 can bind EH domain proteins. The AP2-EH domain complex in integrin $\beta 1$ structures is unable to drive endocytosis probably because it is not bound to receptor.

Chapter 4 – A Dab2 conformational change may regulate CCP activity

I. Introduction

CME is one of the major ways a cell is able to regulate its cell surface proteome and therefore processes such as motility and signal transduction. The multitude of ways by which endocytosis itself is regulated, however, are just beginning to be understood. Regulation can potentially occur at many levels and at various steps of endocytosis. Perhaps the most well-known way that endocytosis is regulated is the selection of receptors for internalization. The endocytosis of some receptors, such as the LDLR and TfnR, is thought to occur regardless of whether they're bound to their ligands [248, 249], while other receptors, typically those with a signaling function, are only targeted for endocytosis when activated by ligand binding. Two types of receptors known to be internalized only upon ligand activation include the ErbB receptor family, which contains the EGFR, and GPCRs [250, 251]. Upon stimulation by ligand, each type of receptor is modified, by ubiquitin for EGFR and phosphorylation for GPCRs, which allows binding of the appropriate adaptor protein [56, 120, 252, 253].

Apart from regulation of cargo selection for endocytosis, the formation of CCPs is also regulated by phospholipids. Proteins specific for CME at the plasma membrane prefer to bind to PI(4,5)P₂, which is enriched at the plasma membrane. Other cellular compartments are enriched in other types of phosphoinositides (PIs); this segregation of PIs within the cell allows for membrane trafficking specificity [254]. For example, PI(3)P is concentrated in early endosomes and the trans-Golgi network contains high levels of PI(4)P [254, 255]. Phosphorylation and dephosphorylation of PIs can also control the affinity of endocytic proteins for the membrane,

because most endocytic proteins have the highest affinity for PIP₂. This, along with changes in phospholipid composition, can control the frequency and localization of CCP formation [254, 256]. The activity of phosphatases, especially synaptojanin, on PIP₂ also regulates detachment of adaptor proteins from CCVs and therefore clathrin uncoating [108].

There are also controls on whether a newly formed CCP progresses through to budding or aborts at an earlier stage. Live-cell imaging of fluorescent clathrin shows two dynamic populations of clathrin on the cell membrane, one with the same fluorescence intensity as whole, purified CCVs and one with a mean intensity and lifetime significantly less than a complete CCV [97]. Overexpression of cargo proteins decreases the amount of these short-lived structures and increases the number of productive CCPs, suggesting that the presence of cargo may regulate the progression of a CCP from early to late stages [97, 215, 236, 257]. This so-called “endocytic checkpoint” presumably functions in a manner similar to mitotic checkpoints, where the process only continues if all necessary conditions have been met, in this case that cargo is present. Energetically, this makes sense for the cell, so that time, energy, and resources are not wasted internalizing an empty pit. However, the molecular mechanism of this proposed checkpoint is not yet known.

The data presented in chapters 2 and 3 suggest ways that Dab2 could potentially regulate the activity and progression of a CCP. In chapter 2, I showed that FCHO2 binds to Dab2 at the same sites as AP2 (Figure 2.2, [65]). This binding of FCHO2 to sites previously thought to be exclusive for AP2 binding could perhaps aid a CCP in transitioning from an early to late stage, if, for example, the Dab2-FCHO2 interaction was necessary for early steps of endocytosis and

Dab2-AP2 needed for later steps. Additionally, the model proposed at the end of chapter 3 (Figure 3.10, [207]) suggests that the binding of Dab2 to EH domain proteins regulates the endocytosis of Dab2 cargo and may play a role in allowing CCPs to pass through the endocytic checkpoint. This then suggests that Dab2 must sense the presence of cargo and then somehow signal to the growing CCP to proceed. One way this “signal” may function is a conformational change occurring in Dab2 upon cargo binding which then releases other Dab2 motifs for interaction with accessory proteins controlling CCP progression and budding.

Here I show that AP2 and FCHO2 may compete for binding to Dab2, although the data is still incomplete. Excitingly, I also show that the C-terminus of the Dab2 protein is able to interact with its PTB domain, evidence of a “closed” form of the protein. This interaction requires the very C-terminal end of the protein and is disrupted by the addition of a C-terminal His tag, similar to what was seen for Eps15/15R (Figure 3.1, [207]). Furthermore, the interaction of the C-terminus of Dab2 with its PTB domain is disrupted by the addition of a cargo peptide, indicating that cargo binding may signal the change from “closed” to “open.”

II. Results

Part 1: Competition between FCHO2 and AP2 for the Dab2 DPFs

The data in chapter 2 indicates that FCHO2 binds to Dab2 directly through the Dab2 DPF motifs, which are known to be an AP2-binding motif (Figure 4.1A, [203]). To investigate whether there is sequential, mutually-exclusive binding of FCHO2 and AP2 to the Dab2 DPF motifs, we analyzed whether there is competition between FCHO2 and AP2 for Dab2 binding.

We purified T7-His-tagged full length FCHO2 and T7-His-tagged appendage ear domain of α -adaptin, which contains the DPF-interacting region. When FCHO2 and AP2 were combinatorially added to immobilized GST-Dab2 central region, slightly less of each bound Dab2 than when added individually (Figure 4.1B).

To learn more about this potential competition between FCHO2 and AP2 for the Dab2 DPF motifs, we asked whether increasing the relative amount of AP2 could prevent binding of FCHO2. The amount of FCHO2 was held constant and increasing amounts of AP2 were added to excess GST-Dab2. When four or eight times more moles of AP2 than FCHO2 were added, AP2 bound to Dab2 and the amount of FCHO2 bound decreased (Figure 4.2, left). We also performed the reciprocal experiment, where the amount of AP2 was held constant and FCHO2 was increased. In this case, AP2 binding remained constant and FCHO2 was not able to compete against it for Dab2 binding (Figure 4.2, right). This suggests that the affinity of AP2 for Dab2 may be higher than that of FCHO2 for Dab2. Additionally, despite adding up to 109 pmol of protein to GST-Dab2, only a small fraction of both AP2 and FCHO2 bound; the intensity of bound FCHO2 was approximately equal to the input lane, which contained less than 1 pmol of protein, and significantly less AP2 bound than was contained in the input. Although AP2 appeared to have a higher binding affinity for Dab2 than FCHO2, considerably more FCHO2 bound to Dab2 compared to AP2. This was surprising, and we wondered whether it might be due to oligomerization of the FCHO2 F-BAR domain, so that, while only one molecule of AP2 bound to each molecule of Dab2, many molecules of FCHO2 were binding each Dab2.

To test this hypothesis, we repeated the competition experiment in Figure 4.2 using a form of FCHO2 containing only the central region and μ HD, the region responsible for Dab2 binding (Figure 2.2). The results were similar; again AP2 was able to compete with FCHO2 when high molar ratios were added, but FCHO2 was not able to compete off AP2 (Figure 4.3). Again, AP2 appeared to have a higher affinity for Dab2 than FCHO2, although much more FCHO2 bound to Dab2 compared to AP2. It is possible this is due to lower affinity interactions of purified AP2 or FCHO2 and DxF motifs on Dab2, which would prevent direct competition between AP2 and FCHO2 for the Dab2 DPF motifs. To better understand what this means for AP2 and FCHO2 binding to Dab2 during CCP formation, this experiment could be repeated with a form of Dab2 where the DxF motifs have been removed. Additionally, although it has not been reported, FCHO2 could be forming oligomeric structures through either its central region or μ HD. It is also possible that our AP2 α -adaptin ear fragment is behaving in a different manner than the AP2 complex would, perhaps by either aggregating or becoming unfolded. For a quantitative measure of binding affinities, a technique such as isothermal titration calorimetry should be used.

Part 2: The Dab2 C-terminus binds its PTB domain

We hypothesized that if Dab2 somehow regulated CCP progression through a conformational change upon cargo binding then this change might involve the cargo-binding PTB domain. We also had found that the C-terminus of Dab2 is essential for its localization (Figure 2.3). For these reasons, we wondered whether Dab2 might undergo a conformational change involving the C-terminus detaching from the PTB domain. First, we tested whether the PTB domain was able to bind the C-terminus. Purified GST-PTB (aa. 1-205) was mixed with

the Dab2 C-terminus (aa. 493-766) or its central region (aa. 206-492). The C-terminus was able to bind the PTB domain but the central region was not (Figure 4.4). Interestingly, the addition of a His tag on the C-terminal end of the C-terminus blocked this binding. This suggested that the very C-terminal end of the protein might be essential for this interaction.

An alignment of the C-termini of mammalian and zebrafish Dab2 proteins showed that this region is highly conserved, even in zebrafish (Figure 4.5A). The conserved region contains a sequence similar to the cargo internalization signal which binds to the PTB, FxNPxY, where the phenylalanine can be substituted with a tyrosine [131, 132]. The C-terminal end of Dab2 contains FGNPFA, where the first F, the N, and the P are in the same position as in cargo molecules and the F is one position before the Y. Thus we wondered whether the very C-terminal end of Dab2 might then interact with the cargo binding pocket of the PTB domain.

To test whether the FGNPFA sequence at the C-terminal end of Dab2 was required for the interaction seen between the PTB domain and the C-terminus, we removed the last 14 amino acids of Dab2 and tested whether the C-terminus would still bind to the PTB domain. While the entire Dab2 C-terminus bound to the PTB domain, removal of the last 14 amino acids, including the FGNPFA sequence, prevented this interaction (Figure 4.5B and C). This indicates that these last 14 residues of the protein are essential for the interaction of the C-terminus with the PTB domain, although we have not yet tested whether they are sufficient for this interaction.

To map the region of the PTB domain required for C-terminal binding, we made use of an S122T mutation in the PTB previously shown to disrupt binding between Dab2 and its cargo in vitro [258]. Dab2-S122T is unable to cluster LDLR into CCPs, suggesting that it is also unable to bind cargo in vivo [142]. However, surprisingly, GST-PTB S122T still bound to the C-terminus (Figure 4.6A-B). When we analyzed the previously published structure of the Dab2 PTB domain in complex with cargo peptide [258], we noted that S122 was primarily important for interacting with the side chain of the tyrosine residue in the FxNPxY (Figure 4.6C). Because this is the one residue not present in the FGNPFA of the Dab2 C-terminus, a mutation in F166, which is required for peptide binding and contacts both the N and P residues of the cargo peptide (Figure 4.6D), might inhibit C-terminus binding. This prediction remains to be tested.

Next we asked whether the binding of cargo molecules to the PTB domain regulates the Dab2 intramolecular interaction. We presumed that, if Dab2 were to undergo a conformational change upon cargo binding which signals to CCPs to proceed with budding, binding of cargo to the PTB domain might cause release of the PTB-C-terminus interaction. This was indeed the case. When a peptide containing the Dab2-binding sequence of the LDLR (INFDNPVYQKT) was added to purified GST-PTB and His-C-terminus, the Dab2 C-terminus was no longer able to bind to the PTB domain (Figure 4.7). A control peptide did not block this interaction. This supports the idea that, even though the S122T mutation did not block C-terminus-PTB binding, the Dab2 C-terminus is likely still binding to the cargo-binding pocket of the Dab2 PTB domain.

Together, these data support a model where the Dab2 exists in a default closed conformation in the cell, where the very C-terminal end of the protein folds back and is bound to

cargo-binding region of the PTB domain. Upon cargo binding, the C-terminus is released from the PTB domain. This open conformation is likely able to interact with different proteins than the closed conformation, and these interactions cause CCPs to bud. One of these proteins that bind differentially to the open vs. closed conformation may be Eps15/15R. At the end of the conserved C-terminal region is the fifth NPF of Dab2, which is of the sequence NPFA_{COOH} (Figure 4.5). As mentioned in Chapter 3, some EH domains prefer to bind to NPFs followed by X_{COOH} [234, 235]. Our data suggests that Eps15 and Eps15R may be included in this group of EH domain proteins, because addition of a C-terminal His tag on the Dab2 C-terminus decreased Eps15/15R binding (Figure 3.1). Overall, we propose that the binding of the C-terminus of Dab2 to its PTB domain inhibits EH domain protein interaction until cargo binds and releases the C-terminus (Figure 4.8). The EH domain proteins then bind to Dab2 and recruit the other proteins necessary for CCP budding. Additional experiments are necessary to verify that EH domain proteins have a higher affinity for the open conformation of Dab2 and to determine whether this conformational change is regulated at all by binding of other endocytic components.

III. Materials and Methods

Plasmids and Peptides

T7-mDab2-206-492-His, T7-His-mDab2-493-766, and T7-mDab2-493-766-His [207], T7-hFCHO2-His [65], and GST-mDab2-1-205 (PTB, [131]) have been described. The insert from the previously described GST-AP2- α ear [65, 203] was cloned into pET21a(+) to create T7-AP2 α ear-His. T7-hFCHO2-281-810-His was created by moving the insert from GFP-hFCHO2-281-810 [65] into pET21a(+). T7-His-mDab2-493-752 was created by inserting a stop codon after amino acid 752 in T7-His-mDab2-493-766. GST-mDab2-1-205 S122T was created from

GST-mDab2-1-205 using site-directed mutagenesis.

The LDLR internalization signal peptide was the sequence: INFDNPVYQKT (Lifetein, South Plainfield, New Jersey). The control peptide was the sequence: QTSYAIFKK.

Protein purification and pulldown assays

All GST and His-tagged proteins were purified as described in Chapters 2 and 3 [65, 207]. His-Dab2-C-terminal fragments were induced in the presence of protease inhibitors [207]. Pulldowns were performed as described [65, 207].

DNA sequence alignment

Dab2 sequences from mammalian and zebrafish *Dab2* genes were aligned using CLC Sequence Viewer (CLC bio, Aarhus, Denmark). Sequences were obtained from GenBank.

Antibodies

The following antibodies were used: mouse anti-T7 (Novagen) and goat anti-GST (GE Healthcare).

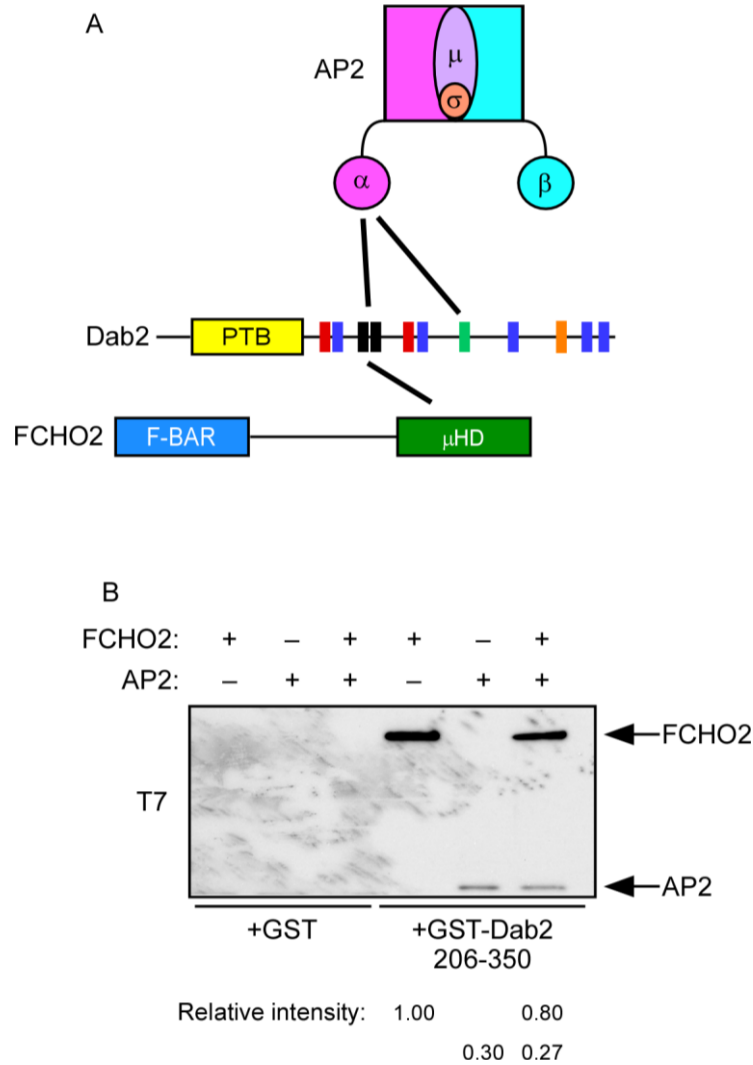


Figure 4.1

Potential competition between AP2 and FCHO2 for Dab2 binding

(A) Diagram of the regions of AP2 and FCHO2 which bind Dab2. (B) Competition between AP2 and FCHO2 for Dab2. Equal molar amounts of purified T7-FCHO2 and T7-AP2 were added to immobilized GST or GST-Dab2 206-350, washed, and Western blotted with T7 antibody. Intensity values are normalized to FCHO2 alone.

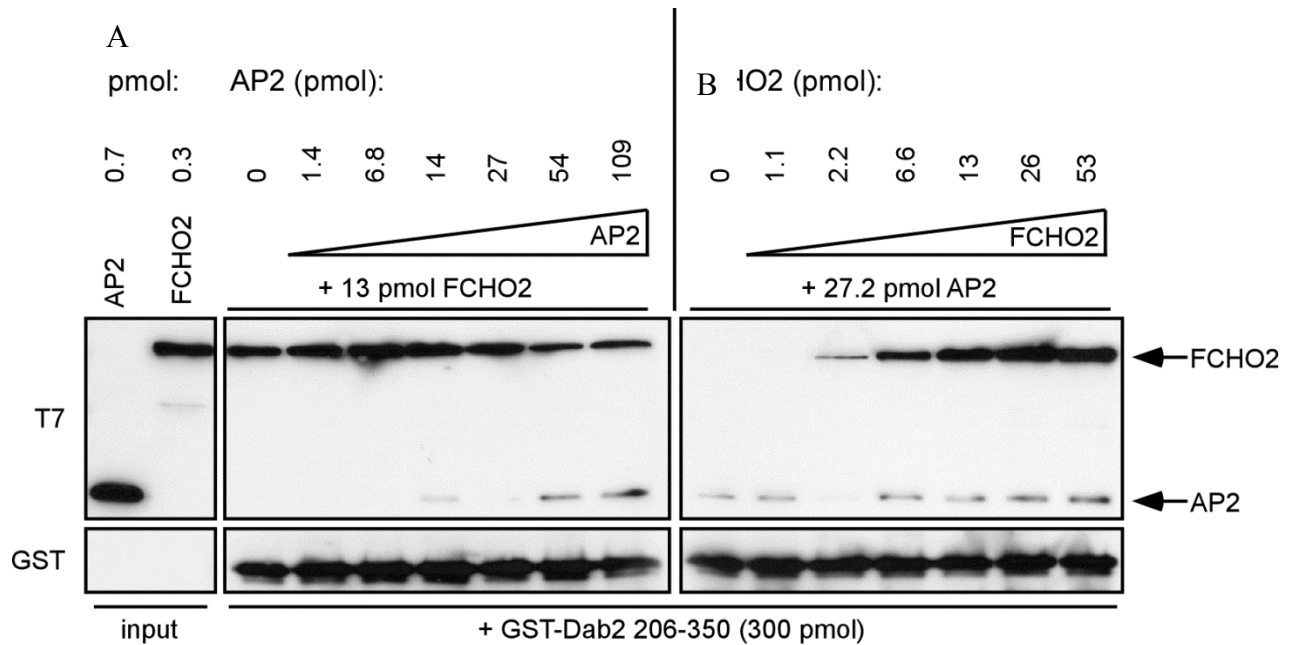


Figure 4.2

AP2 outcompetes FCHO2 for Dab2 binding

(A) A constant amount of T7-FCHO2 and increasing amounts of T7-AP2 were added to immobilized GST-Dab2 206-350. Western blotting was performed with antibodies to T7 and GST. The relative molar amounts of FCHO2 compared to AP2 are shown above. (B) Similar to A, except that the amount of AP2 was held constant and FCHO2 was increased. Relative amounts of AP2 compared to FCHO2 are shown at top. Note that FCHO2 and AP2 were tagged identically, so the signal intensity reflects the molar amount of protein bound. For FCHO2, 13 pmol = 6 μ L, for AP2, 27.2 pmol = 2 μ L, and for Dab2, 300 pmol = 5 μ L. Reactions were carried out in 500 μ L total volume.

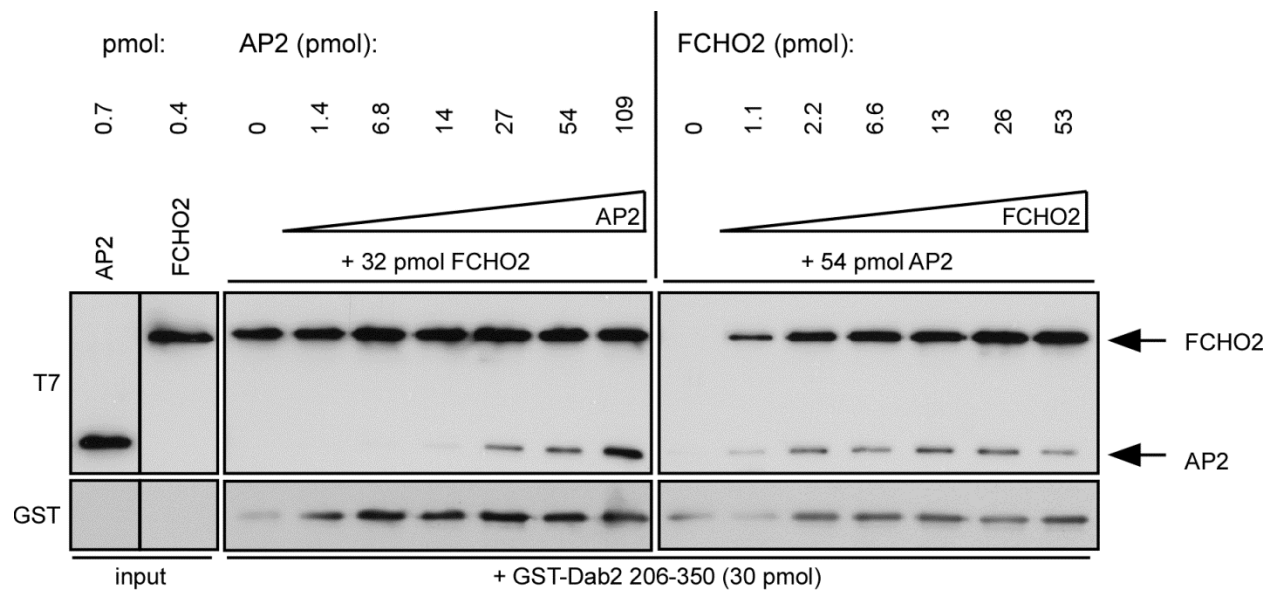


Figure 4.3

Removing the FCHO2 F-BAR domain does not affect competition results

Same as in Figure 4.2, except T7-FCHO2 281-810 was used instead of full length protein.

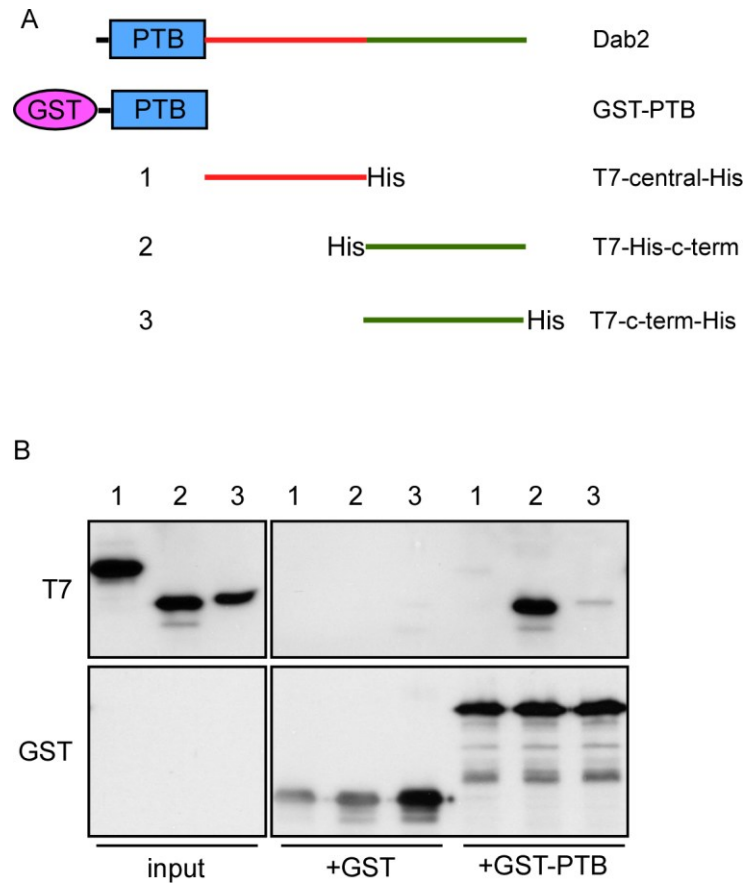


Figure 4.4

The C-terminus of Dab2 binds to its PTB domain

(A) Schematic of the constructs used in (B). GST-PTB contains amino acids 1-205, central is 206-492, and C-terminus is 493-766. (B) Purified Dab2 central region and each of the C-terminal pieces were mixed with immobilized GST or GST-PTB. Samples were then subjected to Western blotting with antibodies to T7 and GST.

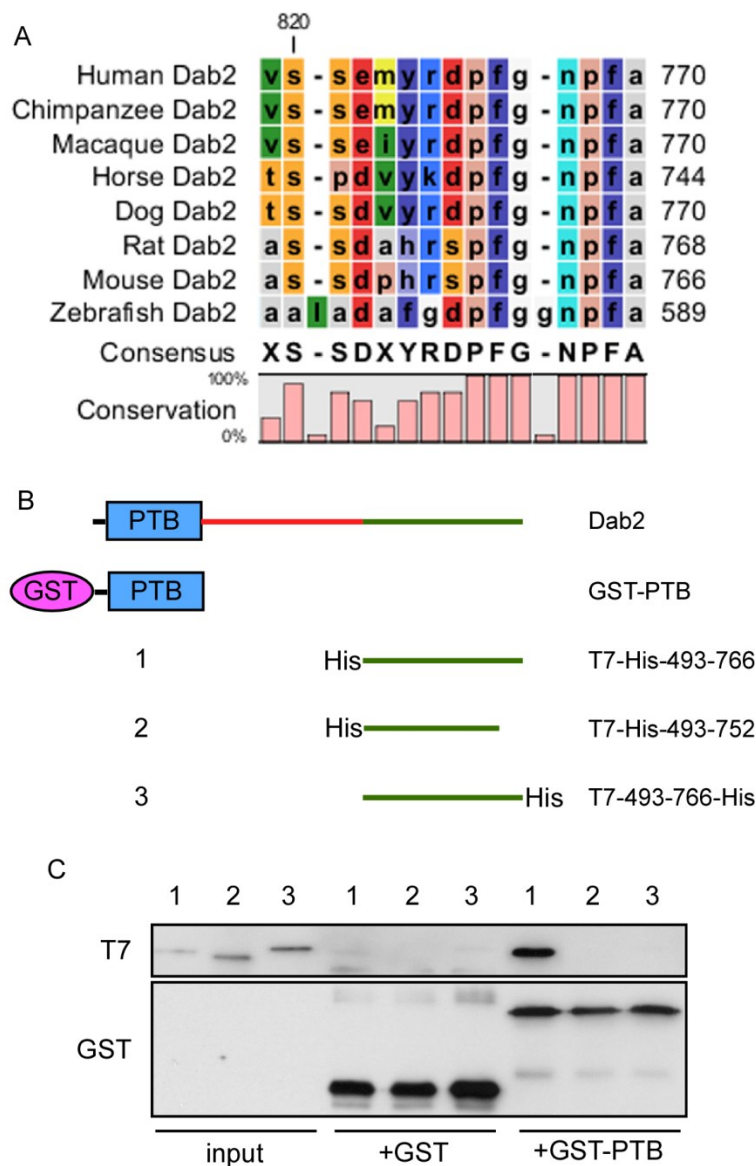
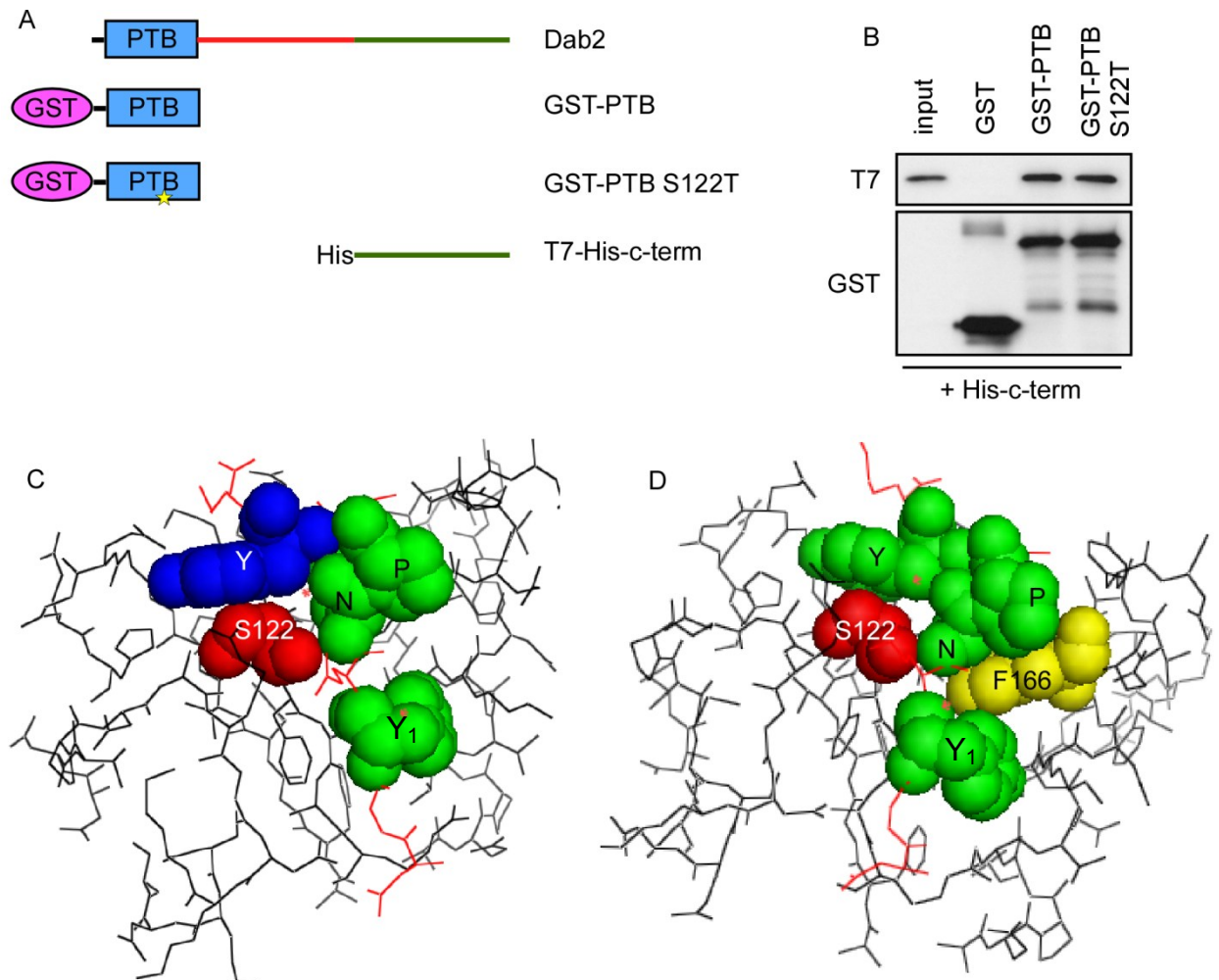


Figure 4.5

The very C-terminal end of Dab2 is required to bind the PTB domain

(A) Alignment of the C-termini of mammalian and zebrafish Dab2. Sequences are the GenBank reference sequences. (B) Schematic of the constructs used in (C) for pulldown. T7-Dab2-493-752 and -493-766 with the His tag at each terminus were mixed with immobilized GST or GST-PTB. Samples were Western blotted and probed with antibodies to T7 and GST.



Structures adapted from [258].

Figure 4.6

The C-terminus still binds a PTB mutant that does not bind cargo

(A) Schematic of Dab2 fragments used for pulldown in (B). T7-Dab2 493-766 was mixed with immobilized GST, GST-PTB (1-205) or GST-PTB S122T. Samples were Western blotted and incubated with antibodies against T7 or GST. (C) and (D) are the crystal structure of the Dab2 PTB domain in complex with the internalization signal of APP from Yun et al [258]. In (C), APP is shown in red lines, with the first Y, N, and P shown in green spheres and its second Y in blue spheres. (The APP internalization signal is of the sequence NGYENPTYK, so it is slightly different from the FxNPxY consensus sequence.) S122 of the Dab2 PTB domain is shown in red spheres. In (D), the molecule is rotated slightly to the right, and the APP amino acids (Y₁xNPxY) are each shown as green spheres. S122 and F166 in the Dab2 PTB domain are shown as red and yellow spheres, respectively.

Images were produced using PyMol.

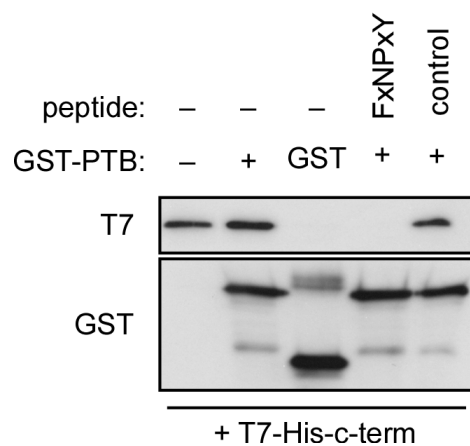


Figure 4.7

Binding of cargo to the Dab2 PTB domain inhibits the C-terminus-PTB interaction

T7-His-Dab2 C-term (amino acids 493-766) was added to immobilized GST or GST-PTB (1-205) with or without 10 μ M peptide. The samples were incubated, washed, and subjected to SDS-PAGE and Western blotting with antibodies against T7 or GST. The FxNPxY peptide is the internalization signal region of the LDLR: INFDNPVYQKT and the control peptide is the sequence: QTSYAIFKK.

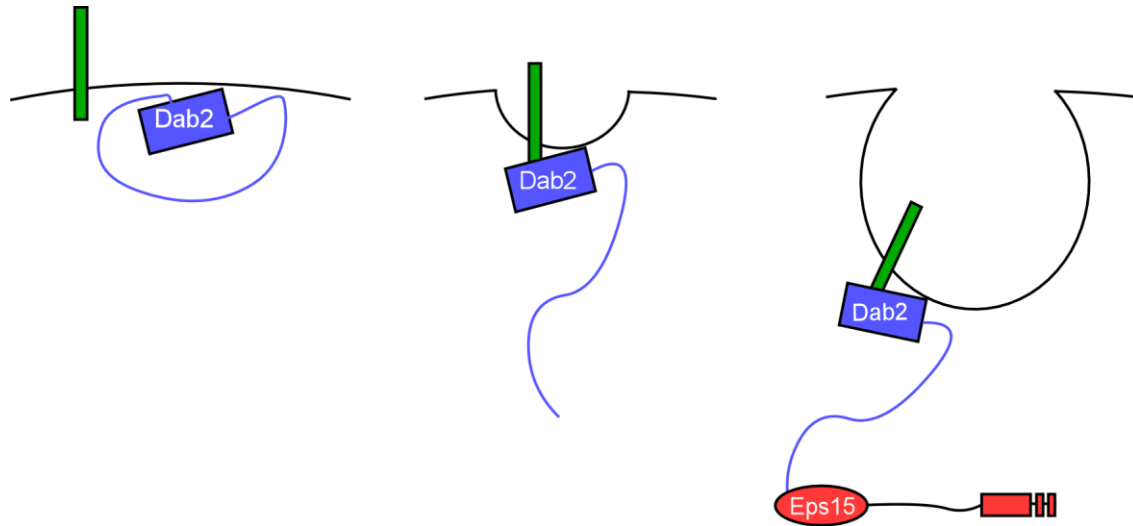


Figure 4.8

Proposed model for a Dab2 conformational change upon cargo binding

Dab2 exists in a closed state where the very C-terminus of the protein is bound to the PTB domain cargo-binding region (left). When cargo binds, the C-terminus is released (center). This frees the C-terminal NPF motif and likely allows it to interact with EH domain proteins such as Eps15, preventing early abortion and allowing the CCP to continue to budding.

Chapter 5 - Discussion

Here I give evidence for three endocytic accessory proteins which interact with the adaptor protein Dab2, the F-BAR protein FCHO2 and the EH domain proteins Eps15/15R and ITSN. Interestingly, FCHO2, Eps15/15R and ITSN each play an important role in controlling the size and shape of endocytic structures. Each of these proteins is also required for efficient uptake of both Dab2-dependent and -independent cargoes, and the interaction of each of these proteins with Dab2 is essential for Dab2-mediated endocytosis. The interaction of Dab2 with the EH domain proteins is necessary for internalization of Dab2 cargo even when AP2 is also present in the CCP, suggesting that the cargo-adaptor interaction somehow controls the activity of the EH domain proteins. Finally, I propose a potential mechanism for this regulation involving a conformational change in Dab2 upon cargo binding; this change may release the Dab2 NPF motifs from the PTB domain and allow EH domain protein binding.

Many additional experiments are needed to fully prove our model that Dab2 undergoes a conformational change and that this regulates its binding to EH domain proteins. The model depends on EH domain proteins binding with higher affinity to the Dab2 C-terminus when the protein is in the open conformation, but this has not yet been tested. This experiment will be easier to interpret using full length Dab2 rather than the PTB domain and C-terminus as separate pieces, but we have been historically unable to produce full length Dab2 in bacteria. However, this may be possible using the conditions under which the Dab2 C-terminus was successfully produced and is a future plan. Additionally, the Cooper lab has successfully grown full length Dab2 in baculovirus, which could also be used. Production of full-length Dab2 will also allow us to test whether the interaction of the C-terminus with the PTB domain may be an

intermolecular, rather than intramolecular, interaction. We recently began a collaboration with Roland Strong's lab to crystallize the Dab2 PTB domain in complex with a C-terminal peptide. This structure will confirm whether the C-terminal end of Dab2 binds to the PTB domain in the cargo-binding pocket and facilitate mapping of the interactions between the two regions, which we have already begun (Figure 4.5 and Figure 4.6). If we are able to identify mutant forms of Dab2 that are constitutively either open or closed, this will enable us to test the biological effects of these conformations on endocytosis. If our model is correct, a constitutively closed Dab2 should be unable to internalize its cargo or bind EH domains with high affinity.

An interesting observation from our mapping of the interaction between the Dab2 C-terminus and PTB domain was that the S122T mutation in the PTB domain blocks cargo binding [258] but did not block C-terminal binding. This may be because S122 primarily contacts the Y in the FxNPxY cargo internalization signal. Tyrosine is required for cargo binding to the PTB domain [132, 133], but the C-terminus does not contain a tyrosine. This suggests, then, that the C-terminus binds to the PTB domain in a different manner from cargo, although cargo binding disrupts the interaction. The crystal structure should help explain how the C-terminus interacts with the PTB domain in a tyrosine-independent manner. It's possible that the second phenylalanine in the C-terminal FGNPFA (in the -1 position compared to the FxNPxY tyrosine) is somehow sufficient for the interaction.

There is precedence for our model that Dab2 undergoes a conformational change. Both AP2 and β -arrestins also undergo conformational changes. Free AP2 binds to phosphoinositides, which stimulates a conformational change which exposes the cargo-binding regions of the μ 2

and $\sigma 2$ subunits [259]. The new conformation is stabilized by phosphorylation by the kinase AAK1, which is activated by assembled clathrin, adding an additional level of regulation [246, 247]. β -arrestin 2 undergoes a conformational change when it binds to phosphorylated GPCRs which increases its affinity for clathrin, allowing it to be incorporated into CCPs [260]. The addition of Dab2 to this list brings the number of adaptors which change their conformations to three and leads to the question of whether additional adaptors are also regulated by conformational changes. ARH, at 308 amino acids and without any NPF motifs, is likely too short for an arrangement similar to Dab2, but the C-terminus of Numb contains an NPF and could potentially be regulated in a similar manner.

Our model that a conformational change in Dab2 regulates its binding to EH domain proteins leaves open the possibility that this change in Dab2 conformation might also regulate binding of other proteins to Dab2. We investigated whether FCHO2 and AP2 competed for Dab2 DPF binding but were unable to make any firm conclusions. It's possible that whether FCHO2 or AP2 binds to Dab2 is determined by the conformation of Dab2. Perhaps one has a higher affinity for the open state of Dab2 and the other, the closed state. When Dab2 mutants are identified that are constitutively open or closed, their binding to FCHO2 and AP2 can be tested.

Early experiments addressing whether there is competition between FCHO2 and AP2 for binding to the Dab2 DPF motifs were inconclusive. One of the problems with these experiments is the presence of additional sites in the central region of Dab2 where the two proteins may potentially be able to bind. Along with the two DPF motifs, there are also two DxF motifs in the fragment of Dab2 used for these experiments. AP2 and FCHO2 likely do not interact with these

sites in a cellular context, since mutation of the two DPF motifs is sufficient to block FCHO2 binding and mutation of the two DPF motifs and the FLDLF motif blocks AP2 binding (Figure 2.2). However, it is possible that concentrated, purified proteins can interact with the DxF motifs. Using a smaller fragment of Dab2 without the two DxF motifs might simplify these experiments.

It was previously thought that Dab2 was required only for direct cargo binding and was not needed for endocytosis of cargoes to which it does not directly bind [142, 143, 145]. However, data presented in chapter 3 suggests a more universal role for Dab2. When Dab2 is depleted, there is a significant decrease in the percent of CCPs which abort early (Figure 3.8), indicating that Dab2 may be important for the endocytic checkpoint to function correctly. This proposed checkpoint ensures that cargo is present before a CCP buds [215, 236]. This defect in the checkpoint probably does not affect the rate of internalization of Dab2-independent cargoes to the extent that it would be noticeable for one round of endocytosis, which is why the effect of Dab2 depletion was not recognized sooner. However, over time there may be a significant effect of Dab2 depletion on global endocytosis. The possible role of Dab2 in the checkpoint also will impact our understanding of how proteins function together during endocytosis. It remains to be seen whether other CLASPs are also important for checkpoint function.

Previous work suggested that both FCHO2 and Eps15 were required for CCP initiation [62]. However, our results do not support that for either protein. When FCHO or EH domain proteins were depleted from our HeLa cells, we observed enlarged CCSs rather than an absence of structures (Figure 2.7 and Figure 3.6). This may be due to incomplete depletion of proteins on

our part, or it may be due to the difference in cell type used. Therefore FCHO and EH proteins may or may not be the CCP initiators in our cells. If the initiator of CME is not FCHO proteins aided by EH domain proteins, what then is? Perhaps AP2 is the initiator of CCPs, as was previously thought. However, our work shows that AP2 can be depleted and Dab2 is still able to function (Figure 2.6 and [142]), implying that AP2 can't be essential for all CCP initiation. Residual AP2 in cells transfected with AP2 siRNA may be sufficient for initiation of CCPs, and Dab2 is then able to compensate for later AP2 functions. Dab2 itself may be able to initiate CCPs, and this may be why it can function when AP2 is depleted. Or it's possible that some other protein, or a combination of these or other proteins, is the true initiator of CCPs. Some of these questions could potentially be addressed using live-cell imaging of fluorescently tagged proteins. If, for example, Dab2 arrives at sites of CCP nucleation before FCHO2 does, FCHO2 is likely not the initiator of that CCP. The question of CCP initiation is a controversial topic and will likely remain so for the foreseeable future.

When FCHO and EH domain proteins are depleted, we saw an increase in the size of CCSs. It's interesting that the depletion of two different types of accessory proteins had the same effect on CCSs. It's possible that both independently are important for CCS shape and size. Or perhaps this is a non-specific effect of accessory protein depletion in our cells. It's also possible that the enlarged structures seen upon FCHO and EH protein depletion indicate that FCHO and EH proteins act in series within the same pathway. This is plausible, since FCHO2 binds to both Eps15 and ITSN (Figure 2.5 and [62]), so the EH domain proteins might be an important link between FCHO proteins and other accessory proteins.

There are of course many questions about CME that remain unanswered, and the speed and complexity of the process prevent many of these questions from being answered definitively. In Chapter 3 we show that integrin $\beta 1$ and TfnR localize to different CCPs on the dorsal side of the cell (Figure 3.9). The CCPs containing integrin $\beta 1$ may be specialized either as a cause or an effect of the different endocytic routes followed by integrin $\beta 1$ and TfnR [241-243]. Further work is needed to understand to what extent cargoes segregate to different CCPs and the mechanism of this segregation. Once cargo is internalized, it is sorted to be either recycled or degraded, but whether the adaptor proteins are used for this sorting remains unknown. With further technical innovation and understanding of the complex interactions that occur during CME, the mechanics of this essential cellular process can be illuminated.

References

1. Traub, L.M., *Regarding the amazing choreography of clathrin coats*. PLoS biology, 2011. **9**(3): p. e1001037.
2. Traub, L.M., *Tickets to ride: selecting cargo for clathrin-regulated internalization*. Nature reviews. Molecular cell biology, 2009. **10**(9): p. 583-96.
3. Traub, L.M., *Sorting it out: AP-2 and alternate clathrin adaptors in endocytic cargo selection*. J Cell Biol, 2003. **163**(2): p. 203-8.
4. McMahon, H.T. and E. Boucrot, *Molecular mechanism and physiological functions of clathrin-mediated endocytosis*. Nature reviews. Molecular cell biology, 2011. **12**(8): p. 517-33.
5. Bonifacino, J.S. and L.M. Traub, *Signals for sorting of transmembrane proteins to endosomes and lysosomes*. Annu Rev Biochem, 2003. **72**: p. 395-447.
6. Conner, S.D. and S.L. Schmid, *Regulated portals of entry into the cell*. Nature, 2003. **422**(6927): p. 37-44.
7. Schmid, S.L., *Clathrin-coated vesicle formation and protein sorting: an integrated process*. Annual review of biochemistry, 1997. **66**: p. 511-48.
8. Maxfield, F.R. and T.E. McGraw, *Endocytic recycling*. Nat Rev Mol Cell Biol, 2004. **5**(2): p. 121-32.
9. Goldstein, J.L., et al., *Receptor-mediated endocytosis: concepts emerging from the LDL receptor system*. Annu Rev Cell Biol, 1985. **1**: p. 1-39.
10. Katzmann, D.J., G. Odorizzi, and S.D. Emr, *Receptor downregulation and multivesicular-body sorting*. Nature reviews. Molecular cell biology, 2002. **3**(12): p. 893-905.
11. Raiborg, C., T.E. Rusten, and H. Stenmark, *Protein sorting into multivesicular endosomes*. Current opinion in cell biology, 2003. **15**(4): p. 446-55.
12. Pearse, B.M., *Clathrin: a unique protein associated with intracellular transfer of membrane by coated vesicles*. Proceedings of the National Academy of Sciences of the United States of America, 1976. **73**(4): p. 1255-9.
13. Ungewickell, E. and D. Branton, *Assembly units of clathrin coats*. Nature, 1981. **289**(5796): p. 420-2.
14. Ungewickell, E. and H. Ungewickell, *Bovine brain clathrin light chains impede heavy chain assembly in vitro*. The Journal of biological chemistry, 1991. **266**(19): p. 12710-4.
15. Ybe, J.A., et al., *Clathrin self-assembly is regulated by three light-chain residues controlling the formation of critical salt bridges*. The EMBO journal, 1998. **17**(5): p. 1297-303.
16. Kirchhausen, T. and S.C. Harrison, *Protein organization in clathrin trimers*. Cell, 1981. **23**(3): p. 755-61.
17. Pearse, B.M. and M.S. Robinson, *Purification and properties of 100-kd proteins from coated vesicles and their reconstitution with clathrin*. The EMBO journal, 1984. **3**(9): p. 1951-7.
18. Dell'Angelica, E.C., et al., *Association of the AP-3 adaptor complex with clathrin*. Science, 1998. **280**(5362): p. 431-4.
19. Lafer, E.M., *Clathrin-protein interactions*. Traffic, 2002. **3**(8): p. 513-20.
20. Owen, D.J., B.M. Collins, and P.R. Evans, *Adaptors for clathrin coats: structure and function*. Annual review of cell and developmental biology, 2004. **20**: p. 153-91.

21. Borner, G.H., et al., *Multivariate proteomic profiling identifies novel accessory proteins of coated vesicles*. The Journal of cell biology, 2012. **197**(1): p. 141-60.
22. Robinson, M.S., *100-kD coated vesicle proteins: molecular heterogeneity and intracellular distribution studied with monoclonal antibodies*. The Journal of cell biology, 1987. **104**(4): p. 887-95.
23. Zaremba, S. and J.H. Keen, *Assembly polypeptides from coated vesicles mediate reassembly of unique clathrin coats*. The Journal of cell biology, 1983. **97**(5 Pt 1): p. 1339-47.
24. Kirchhausen, T., *Clathrin*. Annual review of biochemistry, 2000. **69**: p. 699-727.
25. Folsch, H., et al., *Distribution and function of AP-1 clathrin adaptor complexes in polarized epithelial cells*. The Journal of cell biology, 2001. **152**(3): p. 595-606.
26. Traub, L.M. and G. Apodaca, *AP-1B: polarized sorting at the endosome*. Nat Cell Biol, 2003. **5**(12): p. 1045-7.
27. Hirst, J., et al., *The fifth adaptor protein complex*. PLoS biology, 2011. **9**(10): p. e1001170.
28. Le Borgne, R., et al., *The mammalian AP-3 adaptor-like complex mediates the intracellular transport of lysosomal membrane glycoproteins*. The Journal of biological chemistry, 1998. **273**(45): p. 29451-61.
29. Theos, A.C., et al., *Functions of adaptor protein (AP)-3 and AP-1 in tyrosinase sorting from endosomes to melanosomes*. Molecular biology of the cell, 2005. **16**(11): p. 5356-72.
30. Peden, A.A., et al., *Localization of the AP-3 adaptor complex defines a novel endosomal exit site for lysosomal membrane proteins*. The Journal of cell biology, 2004. **164**(7): p. 1065-76.
31. Burgos, P.V., et al., *Sorting of the Alzheimer's disease amyloid precursor protein mediated by the AP-4 complex*. Developmental cell, 2010. **18**(3): p. 425-36.
32. Virshup, D.M. and V. Bennett, *Clathrin-coated vesicle assembly polypeptides: physical properties and reconstitution studies with brain membranes*. The Journal of cell biology, 1988. **106**(1): p. 39-50.
33. Ahle, S., et al., *Structural relationships between clathrin assembly proteins from the Golgi and the plasma membrane*. The EMBO journal, 1988. **7**(4): p. 919-29.
34. Reider, A. and B. Wendland, *Endocytic adaptors--social networking at the plasma membrane*. Journal of cell science, 2011. **124**(Pt 10): p. 1613-22.
35. Kirchhausen, T., et al., *Structural and functional division into two domains of the large (100- to 115-kDa) chains of the clathrin-associated protein complex AP-2*. Proceedings of the National Academy of Sciences of the United States of America, 1989. **86**(8): p. 2612-6.
36. Heuser, J.E. and J. Keen, *Deep-etch visualization of proteins involved in clathrin assembly*. The Journal of cell biology, 1988. **107**(3): p. 877-86.
37. Shih, W., A. Gallusser, and T. Kirchhausen, *A clathrin-binding site in the hinge of the beta 2 chain of mammalian AP-2 complexes*. The Journal of biological chemistry, 1995. **270**(52): p. 31083-90.
38. Owen, D.J., et al., *The structure and function of the beta 2-adaptin appendage domain*. The EMBO journal, 2000. **19**(16): p. 4216-27.
39. Knuehl, C., et al., *Novel binding sites on clathrin and adaptors regulate distinct aspects of coat assembly*. Traffic, 2006. **7**(12): p. 1688-700.

40. Gaidarov, I. and J.H. Keen, *Phosphoinositide-AP-2 interactions required for targeting to plasma membrane clathrin-coated pits*. The Journal of cell biology, 1999. **146**(4): p. 755-64.
41. Beck, K.A. and J.H. Keen, *Interaction of phosphoinositide cycle intermediates with the plasma membrane-associated clathrin assembly protein AP-2*. The Journal of biological chemistry, 1991. **266**(7): p. 4442-7.
42. Collins, B.M., et al., *Molecular architecture and functional model of the endocytic AP2 complex*. Cell, 2002. **109**(4): p. 523-35.
43. Jost, M., et al., *Phosphatidylinositol-4,5-bisphosphate is required for endocytic coated vesicle formation*. Current biology : CB, 1998. **8**(25): p. 1399-402.
44. Collawn, J.F., et al., *Transferrin receptor internalization sequence YXRF implicates a tight turn as the structural recognition motif for endocytosis*. Cell, 1990. **63**(5): p. 1061-72.
45. McGraw, T.E. and F.R. Maxfield, *Human transferrin receptor internalization is partially dependent upon an aromatic amino acid on the cytoplasmic domain*. Cell regulation, 1990. **1**(4): p. 369-77.
46. Letourneur, F. and R.D. Klausner, *A novel di-leucine motif and a tyrosine-based motif independently mediate lysosomal targeting and endocytosis of CD3 chains*. Cell, 1992. **69**(7): p. 1143-57.
47. Ohno, H., et al., *Interaction of tyrosine-based sorting signals with clathrin-associated proteins*. Science, 1995. **269**(5232): p. 1872-5.
48. Marks, M.S., et al., *Protein targeting by tyrosine- and di-leucine-based signals: evidence for distinct saturable components*. J Cell Biol, 1996. **135**(2): p. 341-54.
49. Kelly, B.T., et al., *A structural explanation for the binding of endocytic dileucine motifs by the AP2 complex*. Nature, 2008. **456**(7224): p. 976-79.
50. Perrais, D. and C.J. Merrifield, *Dynamics of endocytic vesicle creation*. Dev Cell, 2005. **9**(5): p. 581-92.
51. Taylor, M.J., D. Perrais, and C.J. Merrifield, *A high precision survey of the molecular dynamics of mammalian clathrin-mediated endocytosis*. PLoS biology, 2011. **9**(3): p. e1000604.
52. Weinberg, J. and D.G. Drubin, *Clathrin-mediated endocytosis in budding yeast*. Trends in cell biology, 2012. **22**(1): p. 1-13.
53. Praefcke, G.J., et al., *Evolving nature of the AP2 alpha-appendage hub during clathrin-coated vesicle endocytosis*. Embo J, 2004. **23**(22): p. 4371-83.
54. Schmid, E.M., et al., *Role of the AP2 beta-appendage hub in recruiting partners for clathrin-coated vesicle assembly*. PLoS Biol, 2006. **4**(9): p. e262.
55. Brett, T.J., L.M. Traub, and D.H. Fremont, *Accessory protein recruitment motifs in clathrin-mediated endocytosis*. Structure, 2002. **10**(6): p. 797-809.
56. Kazazic, M., et al., *Epsin 1 is involved in recruitment of ubiquitinated EGF receptors into clathrin-coated pits*. Traffic, 2009. **10**(2): p. 235-45.
57. Carbone, R., et al., *eps15 and eps15R are essential components of the endocytic pathway*. Cancer research, 1997. **57**(24): p. 5498-504.
58. Torrisi, M.R., et al., *Eps15 is recruited to the plasma membrane upon epidermal growth factor receptor activation and localizes to components of the endocytic pathway during receptor internalization*. Molecular biology of the cell, 1999. **10**(2): p. 417-34.

59. Slepnev, V.I. and P. De Camilli, *Accessory factors in clathrin-dependent synaptic vesicle endocytosis*. Nat Rev Neurosci, 2000. **1**(3): p. 161-72.
60. van Bergen En Henegouwen, P.M., *Eps15: a multifunctional adaptor protein regulating intracellular trafficking*. Cell communication and signaling : CCS, 2009. **7**: p. 24.
61. Ford, M.G., et al., *Curvature of clathrin-coated pits driven by epsin*. Nature, 2002. **419**(6905): p. 361-6.
62. Henne, W.M., et al., *FCHo proteins are nucleators of clathrin-mediated endocytosis*. Science, 2010. **328**(5983): p. 1281-4.
63. Takei, K., et al., *Functional partnership between amphiphysin and dynamin in clathrin-mediated endocytosis*. Nature cell biology, 1999. **1**(1): p. 33-9.
64. Cocucci, E., et al., *The first five seconds in the life of a clathrin-coated pit*. Cell, 2012. **150**(3): p. 495-507.
65. Mulkearns, E.E. and J.A. Cooper, *FCH domain only-2 organizes clathrin-coated structures and interacts with Disabled-2 for low-density lipoprotein receptor endocytosis*. Molecular biology of the cell, 2012. **23**(7): p. 1330-42.
66. Saffarian, S., E. Cocucci, and T. Kirchhausen, *Distinct dynamics of endocytic clathrin-coated pits and coated plaques*. PLoS biology, 2009. **7**(9): p. e1000191.
67. Heuser, J., *Three-dimensional visualization of coated vesicle formation in fibroblasts*. The Journal of cell biology, 1980. **84**(3): p. 560-83.
68. Frost, A., V.M. Unger, and P. De Camilli, *Boomerangs, Bananas and Blimps: Structure and Function of F-BAR Domains in the Context of the BAR Domain Superfamily*, in *The pombe Cdc15 homology proteins*, P. Aspenström, Editor 2009, Landes Bioscience: Austin, Tex. p. 1-10.
69. Qualmann, B., D. Koch, and M.M. Kessels, *Let's go bananas: revisiting the endocytic BAR code*. The EMBO journal, 2011. **30**(17): p. 3501-15.
70. Frost, A., et al., *Structural basis of membrane invagination by F-BAR domains*. Cell, 2008. **132**(5): p. 807-17.
71. Frost, A., P. De Camilli, and V.M. Unger, *F-BAR proteins join the BAR family fold*. Structure, 2007. **15**(7): p. 751-3.
72. Henne, W.M., et al., *Structure and analysis of FCHo2 F-BAR domain: a dimerizing and membrane recruitment module that effects membrane curvature*. Structure, 2007. **15**(7): p. 839-52.
73. Farsad, K., et al., *Generation of high curvature membranes mediated by direct endophilin bilayer interactions*. The Journal of cell biology, 2001. **155**(2): p. 193-200.
74. Tsujita, K., et al., *Coordination between the actin cytoskeleton and membrane deformation by a novel membrane tubulation domain of PCH proteins is involved in endocytosis*. The Journal of cell biology, 2006. **172**(2): p. 269-79.
75. Shimada, A., et al., *Curved EFC/F-BAR-domain dimers are joined end to end into a filament for membrane invagination in endocytosis*. Cell, 2007. **129**(4): p. 761-72.
76. Masuda, M. and N. Mochizuki, *Structural characteristics of BAR domain superfamily to sculpt the membrane*. Seminars in cell & developmental biology, 2010. **21**(4): p. 391-8.
77. Frost, A., V.M. Unger, and P. De Camilli, *The BAR domain superfamily: membrane-molding macromolecules*. Cell, 2009. **137**(2): p. 191-6.
78. Mattila, P.K., et al., *Missing-in-metastasis and IRSp53 deform PI(4,5)P2-rich membranes by an inverse BAR domain-like mechanism*. The Journal of cell biology, 2007. **176**(7): p. 953-64.

79. Lim, K.B., et al., *The Cdc42 effector IRSp53 generates filopodia by coupling membrane protrusion with actin dynamics*. The Journal of biological chemistry, 2008. **283**(29): p. 20454-72.
80. Wang, L.H., T.C. Sudhof, and R.G. Anderson, *The appendage domain of alpha-adaptin is a high affinity binding site for dynamin*. The Journal of biological chemistry, 1995. **270**(17): p. 10079-83.
81. Koenig, J.H. and K. Ikeda, *Disappearance and reformation of synaptic vesicle membrane upon transmitter release observed under reversible blockage of membrane retrieval*. The Journal of neuroscience : the official journal of the Society for Neuroscience, 1989. **9**(11): p. 3844-60.
82. van der Blik, A.M., et al., *Mutations in human dynamin block an intermediate stage in coated vesicle formation*. The Journal of cell biology, 1993. **122**(3): p. 553-63.
83. Takei, K., et al., *Tubular membrane invaginations coated by dynamin rings are induced by GTP-gamma S in nerve terminals*. Nature, 1995. **374**(6518): p. 186-90.
84. Marks, B., et al., *GTPase activity of dynamin and resulting conformation change are essential for endocytosis*. Nature, 2001. **410**(6825): p. 231-5.
85. Ferguson, S.M. and P. De Camilli, *Dynamin, a membrane-remodelling GTPase*. Nature reviews. Molecular cell biology, 2012. **13**(2): p. 75-88.
86. Ayscough, K.R., *Endocytosis and the development of cell polarity in yeast require a dynamic F-actin cytoskeleton*. Current biology : CB, 2000. **10**(24): p. 1587-90.
87. Ayscough, K.R., et al., *High rates of actin filament turnover in budding yeast and roles for actin in establishment and maintenance of cell polarity revealed using the actin inhibitor latrunculin-A*. The Journal of cell biology, 1997. **137**(2): p. 399-416.
88. Kubler, E. and H. Riezman, *Actin and fimbrin are required for the internalization step of endocytosis in yeast*. The EMBO journal, 1993. **12**(7): p. 2855-62.
89. Qualmann, B., et al., *Syndapin I, a synaptic dynamin-binding protein that associates with the neural Wiskott-Aldrich syndrome protein*. Molecular biology of the cell, 1999. **10**(2): p. 501-13.
90. Qualmann, B. and R.B. Kelly, *Syndapin isoforms participate in receptor-mediated endocytosis and actin organization*. The Journal of cell biology, 2000. **148**(5): p. 1047-62.
91. Ochoa, G.C., et al., *A functional link between dynamin and the actin cytoskeleton at podosomes*. The Journal of cell biology, 2000. **150**(2): p. 377-89.
92. Hussain, N.K., et al., *Endocytic protein intersectin-1 regulates actin assembly via Cdc42 and N-WASP*. Nature cell biology, 2001. **3**(10): p. 927-32.
93. Engqvist-Goldstein, A.E., et al., *RNAi-mediated Hip1R silencing results in stable association between the endocytic machinery and the actin assembly machinery*. Molecular biology of the cell, 2004. **15**(4): p. 1666-79.
94. Fujimoto, L.M., et al., *Actin assembly plays a variable, but not obligatory role in receptor-mediated endocytosis in mammalian cells*. Traffic, 2000. **1**(2): p. 161-71.
95. Merrifield, C.J., et al., *Imaging actin and dynamin recruitment during invagination of single clathrin-coated pits*. Nat Cell Biol, 2002. **4**(9): p. 691-8.
96. Merrifield, C.J., D. Perrais, and D. Zenisek, *Coupling between clathrin-coated-pit invagination, cortactin recruitment, and membrane scission observed in live cells*. Cell, 2005. **121**(4): p. 593-606.

97. Ehrlich, M., et al., *Endocytosis by random initiation and stabilization of clathrin-coated pits*. Cell, 2004. **118**(5): p. 591-605.
98. Prasad, K., et al., *A protein cofactor is required for uncoating of clathrin baskets by uncoating ATPase*. The Journal of biological chemistry, 1993. **268**(32): p. 23758-61.
99. Ungewickell, E., et al., *Role of auxilin in uncoating clathrin-coated vesicles*. Nature, 1995. **378**(6557): p. 632-5.
100. Braell, W.A., et al., *Dissociation of clathrin coats coupled to the hydrolysis of ATP: role of an uncoating ATPase*. The Journal of cell biology, 1984. **99**(2): p. 734-41.
101. Chappell, T.G., et al., *Uncoating ATPase is a member of the 70 kilodalton family of stress proteins*. Cell, 1986. **45**(1): p. 3-13.
102. Schlossman, D.M., et al., *An enzyme that removes clathrin coats: purification of an uncoating ATPase*. The Journal of cell biology, 1984. **99**(2): p. 723-33.
103. Greener, T., et al., *Role of cyclin G-associated kinase in uncoating clathrin-coated vesicles from non-neuronal cells*. The Journal of biological chemistry, 2000. **275**(2): p. 1365-70.
104. Kimura, S.H., et al., *Structure, expression, and chromosomal localization of human GAK*. Genomics, 1997. **44**(2): p. 179-87.
105. Schroder, S., et al., *Primary structure of the neuronal clathrin-associated protein auxilin and its expression in bacteria*. European journal of biochemistry / FEBS, 1995. **228**(2): p. 297-304.
106. Holstein, S.E., H. Ungewickell, and E. Ungewickell, *Mechanism of clathrin basket dissociation: separate functions of protein domains of the DnaJ homologue auxilin*. The Journal of cell biology, 1996. **135**(4): p. 925-37.
107. Xing, Y., et al., *Structure of clathrin coat with bound Hsc70 and auxilin: mechanism of Hsc70-facilitated disassembly*. The EMBO journal, 2010. **29**(3): p. 655-65.
108. Cremona, O., et al., *Essential role of phosphoinositide metabolism in synaptic vesicle recycling*. Cell, 1999. **99**(2): p. 179-88.
109. Wenk, M.R. and P. De Camilli, *Protein-lipid interactions and phosphoinositide metabolism in membrane traffic: insights from vesicle recycling in nerve terminals*. Proceedings of the National Academy of Sciences of the United States of America, 2004. **101**(22): p. 8262-9.
110. Eisenberg, E. and L.E. Greene, *Multiple roles of auxilin and hsc70 in clathrin-mediated endocytosis*. Traffic, 2007. **8**(6): p. 640-6.
111. Warren, R.A., et al., *Distinct saturable pathways for the endocytosis of different tyrosine motifs*. The Journal of biological chemistry, 1998. **273**(27): p. 17056-63.
112. Warren, R.A., F.A. Green, and C.A. Enns, *Saturation of the endocytic pathway for the transferrin receptor does not affect the endocytosis of the epidermal growth factor receptor*. The Journal of biological chemistry, 1997. **272**(4): p. 2116-21.
113. Owen, D.J. and P.R. Evans, *A structural explanation for the recognition of tyrosine-based endocytotic signals*. Science, 1998. **282**(5392): p. 1327-32.
114. Zhang, J., et al., *A central role for beta-arrestins and clathrin-coated vesicle-mediated endocytosis in beta2-adrenergic receptor resensitization. Differential regulation of receptor resensitization in two distinct cell types*. The Journal of biological chemistry, 1997. **272**(43): p. 27005-14.
115. Goodman, O.B., Jr., et al., *Beta-arrestin acts as a clathrin adaptor in endocytosis of the beta2-adrenergic receptor*. Nature, 1996. **383**(6599): p. 447-50.

116. Lohse, M.J., et al., *beta-Arrestin: a protein that regulates beta-adrenergic receptor function*. Science, 1990. **248**(4962): p. 1547-50.
117. Gaidarov, I., et al., *Arrestin function in G protein-coupled receptor endocytosis requires phosphoinositide binding*. The EMBO journal, 1999. **18**(4): p. 871-81.
118. Krupnick, J.G., et al., *Modulation of the arrestin-clathrin interaction in cells. Characterization of beta-arrestin dominant-negative mutants*. The Journal of biological chemistry, 1997. **272**(51): p. 32507-12.
119. Laporte, S.A., et al., *The interaction of beta-arrestin with the AP-2 adaptor is required for the clustering of beta 2-adrenergic receptor into clathrin-coated pits*. The Journal of biological chemistry, 2000. **275**(30): p. 23120-6.
120. Ferguson, S.S., et al., *Role of beta-arrestin in mediating agonist-promoted G protein-coupled receptor internalization*. Science, 1996. **271**(5247): p. 363-6.
121. Hawryluk, M.J., et al., *Epsin 1 is a polyubiquitin-selective clathrin-associated sorting protein*. Traffic, 2006. **7**(3): p. 262-81.
122. Barriere, H., et al., *Molecular basis of oligoubiquitin-dependent internalization of membrane proteins in Mammalian cells*. Traffic, 2006. **7**(3): p. 282-97.
123. Hicke, L., *A new ticket for entry into budding vesicles-ubiquitin*. Cell, 2001. **106**(5): p. 527-30.
124. Haglund, K. and I. Dikic, *The role of ubiquitylation in receptor endocytosis and endosomal sorting*. Journal of cell science, 2012. **125**(Pt 2): p. 265-75.
125. Cohen, J.C., et al., *Molecular mechanisms of autosomal recessive hypercholesterolemia*. Current opinion in lipidology, 2003. **14**(2): p. 121-7.
126. Soutar, A.K., R.P. Naoumova, and L.M. Traub, *Genetics, clinical phenotype, and molecular cell biology of autosomal recessive hypercholesterolemia*. Arterioscler Thromb Vasc Biol, 2003. **23**(11): p. 1963-70.
127. Garcia, C.K., et al., *Autosomal recessive hypercholesterolemia caused by mutations in a putative LDL receptor adaptor protein*. Science, 2001. **292**(5520): p. 1394-8.
128. Eden, E.R., et al., *Use of homozygosity mapping to identify a region on chromosome 1 bearing a defective gene that causes autosomal recessive homozygous hypercholesterolemia in two unrelated families*. American journal of human genetics, 2001. **68**(3): p. 653-60.
129. Norman, D., et al., *Characterization of a novel cellular defect in patients with phenotypic homozygous familial hypercholesterolemia*. The Journal of clinical investigation, 1999. **104**(5): p. 619-28.
130. Mishra, S.K., S.C. Watkins, and L.M. Traub, *The autosomal recessive hypercholesterolemia (ARH) protein interfaces directly with the clathrin-coat machinery*. Proc Natl Acad Sci U S A, 2002. **99**(25): p. 16099-104.
131. Morris, S.M. and J.A. Cooper, *Disabled-2 colocalizes with the LDLR in clathrin-coated pits and interacts with AP-2*. Traffic, 2001. **2**(2): p. 111-23.
132. Howell, B.W., et al., *The disabled 1 phosphotyrosine-binding domain binds to the internalization signals of transmembrane glycoproteins and to phospholipids*. Molecular and cellular biology, 1999. **19**(7): p. 5179-88.
133. Mishra, S.K., et al., *Disabled-2 exhibits the properties of a cargo-selective endocytic clathrin adaptor*. Embo J, 2002. **21**(18): p. 4915-26.
134. Nagai, J., et al., *Mutually dependent localization of megalin and Dab2 in the renal proximal tubule*. Am J Physiol Renal Physiol, 2005. **289**(3): p. F569-76.

135. Calderwood, D.A., et al., *Integrin beta cytoplasmic domain interactions with phosphotyrosine-binding domains: a structural prototype for diversity in integrin signaling*. Proc Natl Acad Sci U S A, 2003. **100**(5): p. 2272-7.
136. Li, S.C., et al., *Structure of a Numb PTB domain-peptide complex suggests a basis for diverse binding specificity*. Nature structural biology, 1998. **5**(12): p. 1075-83.
137. Santolini, E., et al., *Numb is an endocytic protein*. J Cell Biol, 2000. **151**(6): p. 1345-52.
138. Dho, S.E., et al., *Characterization of four mammalian numb protein isoforms. Identification of cytoplasmic and membrane-associated variants of the phosphotyrosine binding domain*. The Journal of biological chemistry, 1999. **274**(46): p. 33097-104.
139. Salcini, A.E., et al., *Binding specificity and in vivo targets of the EH domain, a novel protein-protein interaction module*. Genes & development, 1997. **11**(17): p. 2239-49.
140. Xu, X.X., et al., *Cloning of a novel phosphoprotein regulated by colony-stimulating factor 1 shares a domain with the Drosophila disabled gene product*. J Biol Chem, 1995. **270**(23): p. 14184-91.
141. Zuliani, G., et al., *Characterization of a new form of inherited hypercholesterolemia: familial recessive hypercholesterolemia*. Arteriosclerosis, thrombosis, and vascular biology, 1999. **19**(3): p. 802-9.
142. Maurer, M.E. and J.A. Cooper, *The adaptor protein Dab2 sorts LDL receptors into coated pits independently of AP-2 and ARH*. J Cell Sci, 2006. **119**(Pt 20): p. 4235-46.
143. Keyel, P.A., et al., *A single common portal for clathrin-mediated endocytosis of distinct cargo governed by cargo-selective adaptors*. Mol Biol Cell, 2006. **17**(10): p. 4300-17.
144. Nishimura, T. and K. Kaibuchi, *Numb controls integrin endocytosis for directional cell migration with aPKC and PAR-3*. Developmental cell, 2007. **13**(1): p. 15-28.
145. Teckchandani, A., et al., *Quantitative proteomics identifies a Dab2/integrin module regulating cell migration*. The Journal of cell biology, 2009. **186**(1): p. 99-111.
146. Mok, S.C., et al., *Molecular cloning of differentially expressed genes in human epithelial ovarian cancer*. Gynecol Oncol, 1994. **52**(2): p. 247-52.
147. Mok, S.C., et al., *DOC-2, a candidate tumor suppressor gene in human epithelial ovarian cancer*. Oncogene, 1998. **16**(18): p. 2381-7.
148. Tseng, C.P., et al., *The role of DOC-2/DAB2 protein phosphorylation in the inhibition of AP-1 activity. An underlying mechanism of its tumor-suppressive function in prostate cancer*. J Biol Chem, 1999. **274**(45): p. 31981-6.
149. Schwahn, D.J. and D. Medina, *p96, a MAPK-related protein, is consistently downregulated during mouse mammary carcinogenesis*. Oncogene, 1998. **17**(9): p. 1173-8.
150. Bagadi, S.A., et al., *Frequent loss of Dab2 protein and infrequent promoter hypermethylation in breast cancer*. Breast Cancer Res Treat, 2007. **104**(3): p. 277-86.
151. Karam, J.A., et al., *Decreased DOC-2/DAB2 expression in urothelial carcinoma of the bladder*. Clin Cancer Res, 2007. **13**(15 Pt 1): p. 4400-6.
152. Calvisi, D.F., et al., *Mechanistic and prognostic significance of aberrant methylation in the molecular pathogenesis of human hepatocellular carcinoma*. J Clin Invest, 2007. **117**(9): p. 2713-22.
153. Tong, J.H., et al., *Putative tumour-suppressor gene DAB2 is frequently down regulated by promoter hypermethylation in nasopharyngeal carcinoma*. BMC cancer, 2010. **10**: p. 253.

154. Kleeff, J., et al., *Down-regulation of DOC-2 in colorectal cancer points to its role as a tumor suppressor in this malignancy*. Dis Colon Rectum, 2002. **45**(9): p. 1242-8.
155. Xu, H.T., et al., *Disabled-2 and Axin are concurrently colocalized and underexpressed in lung cancers*. Human pathology, 2011. **42**(10): p. 1491-8.
156. Hannigan, A., et al., *Epigenetic downregulation of human disabled homolog 2 switches TGF-beta from a tumor suppressor to a tumor promoter*. The Journal of clinical investigation, 2010. **120**(8): p. 2842-57.
157. Anupam, K., et al., *Loss of disabled-2 expression is an early event in esophageal squamous tumorigenesis*. World J Gastroenterol, 2006. **12**(37): p. 6041-5.
158. Huang, Y., et al., *Doc-2/hDab2 expression is up-regulated in primary pancreatic cancer but reduced in metastasis*. Lab Invest, 2001. **81**(6): p. 863-73.
159. Morrissey, E.E., et al., *The gene encoding the mitogen-responsive phosphoprotein Dab2 is differentially regulated by GATA-6 and GATA-4 in the visceral endoderm*. J Biol Chem, 2000. **275**(26): p. 19949-54.
160. Kim, J.A., et al., *Feed-back regulation of disabled-2 (Dab2) p96 isoform for GATA-4 during differentiation of F9 cells*. Biochemical and biophysical research communications, 2012. **421**(3): p. 591-8.
161. Zhou, J., et al., *Synergistic induction of DOC-2/DAB2 gene expression in transitional cell carcinoma in the presence of GATA6 and histone deacetylase inhibitor*. Cancer Res, 2005. **65**(14): p. 6089-96.
162. Gertler, F.B., et al., *Drosophila abl tyrosine kinase in embryonic CNS axons: a role in axonogenesis is revealed through dosage-sensitive interactions with disabled*. Cell, 1989. **58**(1): p. 103-13.
163. Gertler, F.B., et al., *Dosage-sensitive modifiers of Drosophila abl tyrosine kinase function: prospero, a regulator of axonal outgrowth, and disabled, a novel tyrosine kinase substrate*. Genes & development, 1993. **7**(3): p. 441-53.
164. Song, J.K., et al., *Disabled is a bona fide component of the Abl signaling network*. Development, 2010. **137**(21): p. 3719-27.
165. Baum, B. and N. Perrimon, *Spatial control of the actin cytoskeleton in Drosophila epithelial cells*. Nature cell biology, 2001. **3**(10): p. 883-90.
166. Kawasaki, F., et al., *The DISABLED protein functions in CLATHRIN-mediated synaptic vesicle endocytosis and exoendocytic coupling at the active zone*. Proceedings of the National Academy of Sciences of the United States of America, 2011. **108**(25): p. E222-9.
167. Howell, B.W., F.B. Gertler, and J.A. Cooper, *Mouse disabled (mDab1): a Src binding protein implicated in neuronal development*. The EMBO journal, 1997. **16**(1): p. 121-32.
168. Howell, B.W., et al., *Neuronal position in the developing brain is regulated by mouse disabled-1*. Nature, 1997. **389**(6652): p. 733-7.
169. D'Arcangelo, G., et al., *Reelin is a ligand for lipoprotein receptors*. Neuron, 1999. **24**(2): p. 471-9.
170. Honda, T., et al., *Regulation of cortical neuron migration by the Reelin signaling pathway*. Neurochemical research, 2011. **36**(7): p. 1270-9.
171. Feng, L. and J.A. Cooper, *Dual functions of Dab1 during brain development*. Molecular and cellular biology, 2009. **29**(2): p. 324-32.
172. Simo, S., Y. Jossin, and J.A. Cooper, *Cullin 5 regulates cortical layering by modulating the speed and duration of Dab1-dependent neuronal migration*. The Journal of

- neuroscience : the official journal of the Society for Neuroscience, 2010. **30**(16): p. 5668-76.
173. Feng, L., et al., *Cullin 5 regulates Dab1 protein levels and neuron positioning during cortical development*. Genes & development, 2007. **21**(21): p. 2717-30.
 174. Seger, R. and E.G. Krebs, *The MAPK signaling cascade*. FASEB journal : official publication of the Federation of American Societies for Experimental Biology, 1995. **9**(9): p. 726-35.
 175. Osborne, J.K., E. Zaganjor, and M.H. Cobb, *Signal control through Raf: in sickness and in health*. Cell research, 2012. **22**(1): p. 14-22.
 176. Hanahan, D. and R.A. Weinberg, *The hallmarks of cancer*. Cell, 2000. **100**(1): p. 57-70.
 177. Xu, X.X., et al., *Disabled-2 (Dab2) is an SH3 domain-binding partner of Grb2*. Oncogene, 1998. **16**(12): p. 1561-9.
 178. Zhou, J. and J.T. Hsieh, *The inhibitory role of DOC-2/DAB2 in growth factor receptor-mediated signal cascade. DOC-2/DAB2-mediated inhibition of ERK phosphorylation via binding to Grb2*. J Biol Chem, 2001. **276**(30): p. 27793-8.
 179. He, J., E.R. Smith, and X.X. Xu, *Disabled-2 exerts its tumor suppressor activity by uncoupling c-Fos expression and MAP kinase activation*. J Biol Chem, 2001. **276**(29): p. 26814-8.
 180. Morin, P.J., *beta-catenin signaling and cancer*. BioEssays : news and reviews in molecular, cellular and developmental biology, 1999. **21**(12): p. 1021-30.
 181. Cadigan, K.M., *TCFs and Wnt/beta-catenin signaling: more than one way to throw the switch*. Current topics in developmental biology, 2012. **98**: p. 1-34.
 182. Cadigan, K.M. and M. Peifer, *Wnt signaling from development to disease: insights from model systems*. Cold Spring Harbor perspectives in biology, 2009. **1**(2): p. a002881.
 183. Dale, T.C., *Signal transduction by the Wnt family of ligands*. The Biochemical journal, 1998. **329** (Pt 2): p. 209-23.
 184. Hocevar, B.A., et al., *Regulation of the Wnt signaling pathway by disabled-2 (Dab2)*. Embo J, 2003. **22**(12): p. 3084-94.
 185. Jiang, Y., C. Prunier, and P.H. Howe, *The inhibitory effects of Disabled-2 (Dab2) on Wnt signaling are mediated through Axin*. Oncogene, 2008. **27**(13): p. 1865-75.
 186. Jiang, Y., W. Luo, and P.H. Howe, *Dab2 stabilizes Axin and attenuates Wnt/beta-catenin signaling by preventing protein phosphatase 1 (PP1)-Axin interactions*. Oncogene, 2009. **28**(33): p. 2999-3007.
 187. Jiang, Y., X. He, and P.H. Howe, *Disabled-2 (Dab2) inhibits Wnt/beta-catenin signalling by binding LRP6 and promoting its internalization through clathrin*. The EMBO journal, 2012. **31**(10): p. 2336-49.
 188. Morris, S.M., et al., *Dual roles for the Dab2 adaptor protein in embryonic development and kidney transport*. Embo J, 2002. **21**(7): p. 1555-64.
 189. Maurer, M.E. and J.A. Cooper, *Endocytosis of megalin by visceral endoderm cells requires the Dab2 adaptor protein*. J Cell Sci, 2005. **118**(Pt 22): p. 5345-55.
 190. Motley, A., et al., *Clathrin-mediated endocytosis in AP-2-depleted cells*. The Journal of cell biology, 2003. **162**(5): p. 909-18.
 191. Hinrichsen, L., et al., *Effect of clathrin heavy chain- and alpha-adaptin-specific small inhibitory RNAs on endocytic accessory proteins and receptor trafficking in HeLa cells*. The Journal of biological chemistry, 2003. **278**(46): p. 45160-70.

192. Conner, S.D. and S.L. Schmid, *Differential requirements for AP-2 in clathrin-mediated endocytosis*. The Journal of cell biology, 2003. **162**(5): p. 773-9.
193. Rappoport, J.Z., et al., *The AP-2 complex is excluded from the dynamic population of plasma membrane-associated clathrin*. The Journal of biological chemistry, 2003. **278**(48): p. 47357-60.
194. Hussain, N.K., et al., *Splice variants of intersectin are components of the endocytic machinery in neurons and nonneuronal cells*. The Journal of biological chemistry, 1999. **274**(22): p. 15671-7.
195. Benmerah, A., et al., *The tyrosine kinase substrate eps15 is constitutively associated with the plasma membrane adaptor AP-2*. The Journal of cell biology, 1995. **131**(6 Pt 2): p. 1831-8.
196. Mishra, S.K., et al., *Functional dissection of an AP-2 beta2 appendage-binding sequence within the autosomal recessive hypercholesterolemia protein*. J Biol Chem, 2005. **280**(19): p. 19270-80.
197. He, G., et al., *ARH is a modular adaptor protein that interacts with the LDL receptor, clathrin, and AP-2*. The Journal of biological chemistry, 2002. **277**(46): p. 44044-9.
198. Morris, S.M., et al., *Myosin VI binds to and localises with Dab2, potentially linking receptor-mediated endocytosis and the actin cytoskeleton*. Traffic, 2002. **3**(5): p. 331-41.
199. Reider, A., et al., *Syp1 is a conserved endocytic adaptor that contains domains involved in cargo selection and membrane tubulation*. The EMBO journal, 2009. **28**(20): p. 3103-16.
200. Uezu, A., et al., *Characterization of the EFC/F-BAR domain protein, FCHO2*. Genes to cells : devoted to molecular & cellular mechanisms, 2011. **16**(8): p. 868-78.
201. Tagwerker, C., et al., *A tandem affinity tag for two-step purification under fully denaturing conditions: application in ubiquitin profiling and protein complex identification combined with in vivocross-linking*. Mol Cell Proteomics, 2006. **5**(4): p. 737-48.
202. Di Fiore, P.P., P.G. Pelicci, and A. Sorkin, *EH: a novel protein-protein interaction domain potentially involved in intracellular sorting*. Trends in biochemical sciences, 1997. **22**(11): p. 411-3.
203. Owen, D.J., et al., *A structural explanation for the binding of multiple ligands by the alpha-adaptin appendage domain*. Cell, 1999. **97**(6): p. 805-15.
204. Kowanez, K., J. Terzic, and I. Dikic, *Dab2 links CIN85 with clathrin-mediated receptor internalization*. FEBS Lett, 2003. **554**(1-2): p. 81-7.
205. Zhou, J., J. Scholes, and J.T. Hsieh, *Characterization of a novel negative regulator (DOC-2/DAB2) of c-Src in normal prostatic epithelium and cancer*. J Biol Chem, 2003. **278**(9): p. 6936-41.
206. Uezu, A., et al., *SGIP1alpha is an endocytic protein that directly interacts with phospholipids and Eps15*. The Journal of biological chemistry, 2007. **282**(36): p. 26481-9.
207. Teckchandani, A., et al., *The clathrin adaptor Dab2 recruits EH domain scaffold proteins to regulate integrin beta1 endocytosis*. Molecular biology of the cell, 2012. **23**(15): p. 2905-16.
208. Li, Y., et al., *Differential functions of members of the low density lipoprotein receptor family suggested by their distinct endocytosis rates*. The Journal of biological chemistry, 2001. **276**(21): p. 18000-6.

209. Maupin, P. and T.D. Pollard, *Improved preservation and staining of HeLa cell actin filaments, clathrin-coated membranes, and other cytoplasmic structures by tannic acid-glutaraldehyde-saponin fixation*. The Journal of cell biology, 1983. **96**(1): p. 51-62.
210. den Otter, W.K. and W.J. Briels, *The generation of curved clathrin coats from flat plaques*. Traffic, 2011. **12**(10): p. 1407-16.
211. Anderson, R.G., J.L. Goldstein, and M.S. Brown, *Localization of low density lipoprotein receptors on plasma membrane of normal human fibroblasts and their absence in cells from a familial hypercholesterolemia homozygote*. Proceedings of the National Academy of Sciences of the United States of America, 1976. **73**(7): p. 2434-8.
212. Willingham, M.C., et al., *Receptor-mediated endocytosis in cultured fibroblasts: cryptic coated pits and the formation of receptosomes*. The journal of histochemistry and cytochemistry : official journal of the Histochemistry Society, 1981. **29**(9): p. 1003-13.
213. Goldenthal, K.L., I. Pastan, and M.C. Willingham, *Initial steps in receptor-mediated endocytosis. The influence of temperature on the shape and distribution of plasma membrane clathrin-coated pits in cultured mammalian cells*. Experimental cell research, 1984. **152**(2): p. 558-64.
214. Mettlen, M., et al., *Cargo- and adaptor-specific mechanisms regulate clathrin-mediated endocytosis*. The Journal of cell biology, 2010. **188**(6): p. 919-33.
215. Loeke, D., et al., *Cargo and dynamin regulate clathrin-coated pit maturation*. PLoS biology, 2009. **7**(3): p. e57.
216. Romer, W., et al., *Actin dynamics drive membrane reorganization and scission in clathrin-independent endocytosis*. Cell, 2010. **140**(4): p. 540-53.
217. Boucrot, E., et al., *Roles of AP-2 in clathrin-mediated endocytosis*. PloS one, 2010. **5**(5): p. e10597.
218. Doria, M., et al., *The eps15 homology (EH) domain-based interaction between eps15 and hrb connects the molecular machinery of endocytosis to that of nucleocytoplasmic transport*. The Journal of cell biology, 1999. **147**(7): p. 1379-84.
219. Puthenveedu, M.A. and M. von Zastrow, *Cargo regulates clathrin-coated pit dynamics*. Cell, 2006. **127**(1): p. 113-24.
220. Licklider, L.J., et al., *Automation of nanoscale microcapillary liquid chromatography-tandem mass spectrometry with a vented column*. Analytical chemistry, 2002. **74**(13): p. 3076-83.
221. Craig, R. and R.C. Beavis, *TANDEM: matching proteins with tandem mass spectra*. Bioinformatics, 2004. **20**(9): p. 1466-7.
222. Keller, A., et al., *Empirical statistical model to estimate the accuracy of peptide identifications made by MS/MS and database search*. Analytical chemistry, 2002. **74**(20): p. 5383-92.
223. Rauch, A., et al., *Computational Proteomics Analysis System (CPAS): an extensible, open-source analytic system for evaluating and publishing proteomic data and high throughput biological experiments*. Journal of proteome research, 2006. **5**(1): p. 112-21.
224. Boettner, D.R., et al., *The F-BAR protein Sypl negatively regulates WASp-Arp2/3 complex activity during endocytic patch formation*. Current biology : CB, 2009. **19**(23): p. 1979-87.
225. Pearse, B.M., *Receptors compete for adaptors found in plasma membrane coated pits*. The EMBO journal, 1988. **7**(11): p. 3331-6.

226. Kirchhausen, T., *Adaptors for clathrin-mediated traffic*. Annual review of cell and developmental biology, 1999. **15**: p. 705-32.
227. Chaudhuri, R., et al., *Downregulation of CD4 by human immunodeficiency virus type 1 Nef is dependent on clathrin and involves direct interaction of Nef with the AP2 clathrin adaptor*. Journal of virology, 2007. **81**(8): p. 3877-90.
228. Chao, W.T. and J. Kunz, *Focal adhesion disassembly requires clathrin-dependent endocytosis of integrins*. FEBS letters, 2009. **583**(8): p. 1337-43.
229. Ezratty, E.J., et al., *Clathrin mediates integrin endocytosis for focal adhesion disassembly in migrating cells*. The Journal of cell biology, 2009. **187**(5): p. 733-47.
230. Cihil, K.M., et al., *Disabled-2 protein facilitates assembly polypeptide-2-independent recruitment of cystic fibrosis transmembrane conductance regulator to endocytic vesicles in polarized human airway epithelial cells*. The Journal of biological chemistry, 2012. **287**(18): p. 15087-99.
231. de Beer, T., et al., *Structure and Asn-Pro-Phe binding pocket of the Eps15 homology domain*. Science, 1998. **281**(5381): p. 1357-60.
232. Miliaras, N.B. and B. Wendland, *EH proteins: multivalent regulators of endocytosis (and other pathways)*. Cell biochemistry and biophysics, 2004. **41**(2): p. 295-318.
233. Sengar, A.S., et al., *The EH and SH3 domain Eps proteins regulate endocytosis by linking to dynamin and Eps15*. The EMBO journal, 1999. **18**(5): p. 1159-71.
234. Paoluzi, S., et al., *Recognition specificity of individual EH domains of mammals and yeast*. The EMBO journal, 1998. **17**(22): p. 6541-50.
235. Yamabhai, M., et al., *Intersectin, a novel adaptor protein with two Eps15 homology and five Src homology 3 domains*. The Journal of biological chemistry, 1998. **273**(47): p. 31401-7.
236. Mettlen, M., et al., *Endocytic accessory proteins are functionally distinguished by their differential effects on the maturation of clathrin-coated pits*. Molecular biology of the cell, 2009. **20**(14): p. 3251-60.
237. Jaqaman, K., et al., *Robust single-particle tracking in live-cell time-lapse sequences*. Nature methods, 2008. **5**(8): p. 695-702.
238. Cao, T.T., R.W. Mays, and M. von Zastrow, *Regulated endocytosis of G-protein-coupled receptors by a biochemically and functionally distinct subpopulation of clathrin-coated pits*. The Journal of biological chemistry, 1998. **273**(38): p. 24592-602.
239. Leonard, D., et al., *Sorting of EGF and transferrin at the plasma membrane and by cargo-specific signaling to EEAI-enriched endosomes*. Journal of cell science, 2008. **121**(Pt 20): p. 3445-58.
240. Mundell, S.J., et al., *Distinct clathrin-coated pits sort different G protein-coupled receptor cargo*. Traffic, 2006. **7**(10): p. 1420-31.
241. Bleil, J.D. and M.S. Bretscher, *Transferrin receptor and its recycling in HeLa cells*. The EMBO journal, 1982. **1**(3): p. 351-5.
242. Iacopetta, B.J. and E.H. Morgan, *The kinetics of transferrin endocytosis and iron uptake from transferrin in rabbit reticulocytes*. The Journal of biological chemistry, 1983. **258**(15): p. 9108-15.
243. Roberts, M.S., et al., *Protein kinase B/Akt acts via glycogen synthase kinase 3 to regulate recycling of alpha v beta 3 and alpha 5 beta 1 integrins*. Molecular and cellular biology, 2004. **24**(4): p. 1505-15.

244. Cao, H., et al., *SRC-mediated phosphorylation of dynamin and cortactin regulates the "constitutive" endocytosis of transferrin*. Molecular and cellular biology, 2010. **30**(3): p. 781-92.
245. Liu, A.P., et al., *Local clustering of transferrin receptors promotes clathrin-coated pit initiation*. The Journal of cell biology, 2010. **191**(7): p. 1381-93.
246. Ricotta, D., et al., *Phosphorylation of the AP2 mu subunit by AAK1 mediates high affinity binding to membrane protein sorting signals*. The Journal of cell biology, 2002. **156**(5): p. 791-5.
247. Honing, S., et al., *Phosphatidylinositol-(4,5)-bisphosphate regulates sorting signal recognition by the clathrin-associated adaptor complex AP2*. Molecular cell, 2005. **18**(5): p. 519-31.
248. Anderson, R.G., M.S. Brown, and J.L. Goldstein, *Role of the coated endocytic vesicle in the uptake of receptor-bound low density lipoprotein in human fibroblasts*. Cell, 1977. **10**(3): p. 351-64.
249. Hopkins, C.R. and I.S. Trowbridge, *Internalization and processing of transferrin and the transferrin receptor in human carcinoma A431 cells*. The Journal of cell biology, 1983. **97**(2): p. 508-21.
250. Beguinot, L., et al., *Down-regulation of the epidermal growth factor receptor in KB cells is due to receptor internalization and subsequent degradation in lysosomes*. Proceedings of the National Academy of Sciences of the United States of America, 1984. **81**(8): p. 2384-8.
251. Hanyaloglu, A.C. and M. von Zastrow, *Regulation of GPCRs by endocytic membrane trafficking and its potential implications*. Annual review of pharmacology and toxicology, 2008. **48**: p. 537-68.
252. Waterman, H., et al., *The RING finger of c-Cbl mediates desensitization of the epidermal growth factor receptor*. The Journal of biological chemistry, 1999. **274**(32): p. 22151-4.
253. de Melker, A.A., G. van der Horst, and J. Borst, *Ubiquitin ligase activity of c-Cbl guides the epidermal growth factor receptor into clathrin-coated pits by two distinct modes of Eps15 recruitment*. The Journal of biological chemistry, 2004. **279**(53): p. 55465-73.
254. Haucke, V., *Phosphoinositide regulation of clathrin-mediated endocytosis*. Biochemical Society transactions, 2005. **33**(Pt 6): p. 1285-9.
255. Clague, M.J., S. Urbe, and J. de Lartigue, *Phosphoinositides and the endocytic pathway*. Experimental cell research, 2009. **315**(9): p. 1627-31.
256. Antonescu, C.N., et al., *Phosphatidylinositol-(4,5)-bisphosphate regulates clathrin-coated pit initiation, stabilization, and size*. Molecular biology of the cell, 2011. **22**(14): p. 2588-600.
257. Carroll, S.Y., et al., *Analysis of yeast endocytic site formation and maturation through a regulatory transition point*. Molecular biology of the cell, 2012. **23**(4): p. 657-68.
258. Yun, M., et al., *Crystal structures of the Dab homology domains of mouse disabled 1 and 2*. J Biol Chem, 2003. **278**(38): p. 36572-81.
259. Jackson, L.P., et al., *A large-scale conformational change couples membrane recruitment to cargo binding in the AP2 clathrin adaptor complex*. Cell, 2010. **141**(7): p. 1220-9.
260. Xiao, K., et al., *Activation-dependent conformational changes in {beta}-arrestin 2*. The Journal of biological chemistry, 2004. **279**(53): p. 55744-53.

Curriculum Vitae

ERIN E MULKEARNS-HUBERT

EDUCATION

Ph.D., Molecular and Cellular Biology

University of Washington and Fred Hutchinson Cancer Research Center
Seattle WA

August 2012

Research Advisor: Jonathan A. Cooper

Thesis Title: The “intelligent adaptor” Dab2 regulates clathrin-mediated endocytosis

B.S., Cellular and Molecular Biology

The Johns Hopkins University

Baltimore MD

May 2003

Graduated with Biology departmental honors

RESEARCH EXPERIENCE

Graduate Research Assistant

University of Washington and Fred Hutchinson Cancer Research Center
Seattle WA

September 2006 – August 2012

Research Advisor: Jonathan A. Cooper, PhD

Research Technician

Brigham and Women’s Hospital and Harvard Medical School
Boston MA

June 2003 – August 2006

Research Advisor: Mel B. Feany, MD, PhD

Undergraduate Research Assistant

Johns Hopkins University School of Medicine
Baltimore MD

June 2002 – May 2003

Research Advisor: Peter Devreotes, PhD

PUBLICATIONS

Teckchandani A, **Mulkearns EE**, Randolph TW, Toida N, Cooper JA. The clathrin adaptor Dab2 recruits EH domain scaffold proteins to regulate integrin β 1 endocytosis. *Mol Biol Cell*. 2012 Aug;23(15):2905-16.

Mulkearns EE, Cooper JA. FCH domain only-2 organizes clathrin-coated structures and interacts with Disabled-2 for low-density lipoprotein receptor endocytosis. *Mol Biol Cell*. 2012 Apr;23(7):1330-42.

Khurana V, Elson-Schwab I, Fulga TA, Sharp KA, Loewen CA, **Mulkearns E**, Tyynelä J, Scherzer CR, Feany MB. Lysosomal dysfunction promotes cleavage and neurotoxicity of tau in vivo. *PLoS Genet*. 2010 Jul 15;6(7):e1001026.

Steinhilb ML, Dias-Santagata D, **Mulkearns EE**, Shulman JM, Biernat J, Mandelkow EM, Feany MB. S/P and T/P phosphorylation is critical for tau neurotoxicity in *Drosophila*. *J Neurosci Res*. 2007 May 1;85(6):1271-8.

GRANTS AWARDED

Viral Oncology Training Grant (T32)

Fred Hutchinson Cancer Research Center
2007 - 2009.

MEETING ABSTRACTS

Mulkearns EE, Cooper JA. FCH domain only-2 organizes clathrin-coated structures and interacts with Disabled-2 for low-density lipoprotein receptor endocytosis. *Keystone Symposia: Membranes in Motion*, Lake Tahoe, CA, January 2012; Abstract 239.

TEACHING AND MENTORING EXPERIENCE

Undergraduate Research Mentor

Fred Hutchinson Cancer Research Center
FHCRC/NMSU Cancer Research Internship Program
Summer 2012

Science and Education Partnership

Fred Hutchinson Cancer Research Center
Summer 2008

Teaching Assistant

University of Washington
Foundations in Molecular Cell Biology
Fall 2007

SCIENCE WRITING

Mulkearns, Erin E. “Small Molecules Make a Big Difference.” Northwest Science & Technology, Fall 2008.

Mulkearns, Erin E. “Stories Make History Memorable.” Northwest Science & Technology, Fall 2008.